Project Report
NOAA-18

An Assessment of the Operational Utility of a GOES Lightning Mapping Sensor

M.E. Weber
E.R. Williams
M.M. Wolfson
S.J. Goodman

MIT LINCOLN LABORATORY
COPY 0355
G18D1445894

13 February 1998

Lincoln Laboratory
MASSACHUSETTS INSTITUTE OF TECHNOLOGY
LEXINGTON, MASSACHUSETTS

Prepared for the National Oceanic and Atmospheric Administration under Air Force Contract F19628-95-C-0002.

No distribution of this report shall be made to DTIC.

Transmittal outside the Department of Defense, other than initial distribution to DoD contractors, must have prior approval of the Lincoln Laboratory Program Manager.

No secondary distribution is authorized without prior written approval of the Lincoln Laboratory Program Manager.

MASSACHUSETTS INSTITUTE OF TECHNOLOGY
LINCOLN LABORATORY

AN ASSESSMENT OF THE OPERATIONAL UTILITY OF A GOES LIGHTNING MAPPING SENSOR

M.E. WEBER
E.R. WILLIAMS
M.M. WOLFSON
Group 43

S.J. GOODMAN
NASA/Marshall Space Flight Center

PROJECT REPORT NOAA-18

13 FEBRUARY 1998

No distribution of this report shall be made to DTIC.

Transmittal outside the Department of Defense, other than initial distribution to DoD contractors, must have prior approval of the Lincoln Laboratory Program Manager.

No secondary distribution is authorized without prior written approval of the Lincoln Laboratory Program Manager.

LEXINGTON MASSACHUSETTS

ABSTRACT

This report evaluates the incremental operational benefits of a proposed Lightning Mapping Sensor (LMS) for NOAA's Geostationary Operational Environmental Satellites (GOES). If deployed, LMS would provide continuous, real-time surveillance of total lightning activity over large portions of the North and South American continents and surrounding oceans. In contrast to the current National Lightning Detection Network, LMS would monitor total lightning activity, including the dominant intracloud component which is estimated to occur with order of magnitude greater frequency than cloud-to-ground lightning and may occur ten minutes or more in advance of a storm's first ground flash.

Quantitative yearly benefit estimates–expressed as reductions in human casualty, property damage and business operating costs–are derived for the following categories of potentially enhanced operational capability:

1. Improvements to the lead time and/or the reliability of warnings for tornadoes, damaging thunderstorm winds and hail;

2. Augmented warning capability for thunderstorm flash floods in mountainous areas where the NEXRAD weather radar network's coverage is incomplete owing to beam blockage;

3. Improvements in information provided to commercial airlines on hazardous convective weather, particularly over oceanic regions where current sensor coverage is limited; and

4. More reliable warnings of lightning ground strike hazard.

These benefits estimates are based on our assessment of LMS' ability to enhance warning or decision making capability beyond that achievable with current operational sensors.

Significant technical insight into these potential benefit areas was developed through analysis and operational observations from a total lightning demonstration program at the Melbourne, FL Weather Forecast Office. In addition, we conducted a literature search and interviews with personnel experienced with convective weather impacts on human safety and economic activities and the applications of lightning sensing technology. Models were developed for each benefit category to quantify the effect of the estimated warning/decision-making improvements in reducing casualty and/or economic disruption.

In aggregate, our analysis indicates that yearly reductions of approximately 10 convective weather related fatalities, 150 injuries and $40 million in property damage and business operating costs might be realized through deployment of LMS on GOES East and West platforms. Although they are a relatively small fraction of the total societal toll of the convective weather phenomena considered, these benefits–in monetized terms–significantly exceed the estimated costs of the sensor.

We note finally that realization of these benefits will require the existence of algorithms for reliably alerting operational personnel to appropriate lightning signatures and appropriate data communications, processing and display infrastructure. Development of these capabilities must be pursued aggressively if LMS benefits are to be fully realized.

ACKNOWLEDGMENTS

We gratefully acknowledge contributions from members of the technical oversight committee and the persons interviewed during the fact-finding phase of this study. These contributors are listed individually in Appendix A. Bob Boldi, Anne Matlin, Mike Moore, Melissa Nischan, Dale Rhoda, and Joe Cullen of Lincoln Laboratory assisted in data analysis, fact-finding and graphics preparation. Leslie Mahn invested extraordinary effort in the preparation of this report. Ravi Raghavan, Dennis Buechler, and Rahul Ramachandran of the NASA Global Hydrology and Climate Center in Huntsville, AL assisted in the analysis of the Lightning Imaging Sensor Data Application Demonstration (LISDAD) database. Steve Hodanish, at the Melbourne, FL Weather Forecast Office, was a key contributor to the identification and analysis of the Florida Severe Storm cases.

TABLE OF CONTENTS

Section	Page
Abstract	iii
Acknowledgments	v
List of Illustrations	xi
List of Tables	xiii
1.0 Introduction	1
2.0 Background	3
2.1 Lightning and Thunderstorm Convective Processes	3
2.2 The Lightning Imaging Sensor Data Application Demonstration (LISDAD)	5
2.3 Lightning Mapping Sensor (LMS)	7
3.0. SEVERE STORM WARNINGS (TORNADO, HAIL, THUNDERSTORM WINDS)	9
3.1. Current Costs to Society	9
3.2. Technical Basis for LMS Benefit	10
3.2.1. Updraft Velocity, Radar Cloud Top Height and Lightning Flash Rate	10
3.2.2. Lightning and Tornadoes	12
3.2.3. Total Lightning Benefit in the Severe Storm Context	13
3.3. Benefits Model for LMS Severe Weather Warning	19
3.3.1. Lead Time Assumptions	19
3.3.2. Tornado	20
3.3.3. Severe Weather Warnings	24
3.4. Discussion	27
4.0. THUNDERSTORM FLOOD WARNING	29
4.1. Current Costs to Society	29
4.2. Technical Basis for Benefit	30
4.3. Benefits Model for Thunderstorm Flood	31
4.4. Discussion	35

TABLE OF CONTENTS
(Continued)

Section	Page
5.0. AVIATION WEATHER	37
5.1. Introduction and Existing Sensor Description	37
5.1.1. NEXRAD	37
5.1.2. TDWR and ASR-9	38
5.1.3. NLDN	39
5.1.4. Geostationary Satellite	40
5.1.5. Airborne Weather Radar	40
5.1.6. Visual Detection	41
5.2. Technical Basis for LMS Benefits to Aviation	41
5.2.1. Proxy for Radar Reflectivity	41
5.2.2. Microburst Prediction	49
5.2.3. Aircraft Lightning Strike Prevention	50
5.3 Benefits Categories	50
5.3.1. Summary of Aviation Benefits Categories	50
5.4 Benefits Calculations	51
5.4.1 Assumptions	51
5.4.2 More Efficient Routing by Providing a Proxy for VIL and Echo Tops	54
5.4.3 Microburst Prediction	60
5.4.4. Lightning Strike to Aircraft	62
5.5 Summary	63
6.0 GROUND STRIKE WARNING	65
6.1. Personal Injury, Death and Property Damage	65
6.1.1. Current Costs to Society	65
6.1.2. Technical Basis for LMS Benefit	66
6.1.3. LMS Ground Strike Warning Benefit Model	67
6.1.4. Discussion	73
6.2. Economic Disruptions Due to Ground Strike Threat	73
6.2.1. Overview	73
6.2.2. Lightning Advisories at the NASA Kennedy Space Center	74
6.2.3. Electric Power Generation and Distribution	77

TABLE OF CONTENTS
(Continued)

Section	Page
7.0. Summary, Discussion and Recommendations	79
7.1 Aggregate Benefits	79
7.2 Confidence in Assumptions	80
7.3 Open Issues	81
7.3.1 Phenomenology	81
7.3.2 Algorithms	82
7.3.3 System Architecture	82
GLOSSARY	85
REFERENCES	87
APPENDIX A: STUDY PARTICIPANTS	95
APPENDIX B: TWO-DIMENSIONAL MAPPING OF LIGHTNING DATA	97
APPENDIX C: POTENTIAL LMS BENEFITS FOR TROPICAL STORM FORECASTING/WARNING, FOREST FIRE MANAGEMENT, AND QUANTITATIVE PRECIPITATION FORECASTS	101
1. Tropical Storms and Hurricanes	101
1.1. Introduction	101
1.1.1. Lightning and Hurricane-Spawned Tornadoes	101
1.1.2. Lightning and Hurricane Intensity Changes	102
2.0. Lightning and Forest Fires	104
2.1. Introduction	104
2.2. Fire Preparedness and Operations	104
2.3. DOI Perspective on Satellite Lightning Mapping	105
3.0. Total Lightning Assimilation and Quantitative Precipitation Forecasting	106

LIST OF ILLUSTRATIONS

Figure		Page
1.	Depiction of intracloud and cloud-to-ground lightning in prototype electrostatic structures	4
2.	LISDAD block diagram.	5
3.	Antenna site locations for the Lightning Detection and Ranging (LDAR) system at Kennedy Space Center (adapted from Lennon and Maier, 1991).	6
4.	Map showing proposed coverage of GOES West and East satellites (H. Christian, 1997).	8
5.	Comparison of total lightning flash rate and high-resolution radar measurements of cloud top height for a large Florida storm.	11
6.	Comparison of NEXRAD scanning strategies in non-severe and severe weather conditions.	12
7.	Operational LISDAD display at Melbourne, FL WFO.	14
8.	Histogram of maximum LDAR flash rate for nonsevere and for severe storms.	15
9.	Evolution of LDAR flash rate (top) and differential radial velocity for a microburst-producing hailstorm on May 22, 1997.	17
10.	Warning/response model for evaluating LMS imposed warning benefits.	22
11.	Fatalities attributed to flash floods during the period 1990-1995.	30
12.	Annual flash flood fatalities by location of victims, 1990-1995.	34
13.	Schematic showing the NEXRAD Severe Weather Mode scan and our adopted definition of "three-dimensional" coverage.	37
14.	NEXRAD three-dimensional coverage envelope as described in text.	38
15.	Locations of FAA wind shear detection radars (TDWR and ASR-9 with WSP) and weather reflectivity radars (ASR without WSP) relative to NEXRAD three-dimensional coverage envelope.	39
16.	Map of NLDN detection efficiency in percent. Contours are in intervals of 10 percent (figure from Global Atmospherics, Inc.).	40
17.	Four-panel plot showing LDAR, VIL and Echo Tops from NEXRAD, and NLDN data at 2034 UT on August 16, 1996.	43
18.	Six of the four-panel plots described in Figure 17 are shown for August 16, 1996.	44

LIST OF ILLUSTRATIONS
(Continued)

Figure		Page
19.	Four-panel plot showing LDAR, VIL and Echo Tops from NEXRAD, and NLDN data at 1941 UT on March 29, 1997.	45
20.	Six of the four-panel plots described in figure 19 are shown for March 29, 1997	46
21.	Four-panel plot showing LDAR, VIL and Echo Tops from NEXRAD, and NLDN data at 1638 UT on April 23, 1997.	47
22.	Six of the four-panel plots described in figure 21 are shown for April 23, 1997.	48
23.	Linear regression between vertically integrated liquid water (VIL) pixel values and lightning flash rate densities.	49
24.	Lightning ground flash density for the years 1992-1995 is shown in panels (a) through (d), respectively.	56
25.	Distribution of delay between first IC and first CG flash in Florida thunderstorm.	66
26.	Data used in estimating LMS benefit for human warnings of lightning ground strike.	68
27.	Model for estimating LMS benefit for human warning of lightning ground strike.	69
B-1.	Comparison of VIL and ASR reflectivity for uncorrected ASR reflectivity (boxes) and corrected ASR reflectivity (triangles), where the correction is applied only to reflectivities greater than 18 dBZ (Troxel and Engholm, 1990).	98
C-1.	Lightning flashes in the eyewall and rainbands of Hurricane Linda as observed by the NASA Optical Transient Detector on 12 September 1997.	103
C-2.	Evolution of surface pressure of the Superstorm as a function of time, both during the assimilation period and the prediction period (Alexander, et al., 1997).	107
C-3.	Comparison of precipitation distribution forecasts on 13 March (derived from the control data) with forecasts using SSM/I and GOES IR data only and with forecasts predicted by the model when lightning data were also assimilated.	108

LIST OF TABLES

Table		Page
1.	National Weather Service Natural Hazards Statistics Compilation Gathered from "Storm Data, 1990-1995 Averages"	9
2.	Average Annual Tornado Fatalities by Decade from 1940-1991	9
3.	LISDAD Severe Storm Summary	16
4.	LDAR Lightning "Jump" vs. Melbourne NWS Severe Storm Warning	18
5.	Figures of Merit for National Weather Service Severe Weather Warnings, Pre- and Post-WSR-88D Implementation	20
6.	Tornado Fatality Reduction Calculations for Current Warning System and for Improved Lead Times and Probability of Detection Based on Use of LMS	24
7.	Tornado Injury Reduction Calculations for Current Warning System and for Improved Lead Times and Probability of Detection Based on Use of LMS	24
8.	Thunderstorm Wind Fatality Reduction Calculations for Current Warning System and for Improved Lead Times and Probability of Detection Based on Use of LMS	25
9.	Thunderstorm Wind Injury Reduction Calculations for Current Warning System and for Assumed Lead Time and Probability of Detection Improvements with Use of LMS	26
10.	Hail and Thunderstorm Wind Property Damage Reduction Calculations for Current Warning System and for Improved Lead Times and Probability of Detection Based on Use of LMS	27
11.	Flash Flood Casualties and Property Damage, from NWS Natural Hazards Statistics, 1990-1995 Averages	29
12.	Average Annual Flood Fatalities by Decade, from 1940-1991	29
13.	Percentage Bias of Radar Versus Rain Gage Estimates of Precipitation	31
14.	Annual Flash Flood Fatalities for Current Warnings, Warnings Supplemented by NLDN and Warnings Supplemented by LMS	33
15.	Annual Flash Flood Injuries for Current Warnings, Warnings Supplemented by NLDN and Warnings Supplemented by LMS	33
16.	Annual Flash Flood Property Damage ($M) for Current Warnings, Warnings Supplemented by NLDN and Warnings Supplemented by LMS	34
17.	Dates, Times, and Description of LISDAD Cases Analyzed	42
18.	Aviation Benefits Categories and Existing Sensor Coverage	51
19.	Estimates of the Percentage of International Flights Deviating due to Convection and the Delay (in minutes) Incurred per Deviating Flight	58
20.	Summary of Annual LMS Aviation System Benefits ($M)	64

LIST OF TABLES
(Continued)

Table		Page
21.	NWS Natural Hazards Statistics Compilation for Storm Data, Annual Average for 1990-1995	65
22.	Lightning Warning Time t_w, Relative to Beginning of the Threat Period	70
23.	Fractional Residual Threat (FT) for Cloud-to-Ground Lightning	71
24.	Annual Lightning Fatalities vs. Warning Scenario	71
25.	Annual Lightning Injuries vs. Warning Scenario	72
26.	Annual Lightning Casualties vs. Warning Scenario, Assuming that only 25 Percent of Exposed Individuals Receive Automated System Warning	73
27.	Breakdown of KSC Personnel Affected by Lightning Advisories	76
28.	Summary of LMS Annual Benefits Estimates	79
29.	LMS Benefits for Severe Weather, Flash Flood and Ground Strike Expressed Relative to Total Societal Toll and Relative to Current Warning System Benefit	80
30.	Partial list of LMS Data Processing Algorithms Necessary for Realization of Operational Benefits	82
B-1.	Default Kernel Weights for Spatially Distributing Lightning Strikes Sum of Weights = 48.8.	97
B-2.	Compilation of Color Bar Thresholds Used to Compare VIL, NLDN, and LDAR Data to NWS Levels. The NWS Level Correspondence to ASR Reflectivity is also Given	99
C-1.	Lightning flashes in the eyewall and rainbands of Hurricane Linda as observed by the NASA Optical Transient Detector on 12 September 1997.	103
C-2.	Evolution of surface pressure of the Superstorm as a function of time, both during the assimilation period and the prediction period (Alexander, et al., 1997).	107
C-3.	Comparison of precipitation distribution forecasts on 13 March (derived from the control data) with forecasts using SSM/I and GOES IR data only and with forecasts predicted by the model when lightning data were also assimilated.	108

1.0 INTRODUCTION

This report, commissioned by NOAA's National Environmental Satellite, Data and Information Service (NESDIS), evaluates quantitative incremental benefits of a proposed geostationary total Lightning Mapping Sensor (LMS). Recognizing that the introduction of new sensors on its satellite fleet is complicated by programmatic and funding constraints, NESDIS is attempting to better understand potential benefits of emerging technologies before embarking on costly development programs. This study represents an attempt by NESDIS to expose objective rationale for improving its Geostationary Operational Environmental Satellite (GOES) mission, specifically in areas of 1) severe convective weather warnings, and 2) aviation weather support.

The Lightning Mapping Sensor has been developed by NASA's Marshall Space Flight Center (MSFC). It detects and localizes optical emissions from lightning, which are transmitted through the cloud-top and may be detected during both day- and night-side operations using suitable processing. A prototype system, the Operational Transient Detector (OTD), has been in low-earth orbit since April 1995 as a proof-of-concept demonstration. In November 1997, a follow-on Lightning Imaging Sensor (LIS) was deployed on the Tropical Rainfall Measuring Mission (TRMM) satellite, featuring improved sensitivity and angular registration to support studies dealing with cloud processes and the climatology of rainfall and lightning. In geosynchronous orbit, the LMS would provide continuous, real-time surveillance of lightning activity over large portions of the North and South American continents and surrounding oceans. It would potentially enhance operational weather forecasting capabilities as well as provide data for scientific studies of convective processes on a continental or global scale. In contrast to the current National Lightning Detection Network (NLDN), LMS would monitor <u>total</u> lightning activity, including the dominant intracloud (IC) component, which is estimated to occur with order of magnitude greater frequency than cloud-to-ground (CG) lightning and may occur ten minutes or more in advance of the first ground flash in a storm.

This report quantitatively evaluates possible operational benefits of LMS in areas of primary utility to the U.S. public:

1. Improved National Weather Service (NWS) convective weather warning;

2. Reduced toll from cloud-to-ground lightning strikes owing to more reliable identification of electrically active storms; and

3. Improved efficiency and/or safety in aviation system operation through provision of relevant information on thunderstorm phenomena to pilots, airline flight dispatch personnel and Air Traffic Controllers.

These benefits are estimated based on assessments of LMS' ability to enhance warning or decision making capability beyond that achievable with current operational sensors. In the context of this study, the most relevant elements of this current system are the weather radar networks–the NWS WSR-88D or NEXRAD, the FAA's Terminal Doppler Weather Radar (TDWR), and Doppler-augmented Airport Surveillance Radar–the GOES satellite visible and IR imagers, and the NLDN. LMS incremental benefits are characterized using such metrics as human casualty and property damage prevention, and reduction of airline operating costs. Although not the focus of this report, such metrics may be monetized in order to establish a "benefits-cost ratio" to support decision making for LMS procurement.

The data collected and analyzed for this study build on ongoing activities addressing the use of total lightning data for NWS, FAA, and NASA applications. Key data and operational feedback pertinent to NWS warning responsibilities have been obtained through an ongoing demonstration program at the Melbourne, FL Weather Forecast Office (WFO). This activity is described in Section 2.

Additional insight into the potential utility of LMS data has been obtained through literature review, discussion amongst members of a "Technical Oversight Committee" for this study, and phone interviews with personnel familiar with the technical and operational issues we considered. Appendix A lists members of the Technical Oversight Committee and the individuals who were interviewed as part of this study.

The remainder of this report is organized as follows. In Section 2, we provide background information on lightning in relation to relevant meteorological phenomena and on the sensing capabilities of LMS. In addition, we describe the Melbourne, FL WFO total lightning demonstration that provided significant technical input to our analysis. Potential benefits for core NWS warning responsibilities are presented in the following sections. Section 3 treats severe weather warnings and Section 4 deals with thunderstorm floods. Potential enhancements to aviation operations are evaluated in Section 5. Finally, in Section 6 we consider the extent to which "precursory information" on ground strikes, provided by LMS' ability to detect IC lightning activity, might reduce casualty and economic loss from CG lightning. Results are summarized in Section 7. There we also discuss issues relative to phenomenology, LMS sensing capability, required algorithms and warning dissemination infrastructure.

Discussion of additional areas of potential LMS benefit–tropical storm/hurricane monitoring, forest fire management, and quantitative precipitation forecasting–is provided in Appendix C. We chose not to include these areas in the body of the report owing to lack of sufficient information to quantify a benefit.

2.0 BACKGROUND

2.1 Lightning and Thunderstorm Convective Processes

The electrification of thunderclouds is closely coupled to the vertical air motions and associated microphysical conditions which define the convective stage of the storm. Laboratory studies, field measurements and numerical models are all consistent with the widely accepted hypothesis that charge separation during the active phase of thunderclouds occurs through a non-inductive, ice-ice interaction that occurs within specific temperature ($T < -10^{\circ}C$) and liquid water content ($0.1\ gm/m^3 < L < 5\ gm/m^3$) regimes. A sustained and vigorous updraft is required to generate the necessary values of L and the charge carrying hydrometeors at altitudes with environmental temperatures of $-10^{\circ}C$ and below. Owing to the different terminal fall speeds of the more massive negatively charged hydrometeors and the ice crystals/snowflakes to which positive charge is transferred, the updraft also plays a crucial role in the macroscopic separation of electric charge in a thundercloud.

As a result of this charging process, active thunderstorms exhibit a bipolar charge distribution with negative charge distributed near and below the mid-level ice-ice interaction region, topped by positive charge in the upper cloud (Figure 1a). Initial lightning activity typically commences several minutes after moderate intensity (>35 dBz) radar echoes form in the mixed phase region of the cloud; these are almost invariably intracloud (IC) discharges between the mid-level negative and upper positive regions of the thundercloud dipole. Relative to subsequent cloud-to-ground (CG) flashes, the IC lightning is characterized by higher occurrence frequencies and smaller energy dissipation (i.e., charge transfer) per flash. IC lightning rates may vary from a few per minute in small, air-mass thunderstorms to more than one per second in severe thunderstorms.

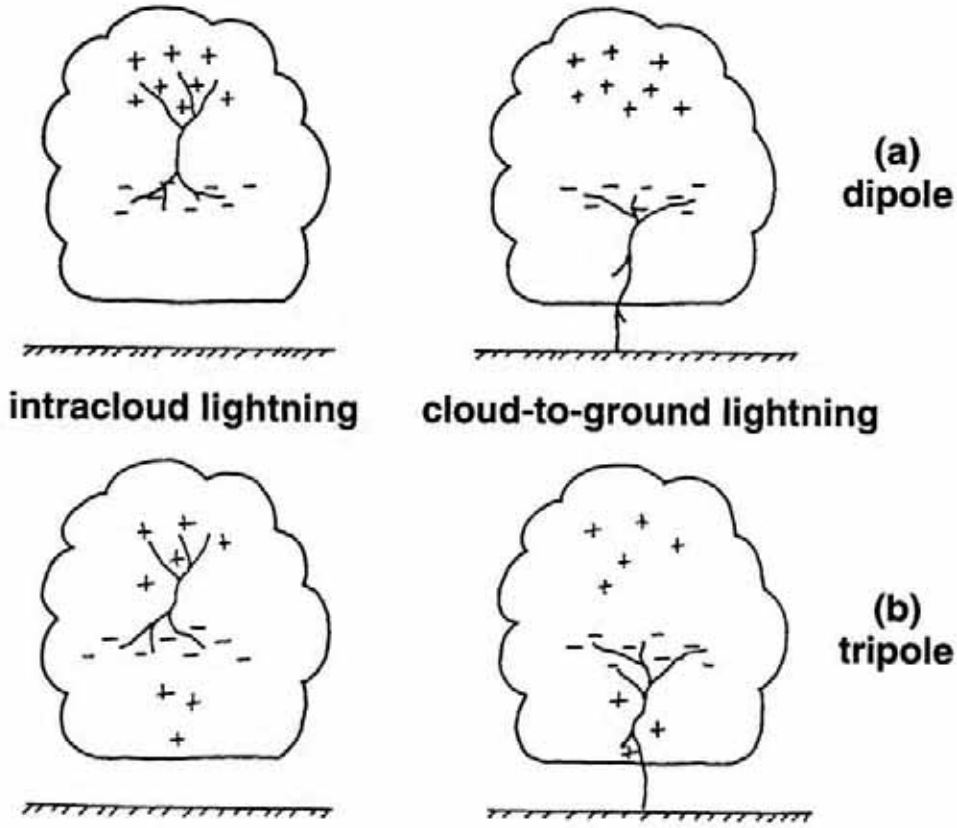

Figure 1. Depiction of intracloud and cloud-to-ground lightning in prototype electrostatic structures: (a) dipole and (b) tripole (from Williams, et al., 1989)

Ground (CG) flashes are normally not manifest until the thunderstorm reaches its "mature" phase, characterized by significant, descending precipitation accumulations and downdrafts in some portions of the cloud. Laboratory experiments indicate that the sign of charge transfer in ice-ice interactions reverses at temperatures near and above freezing; thus graupel particles descending through the lower portions of the cloud may acquire positive charge. Intensification of electrostatic fields in the lower portion of the resulting tripolar thunderstorm charge distribution (Figure 1b) may be the impetus for the onset of CG lightnings.

A number of observational studies (e.g., Workman and Reynolds, 1949; Goodman et al., 1988; Williams et al., 1989; Stanley, et al., 1997) emphasize the correlation between total lightning occurrence rates and observable quantities related to thunderstorm updraft vigor such as cloud-top height, cloud water mass, etc. Such studies further emphasize that surface manifestations of vigorous convection such as strong winds (e.g., "downbursts"), heavy precipitation and hail may occur minutes after the maximum lightning rates. This temporal sequence, presumably the result of the "descent time" of precipitation and downdrafts originating in the cloud's mid-levels, indicates that monitoring of total lightning may provide predictive signals for the occurrence of operationally significant weather. Further, the intensity of these convective manifestations is in general proportional to lightning rate, *albeit* with considerable storm-to-storm variation in the "constant of proportionality."

Operational utilization of such relationships between lightning and thunderstorm precipitation and wind fields forms the basis for the LMS benefits areas discussed in Sections 3 through 5 of this report. A growing base of operational experience with the deployed National Lightning Detection Network (NLDN) provides at least qualitative evidence that monitoring lightning data yields operational benefits. For example, the authors' interviews with NWS forecasters exposed a high degree of enthusiasm for utilization of NDLN data, particularly in regions of poor radar coverage such as the mountainous regions of the western U.S. Corresponding experience with total lightning data is largely absent, the notable exception being the demonstration program at the Melbourne, FL WFO described below.

2.2 The Lightning Imaging Sensor Data Application Demonstration (LISDAD)

This NASA-funded demonstration program utilizes total lightning measurements from the Lightning Detection and Ranging (LDAR) system at Kennedy Space Center (KSC) to approximate–on a local basis–the operational capabilities of an LMS (Raghavan, et al., 1997). These data are integrated with radar-derived products and displayed in real-time to working forecasters at the Melbourne, FL Weather Forecast Office (WFO). The LISDAD processing/display platform is a Sun engineering workstation, with inputs as shown in Figure 2 from LDAR and–through a circuitous path–from the Melbourne WSR-88D and the NLDN. The workstation is located in the "mesoscale operations center" at the WFO and is used during convective weather outbreaks in conjunction with other operational displays such as the WSR-88D Principal User Display (PUP) and GOES satellite VIS/IR displays. Figure 7 in Section 3 illustrates the operation of LISDAD during a period of severe thunderstorm activity to the south of Melbourne.

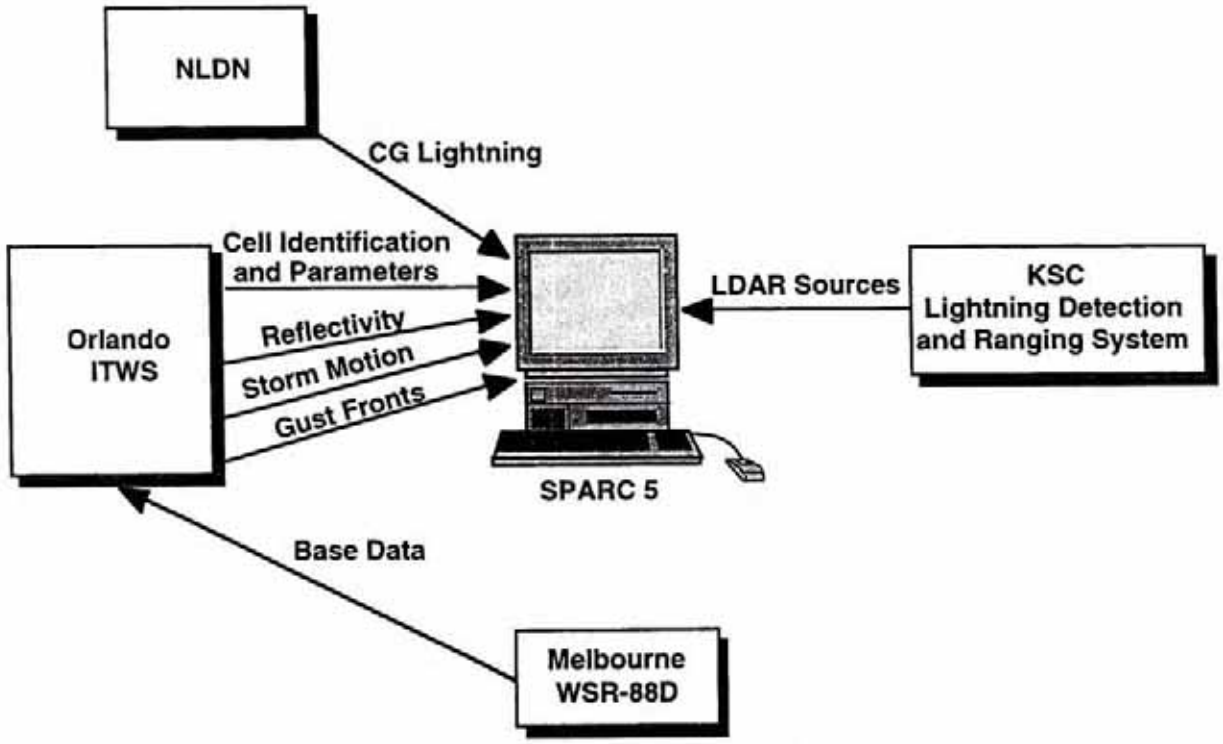

Figure 2. LISDAD block diagram.

LDAR detects radio noise from lightning in a 6 MHz band at 63 MHz, using an array of seven antennae (Lennon and Maier, 1991). The receiving antennae are deployed at the center and around the perimeter of a 10 km radius circle (Figure 3), and are linked via microwave channels. Radio noise source locations are estimated using measurements of the differential time of arrival for large, common pulses at the separated antennae. The system typically yields 20-40 radio noise source locations for a flash within the network. The accuracy of source locations is a function of position relative to the receiving array, generally decreasing (particularly along the radial axis with respect to the array center) with distance. The RMS error for LDAR lightning source locations varies from a few tens of meters inside the network to about 10 km at a range of 90 km (about 1/3 the width of the Florida peninsula). For most of the storm cases we have analyzed then, LDAR's spatial location accuracy equals or exceeds the resolution that would be provided by LMS.

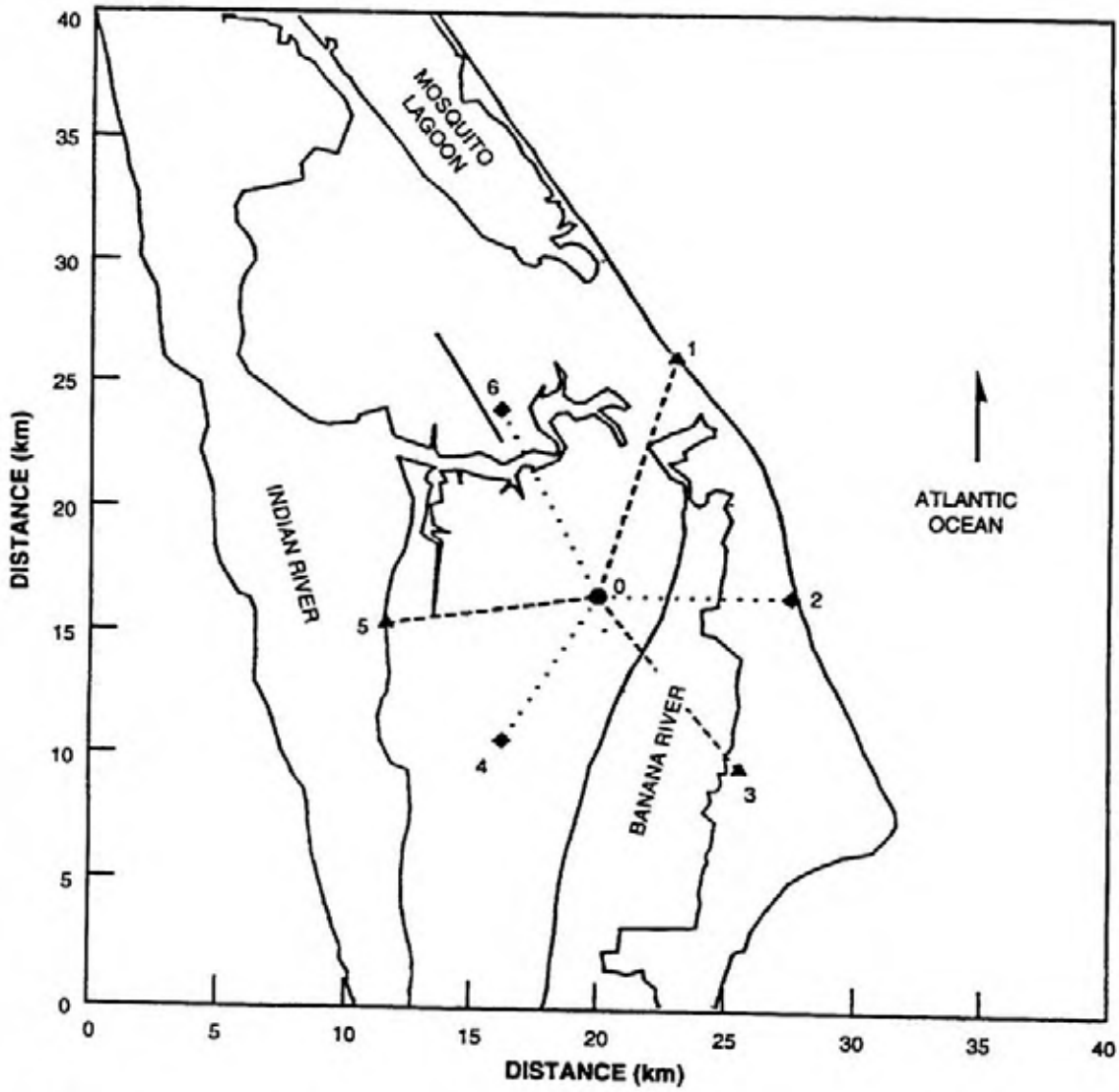

Figure 3. Antenna site locations for the Lightning Detection and Ranging (LDAR) system at Kennedy Space Center (adapted from Lennon and Maier, 1991).

LDAR source locations are computed using a processor at KSC and transmitted along with reception time to the Melbourne WFO via wide-band telephone line. The LISDAD processor groups these sources into "flashes" on the basis of time-space proximity: the grouping algorithm applies a tolerance window of approximately 300 ms in time and 5 km in space. The plan projection of the centroids of these flash groups is computed and used as the basic lightning "unit" for subsequent processing and display.

For reasons of cost and effort minimization, LISDAD's connection to the Melbourne WSR-88D was established via the Lincoln Laboratory Integrated Terminal Weather System (ITWS) prototype at the Orlando International Airport. A previously established wide-band phone link brings WSR-88D "base data"–full-resolution reflectivity and Doppler velocity imagery for each elevation tilt–to the ITWS site. Here, a dedicated workstation implements robust ground clutter suppression algorithms, generates a 4x4 km resolution "composite-maximum" reflectivity image, and processes the volumetric base data using the National Severe Storms Laboratory's (NSSL) Storm Cell Identification Algorithm (SCIT) (Johnson, et al., 1998, in press). This algorithm–a prototype for enhanced implementations of the WSR-88D operational algorithm suite–identifies and tracks individual storm cells and computes for each cell radar-measurable parameters such as maximum reflectivity, vertically integrated liquid water (VIL) and radar cloud top height.

LISDAD's data integration window for estimating and updating displayed lightning rates is one minute; latency for these estimates is less than 15 seconds. Radar measurables are updated on a five-minute strobe corresponding to the volume scan time for the WSR-88D. Processing time may impose several minutes of additional latency.

2.3 Lightning Mapping Sensor (LMS)

The LMS (Christian, et al., 1989) detects energy in a narrow band in the near infrared window (777.4 nm), corresponding to one of the strongest lightning emission lines. Wide field of view optics and a narrow-band filter precede a sensitive Charge Coupled Device (CCD) detector array. Pixel footprint, approximately 10 x 10 km, is matched to the typical footprint of lightning optical emissions when diffused through thunderstorm turrets. The CCD frame integration time is 2 ms. This optimizes the signal-to-noise ratio for the detection of lightning optical pulses in the presence of bright sunlit cloud backgrounds. The on-board Real Time Event Processor (RTEP) tracks and subtracts the background illumination at each pixel. Taken together, these filtering techniques allow for day and nighttime operation with a detection efficiency estimated to exceed 0.9.

Figure 4 shows the coverage pattern of LMS, assuming the envisioned operational deployment of identical sensors on GOES East and West. Coverage extends in latitude from the U.S.-Canadian border to the tip of South America, and in longitude from west of the Hawaiian Islands to the Mid-Atlantic.

Measurements using prototype versions of the LMS on high-flying aircraft and low-earth orbiting satellites have not indicated that reliable discrimination between cloud-to-ground and intracloud lightning is possible. It is envisioned that integration with NLDN data will be necessary in applications where differentiation of CG and IC lightning is required.

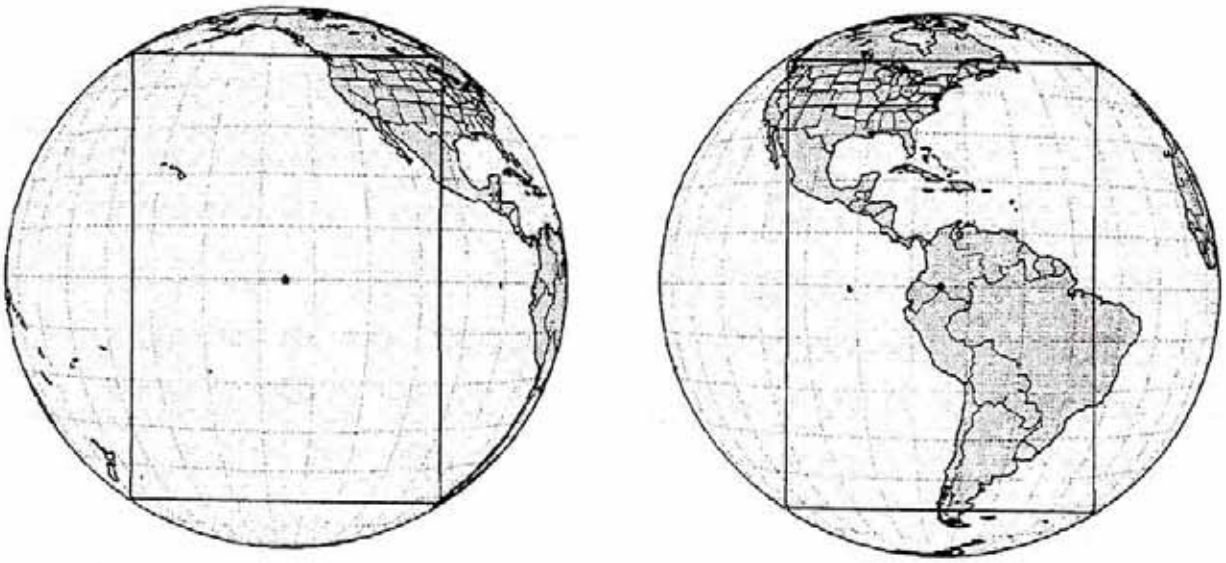

Figure 4. Map showing proposed coverage of GOES West and East satellites (H. Christian, 1997).

3.0. SEVERE STORM WARNINGS (TORNADO, HAIL, THUNDERSTORM WINDS)

3.1. Current Costs to Society

While relatively rare, severe weather outbreaks may cause significant and concentrated property damage, human injury and fatalities. Tables 1 and 2 are National Weather Service tabulations of the magnitude of this destruction. Table 1 provides 1990-1995 averages for all severe weather types while Table 2 shows decadal averages for tornado fatalities. Allowing for considerable year-to-year variability, these statistics suggest that in the current era, these three phenomena account for roughly 70 fatalities, 1500 injuries and $1.5B dollars of property damage per year. The decadal averages of Table 2 indicate that tornado fatalities at least, have clearly trended downwards over the last fifty years; with the growth in population over that period in the states where tornado fatalities are concentrated, the fatality rate per 100,000 population has decreased by a factor of five. Presumably this reflects improved building standards, warning mechanisms and public education.

Table 1.
National Weather Service Natural Hazards Statistics
Compilation Gathered from "Storm Data, 1990-1995 Averages"

	Fatalities	Injuries	Damage ($M)
Tornado	44	1000	590
Thunderstorm Winds	27	440	390
Hail	0	70	640

Table 2.
Average Annual Tornado Fatalities by Decade from 1940-1991

Years	Tornado Fatalities (per year)
1940-1949	154
1950-1959	135
1960-1969	94
1970-1979	99
1980-1989	52
1990-1991	46
Average (51 years)	112

National Weather Service issues separately "severe thunderstorm" and "tornado" warnings, the former targeted primarily towards property-damage prevention and the latter towards human

safety. Clearly, a significant portion of the destruction from these violent phenomena may not be preventable with warnings generated within a few minutes to tens of minutes before their onset. Little can be done in these last minutes to prevent damage to crops, buildings, above-ground power and communication lines, etc. The most violent tornadoes (F4 and F5) can obliterate many above-ground structures, requiring that threatened individuals be able to reach suitable basements or storm shelters. The recent Jarrell, Texas tornado caused tens of fatalities to warned residents who sought shelter in permanent homes.

Automobiles, airplanes, boats and livestock may, however, be moved to more secure stowage on short notice. Injury and fatalities from storm winds and from less violent tornadoes will be reduced to the extent that severe weather warnings persuade people to remain indoors or otherwise take appropriate actions to minimize their exposure to falling trees and wind-borne projectiles.

In the following sections, we review information relevant to the contention that monitoring of total lightning activity may complement other sensors, in particular the WSR-88D Doppler radar network, in allowing NWS personnel to issue timely and accurate severe weather warnings. The potential magnitude of this improvement is estimated as is its resulting benefit in reducing the toll severe weather exacts on our society.

3.2. Technical Basis for LMS Benefit

3.2.1. Updraft Velocity, Radar Cloud Top Height and Lightning Flash Rate

In many kinds of severe convective weather, the updraft strength is an important if not leading determinant of the degree of storm severity. Strong physical reasons have evolved for believing that the updraft maximum aloft systematically precedes manifestations of severe weather at the surface with lead times in the range of 5-20 minutes. Specific examples of such severe weather are microbursts and severe winds, large hailstones and tornadoes. In the microburst case, the updraft is responsible for the accumulation of condensate aloft which ultimately forces the downdraft and the surface wind. In the hailstone case, it is the updraft levitation of ice particles in the airstream of supercooled water that promotes the growth of these particles to hailstone size. In the case of the tornado (see Section 3.2.2.), the updraft is an essential ingredient in vortex stretching and the concentration of angular momentum which is the tornado funnel.

Despite the great importance of the updraft in forcing severe weather, vertical air motions are not directly observable with Doppler radar and so are not routinely monitored and studied. This substantial inadequacy has led to the adoption of proxy quantities such as VIL, radar cloud top height and lightning flash rate, all of which have strong physical connections with updraft strength. Previous observations have shown the maximum in radar cloud top height to precede strong surface winds and microbursts (Byers and Braham, 1949; Goodman, et al., 1988; Williams, et al., 1989; Laroche, et al., 1991; Stanley, et al., 1997), large hail (Donaldson, 1958, 1962; Lemon, 1977; Carey and Rutledge, 1996), mesocyclones (Burgess and Lemon, 1990) and tornadoes (Donaldson, 1962; Lemon, 1977). The recognition of the cloud top precursor is not as widely known as it might otherwise be simply because radar cloud top height is not a carefully scrutinized variable. The reasons for this are only partly clear, but one contributor may be the problems arising with sector-scanning radar in obtaining reliable measurements of radar cloud top (Howard, et al., 1997), a point emphasized further below.

The lightning flash rate has particular value as a proxy variable for storm updraft because it often tracks closely with the radar cloud top (Byers and Braham, 1949; Frost, 1954; Williams, 1985; Stolzenberg, 1994) and is measurable more continuously than the 5-6 minute update of the NEXRAD radar scans. Figure 5 illustrates the tight relationship between total lightning flash rate and cloud top height when both quantities are measured accurately and with fine space-time resolution. In this case, the radar cloud top variations in an active Florida thunderstorm were monitored with a vertically scanning X-band radar making one complete revolution in azimuth every minute. The tightly spaced vertical scans in these observations are particularly well suited for observations of the cloud vertical development. In this figure both the cloud top height and the fifth power of the cloud top height are plotted, following predictions by Vonnegut (1963) and analysis by Williams (1985) supporting this strong power law dependence. Times of maximum cloud top height are closely in phase with the maximum flash rate. Furthermore, doublings of flash rate are associated with rather modest changes (2-3 km or 15-20 percent changes) in cloud height. The strong sensitivity underscores the value of the lightning measurements.

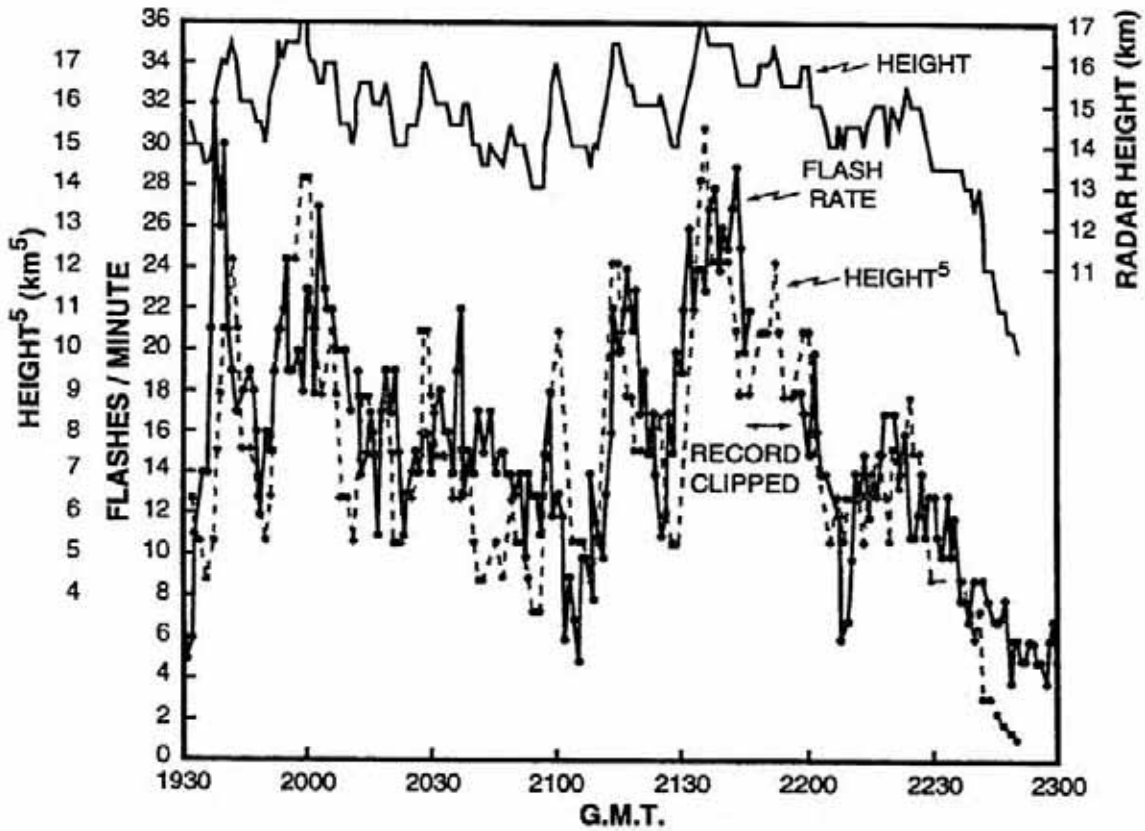

Figure 5. Comparison of total lightning flash rate and high-resolution radar measurements of cloud top height for a large Florida storm.

The limitations of conventional NEXRAD radar scanning in depicting the delicate variation of radar cloud top shown in Figure 5 are increasingly recognized. The recent study by Howard, et al. (1997) documents well these limitations. Figure 6 illustrates the basic problem. For storms at certain ranges from the radar, the sampling resolution of the cloud top with discrete radar tilt

angles may not even be adequate to document the subtle height variations in Figure 5 (1-3 km) with which the factor-of-two variations in total flash rate are associated.

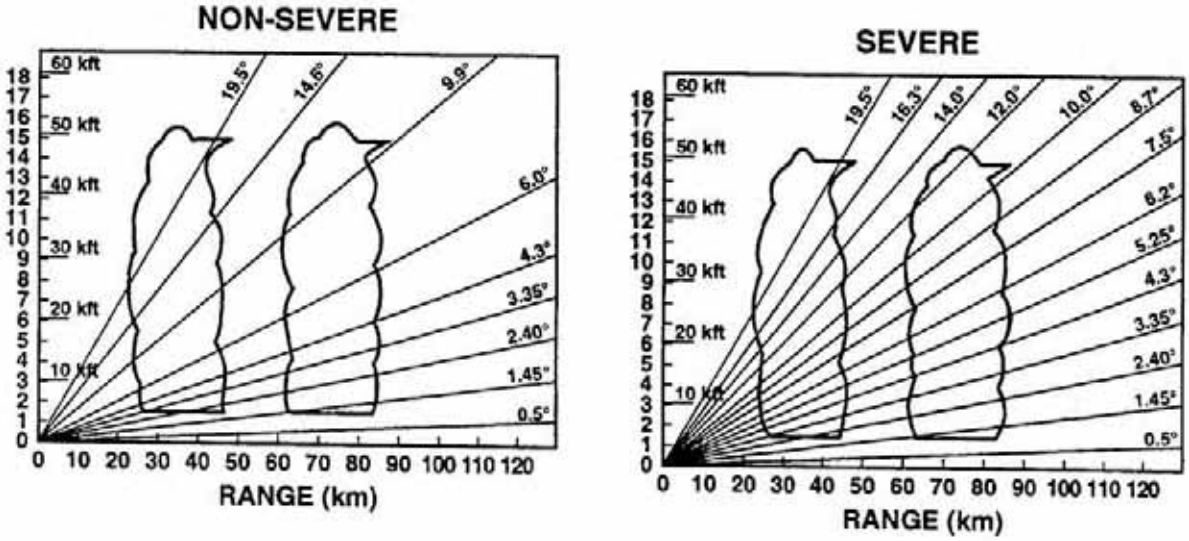

Figure 6. Comparison of NEXRAD scanning strategies in non-severe and severe weather conditions.

Our experience with LISDAD over two summers in Florida strongly supports the conclusions drawn by Howard et al. (1997): the life cycle of Florida thunderstorms is often not well depicted through the use of NEXRAD radar cloud top height because of frequent sampling limitations. Lightning observations therefore may provide an important role as an observation complementary to radar.

3.2.2. Lightning and Tornadoes

The theoretical basis for tornadogenesis–vortex stretching–is well established. Vertical vortex stretching, which is equivalent to the concentration of the angular momentum in the vertical, is proportional to the product of the vertical velocity gradient, dw/dz, and the radial gradient of horizontal velocity, du/dr. The ice skater analogy is applicable here: horizontally convergent air is the skater's arms drawn inward. Such action spins up the skater and spins up the vortex. The updraft (or downdraft) is essential here and this feature is believed to be a fundamental link between lightning activity and tornadogenesis.

Despite this theoretical understanding and a network of Doppler radars sensing radial velocity throughout the U.S., the accurate prediction of tornadoes in space and time remains problematic. What the radars do disclose is that the concentration of angular momentum from the synoptic scale to the mesoscale to the tornado scale is an episodic process (Burgess and Lemon, 1990). Furthermore the radar observations have shown that systematic variations in cloud top height (Donaldson, 1958,1962; Lemon, 1977; Adler and Fenn, 1981; Negri, 1982)–and by inference systematic variations in updraft velocity–are closely associated with the concentration of angular momentum (Burgess and Lemon, 1990). Based on the frequently observed in-phase relationship between total lightning activity and cloud top height (Byers and Braham, 1949; Frost, 1954; Williams, 1985; Goodman, et al., 1988; Stolzenberg, 1994; Tapia, et al., 1997), it is expected that total lightning activity will provide a quantitative indicator for mesocyclone spin-up and consequently a precursor to tornadic touchdown. Recent observations of total lightning

activity with the NASA space-based Optical Transient Detector (Buechler, et al., 1996) support this expectation. The latter study and the common report by severe storm chase teams that ground flashes are frequently absent in the vicinity of tornadic storm wall clouds and the tornado funnel are consistent with the idea that the extraordinary vertical development of these storms suppresses the ground flashes and amplifies the cloud flash rate (Williams, 1997). Hence there is a need for recording total lightning activity for the diagnosis of tornadic storms (MacGorman, 1993; Williams, 1997).

With the advent of Doppler radar, the radial Doppler couplet for the mesocyclone provides additional information on potential tornadogenesis, but this observation is still incomplete. The mesocyclone detection is in effect only one of two terms in the equation for vortex stretching. Furthermore, the false alarm problem remains. The concentration of angular momentum to form the mesocyclone frequently does not proceed to the formation of the smaller scale tornado on the ground. Burgess (1997) reports that only 30-50 percent of mesocyclones lead to tornadoes at the surface.

On the basis of the quoted observations and the foregoing discussion, two possible benefits from lightning in the tornado problem are identified. Both benefits are best achieved by merging total lightning observations with the radar observations. The first benefit is a possible improvement in lead time for tornado touchdown where the threat to life and property commences. This benefit is based on the information contributed by total lightning to the updraft term in the equation for vortex stretching. The second benefit is an expected reduction in the tornado false alarms based on radar mesocyclone detection alone. The lightning behavior may well be an important further discriminant of those mesocyclones that consistently progress to full-fledged tornadoes. This second benefit may be, equivalently, viewed as a capability to increase the probability for tornado detection while maintaining an acceptable false-alarm rate.

3.2.3. Total Lightning Benefit in the Severe Storm Context

The benefits accruing from space-based lightning observations need to be clearly identified before they can be quantified. In the case of severe storms, an immediate problem arose in the present study with the identification of benefits from total lightning for one simple reason: the literature is devoid of case studies in which the total flash rate is reliably documented over the lifetime of a severe storm. The literature on severe storm electrification has been recently reviewed (Williams, 1997). The available results demonstrate two facts: (1) the total flash rate in most severe weather is extraordinarily high, (2) the lightning activity is overwhelmingly dominated by intracloud activity not currently displayed by the NLDN.

The absence of more detailed information relating total lightning with severe weather is attributable to the difficulty with recording all lightning flashes with single sensors on the ground and the difficulty of sampling the severe weather on the ground in space and in time. Perhaps the most thoroughly documented example of total lightning (intracloud and ground flashes) in severe weather (and to be sure, this one has its limitations too) is the tornadic thunderstorm whose lightning was observed with the Optical Transient Detector (Buechler, et al., 1996).

The deficiencies noted above for ground-based documentation of total lightning activity in severe weather have been largely remedied over the past two years with the development of LISDAD (Section 2) and its utilization in an operational setting at the Melbourne WFO. With this new observational system, an ensemble of severe weather cases in Florida has been assembled which are showing consistent behavior.

The key LISDAD component in evaluating benefits from total lightning activity in severe storms is the LDAR system, whose accuracy and reliability in mapping lightning over a large area in Florida has been demonstrated for more than two decades (Lhermitte and Krehbiel, 1979; Krehbiel, 1981; Lhermitte and Williams, 1985; Nisbet, et al., 1990; Mazur, et al., 1997). LISDAD has also been very successful in the documentation of severe storms because it is generally operational in all weather and is monitored routinely by forecasters at the Melbourne NWS office who also acquire and document severe storm observer reports.

The operation of LISDAD is illustrated in Figure 7. Individual cells in NEXRAD radar observations are identified by the NSSL SCIT algorithm and are automatically circled on the display. The entire history of LDAR lightning flash rate, NLDN ground flash rate, and various radar measurables (maximum reflectivity, vertical integrated liquid water (VIL), radar cloud top height, etc.) for each cell are monitored and can be displayed in a "pop-up box" (in real time or in playback mode after the fact) as shown in the figure.

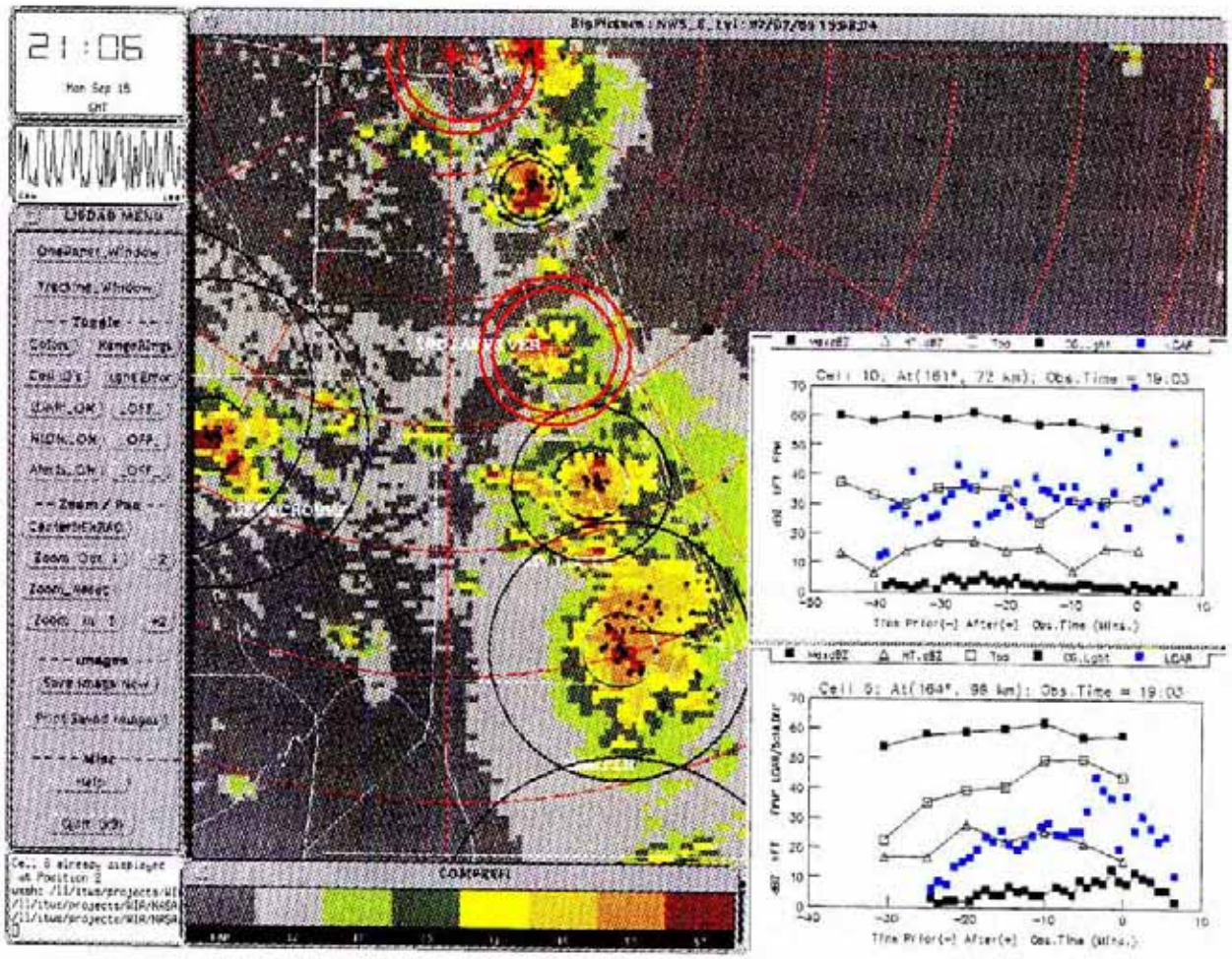

Figure 7. Operational LISDAD display at Melbourne, FL WFO.

LISDAD first became operational in August of 1996 but very little severe weather occurred late that summer. The histories of approximately 100 nonsevere thunderstorms were however documented and studied. Beginning in March of 1997 and extending into the summer months, numerous severe storms occurred which included examples of wind, hail and tornadoes, all of

which were documented in surface observer reports. The number of severe weather cases in July 1997 (31) far exceeded the number in July 1996. This ensemble of cases enabled the compilation of results presented here.

Figure 8 summarizes the distribution of peak flash rates (total lightning as observed by the LDAR system) for storms from 1996 and 1997. Both nonsevere and severe are included. The flash rates for the nonsevere cases are generally less than 60 flashes per minute (1 per second) and most commonly less than 10 per minute. In contrast, the flash rate for the severe cases are greater than 100 flashes per minute. There appears to be a "gray" area in the vicinity of 100 flashes per minute where the distinction between severe and nonsevere is not clearly decided on the basis of flash rate alone. Several storms also were documented and included in Figure 8 that displayed LDAR lightning flash rates in excess of 100 flashes per minute and for which no severe storm report was logged. If in fact these storms were not severe, they would present false alarms to a stand-alone lightning detection system. In some cases, the observed storms occurred over sparsely populated areas where severe weather may have been missed. This situation was not always the case, however. The largest single uncertainty in this substudy is the truthing on storm severity.

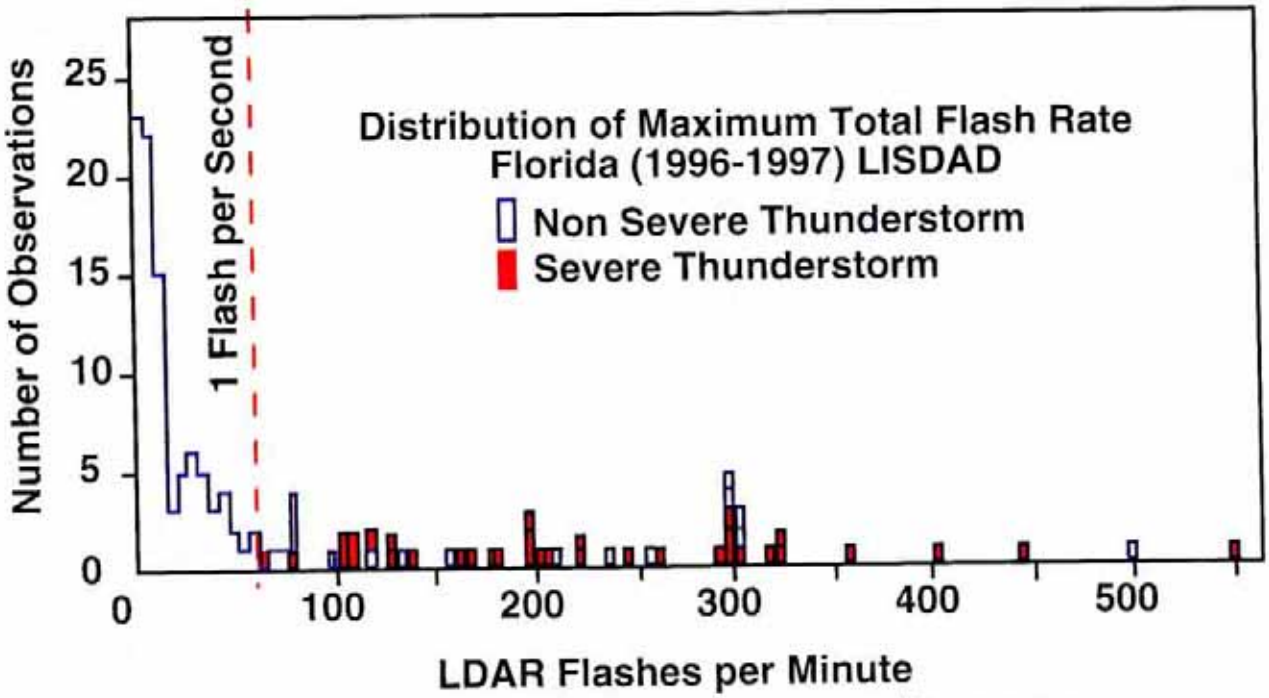

Figure 8. Histogram of maximum LDAR flash rate for nonsevere and for severe storms.

Table 3 tabulates the peak flash rates for the severe cases shown in Figure 8 and includes for comparison the maximum ground flash rate recorded by the NLDN. These values vary from 4 to 22 per minute and are invariably at least one order of magnitude less than the intracloud flash rate inferred from the LDAR observations.

Table 3.
LISDAD Severe Storm Summary

1997	Severe Weather Description	NSSL SCIT Cell ID#	Total Lightning: Peak LDAR Flash Rate (flashes/min)	LDAR Lightning 'Jump' (flashes/min/min)	Cloud-to-Ground Lightning: NLDN Peak Rate (flashes/min)	t_0 (UT)	t_1 (UT)	t_2 (UT)
April 23	tornado/hail	4	195	60	4	1237	1242	1320
May 22	1" hail/wind	5	290	75	5	1838	1849	1847-1852
June 13	nickel size hail	1	410	90	10	1852	2003	2110
July 1	dime size hail	9	106	62	4	2013	2017	2005
July 1	dime to quarter size hail	18	130	32	5	2033	2045	2045
July 5	wind damage	9	170	32	5	1707	1721	1730
July 6	waterspout	8	86	78	2	1829	1830	1842
July 6	wind damage; dime size hail	2	225	35	21	1938	1945	2001
July 7	golf ball hail	23	425	85	20	2334	2344	2350
July 8	nickel size hail	2, 5	180	50	10	1941	1947	1948
July 8	wind damage	19	170	32	8	2007	2027	2035
July 8	wind damage	19	120	20	6	2121	2131	2130
July 9	wind; quarter size hail	6, 11	215	50	5	1844	1850	1900
July 9	wind	1	60	30	2	1920	1922	1924
July 9	dime size hail	2	325	65	20	2132	2140	2143
July 9	quarter size hail	2	325	65	20	2132	2140	2208
July 11	tornado/water spout	4	170	50	8	1730	1746	1758
July 12	1.25 inch hail	12	200	44	8	2103	2117	2140
July 15	golf ball size hail	17	140	70	3	2033	2035	2058
July 16	dime size hail	10	116	22	3	2027	2030	2038
July 16	funnel cloud; wind	6	550	220	18	2323	2325	2330
July 29	golf ball hail	2	270	80	22	2112	2114	2124
July 31	dime size hail	14	300	60	1	2017	2032	2035
August 23	wind damage	2	270	100	8	1958	1959	–
August 23	wind	2	310	100	10	2032	2034	2030
1996								
August 10	wind	4	100	28	20	2204	2208	?
August 14	waterspout	14	44	21	5	1952	1954	2025
August 16	no severe weather report	2	240	70	10	2051	2054	no report
August 16		18	260	80	10	2040	2056	no report

t_0 = time of rapid increase in LDAR flash rate (the lightning 'jump')
t_1 = time of peak LDAR flash rate
t_2 = time of first observer report of storm severity

In addition to the extraordinary flash rates of the severe cases investigated with LISDAD there is a second distinguishing feature of the ensemble of severe storms which may be more important in the context of benefits. When the total lightning history is examined for the severe storm cases tabulated in Table 3, one finds sudden increases in the lightning rate–lightning "jumps"–a few minutes ahead of the peak flash rate and many minutes ahead of the severe weather report on the ground. These jumps, also tabulated in Table 3, are typically 30-60 flashes/min per minute and are easily picked out of the record as anomalously large derivatives in the flash rate. In only two of the cases in Table 3 did the jump time lag the time of surface detection of storm severity. An example of two lightning jumps prior to two severe weather episodes on the runways at Orlando International Airport on May 22, 1997 is shown in Figure 9.

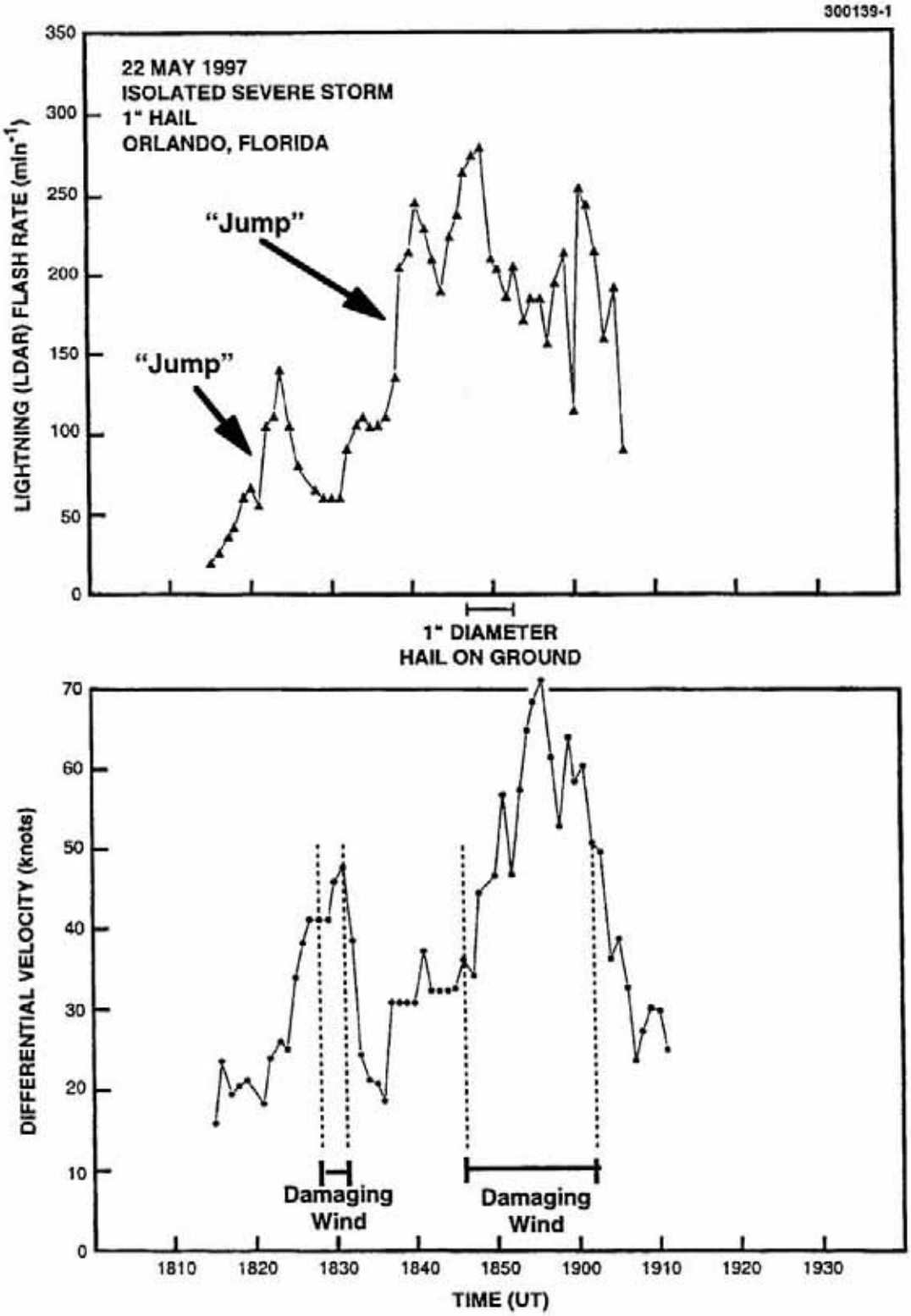

Figure 9. Evolution of LDAR flash rate (top) and differential radial velocity for a microburst-producing hailstorm on May 22, 1997.

Three specific times of interest are tabulated for all the cases in Table 3 in the right hand columns, where it is seen that the lightning "jump" time provides an advanced indication of severe weather, with a lead time ranging from 2 to 43 minutes. The possible importance of these LDAR "jump" times as a benefit for National Weather Service severe storm warning is shown in Table 4. Here are shown all LISDAD-documented cases of severe weather for which both the lightning "jump" time and the time of official severe weather warning were available. In most cases, the "jump" time led the official warning time by intervals ranging from 4 to 15 minutes.

Table 4.
LDAR Lightning "Jump" vs. Melbourne NWS Severe Storm Warning
(the latter issued on the basis of radar observations)

1997	Severe Weather Description	Time of LDAR Lightning "Jump" Time	Time of NWS Severe Storm Warning	Incremental Lead Time
July 1	dime size hail	2013 UT	2024 UT	11 min
July 5	wind	1707 UT	1711 UT	4 min
July 6	tornado	1829 UT	1842 UT	13 min
July 6	wind; dime size hail	1938 UT	2001 UT	23 min
July 7	golf ball size hail	2334 UT	2355 UT	21 min
July 8	nickel size hail	1941 UT	1937 UT	- 4 min
July 8	wind	2010 UT	2025 UT	15 min
July 9	wind; quarter size hail	1844 UT	1855 UT	11 min
July 9	quarter size hail	1859 UT	1855 UT	- 4 min
July 9	dime size hail	2057 UT	2109 UT	12 min
July 11	tornado/ waterspout	1730 UT	1744 UT	14 min
July 12	1.25 inch hail	2103 UT	2120 UT	17 min
July 16	funnel cloud; wind	2325 UT	2323 UT	- 2 min
July 18	quarter size hail	2159 UT	2203 UT	4 min
July 25	funnel cloud; wind	2257 UT	2303 UT	6 min
July 29	golf ball size hail	2112 UT	2114 UT	2 min
July 31	dime size hail	2014 UT	2026 UT	12 min
July 31	dime size hail	2017 UT	2026 UT	9 min
				Average 9 min

The physical basis for the lead time associated with the "jump" in total lightning flash rate in severe storms follows in the same vein as earlier findings on a total lightning precursor to microbursts in non-severe thunderstorms (Goodman, et al., 1988; Williams, et al., 1989; Laroche, et al., 1991; Malherbe, et al., 1992; Williams, et al., 1995; Stanley, et al., 1997). Graupel particles (as distinct from large hailstones) in the mixed phase region of the storm are responsible

for the charge separation that causes lightning. The updraft phase invigorates the growth of these ice particles. The downdraft which is likely responsible in different ways for severe weather on the ground, is forced by gravitational loading and evaporation of the condensate (both liquid and solid phase) which in turn is produced by the updraft. Therefore the severe weather on the ground naturally lags the intracloud lightning activity. The systematic lead times seen by McCann (1983) in satellite observations of V-signatures associated with overshooting tops are undoubtedly another manifestation of updraft-leading-downdraft and intracloud lightning-leading-severe weather.

Tornadoes receive special recognition in the severe weather context. The list of severe storms in Table 3 includes several tornadoes (and waterspouts), and additional attention was given to two of these cases (July 11 and April 23). Analysis of mesocyclonic shear in both cases showed evidence for mesocyclonic intensification in concert with a strong updraft and peak lightning rate, and a tornado on the ground associated with the descent of upper level vorticity and the decline in lightning rate. Here again the downdraft appears to be transporting angular momentum from the mesocyclone aloft down to the surface to make the tornado. A consistent scenario emerging from NOAA's studies of tornadoes in VORTEX (Rasmussen and Straka, 1996) includes the downdraft as a key feature in tornadogenesis at the ground.

One of the tornado cases in Table 3 (July 11, 1997) was not flagged as severe in real time on the basis of the radar observations. The storm did however show a high LDAR flash rate (170 per minute) and a lightning "jump." This circumstance supports the value of total lightning as an additional indicator of storm severity.

3.3. Benefits Model for LMS Severe Weather Warning

3.3.1. Lead Time Assumptions

Table 5 reproduces information from briefing charts provided by Don Burgess of the WSR-88D Operational Support Facility, Norman, Oklahoma. These summarize NWS severe weather and tornado warning accuracies and average lead times tabulated prior to and after implementation of the WSR-88D network. The standard meteorological definitions for probability of detection, probability of false alarm and critical success index pertain. The warning lead times tabulated are the average for the events that were detected. Note that tornado warnings were verified only against tornado reports but the severe weather warning figures allowed verification against reports of any form of severe weather (e.g., a hail warning would be validated by a damaging wind report, etc.). For subsequent benefits calculations, we will utilize the tabulated post-WSR-88D detection probability and warning lead time to represent current NWS warning performance.

Table 5.
Figures of Merit for National Weather Service Severe Weather Warnings, Pre- and Post-WSR-88D Implementation

	Probability of Detection	Probability of False Alarm	Critical Success Index	Average Warning Lead Time (min)
Tornado Warnings				
Before WSR-88D	0.40	0.76	0.12	4.7
After WSR-88D	0.58	0.74	0.20	7.6
Severe Weather Warnings				
Before WSR-88D	0.65	0.54	0.38	13
After WSR-88D	0.80	0.46	0.50	16

Table 4 in the preceding subsection provides a means for estimating the incremental lead time for severe weather warnings that might occur through observations of the total lightning jumps that have systematically preceded severe weather reports at our Florida LISDAD site. For the cases in this table, the point of highest total lightning derivative (i.e., "jump") preceded the Melbourne WFO's severe weather warnings (presumably issued based primarily on WSR-88D measurements) by an average of nine minutes. Personnel at the Melbourne WFO currently employ a five-sample (i.e., five-minute) moving window in estimating the lightning rate derivative during operations. This implies a 2.5 minute "processing" delay in detecting the jump. Thus, we assume that LMS' measurements would on average increase the current severe weather lead time by 6.5 minutes; that is, to 22.5 minutes. Burgess' data show that current tornado warning lead times average slightly less than 1/2 of that for all severe weather warnings. We assume that this same proportional reduction would apply to warnings issued using LMS data; thus, the lead time assumed with LMS for tornado warnings is 22.5 x (7.6/16) = 10.7 minutes.

The LISDAD program at Melbourne, FL has not been in operation long enough to provide clear indications of how much the total lightning data might increase the probability of detection for severe weather outbreaks. It is reasonable to expect that an independent measurement indicative of storm conditions likely to result in severe weather would indeed improve this metric but this remains to be proven. The importance of this point will be emphasized in subsequent discussion.

3.3.2. Tornado

Figure 10 illustrates the major elements of a simple model used to explore the value of more timely tornado warnings provided via monitoring of the "lightning jumps" observed to precede Florida severe weather episodes. This analysis is applied again (with different model parameters) in subsequent analysis of general "severe weather" warnings. We presume, in the tornado case, that the major potential benefit associated with improved warnings is reduction of human death and injury.

The tornado threat is modeled probabilistically as existing at a uniform level over 30 minutes–roughly equal to the time for the core of a severe thunderstorm system to approach and pass over a given point. Warnings are assumed to occur only during this threat period but their probability is "front loaded" so as to achieve average warning lead times (relative to tornado occurrence) consistent with the assumptions described above. Mathematically, the probability density of tornado warning time, t_w , is taken to be exponential:

$$p(t_w) = b\exp(-bt_w)/\{1-\exp(-30b)\} \qquad 0 < t_w < 30 \text{ minutes} \tag{1}$$

with the time origin corresponding to the beginning of the threat period.

The average lead time (LT) for tornado warnings

$$LT = \langle t_{torn} - t_w \rangle = \int \left\{ t_{torn} - t_w \right\} \; p(t_{torn}) \; p(t_w) \; dt_{torn} \; dt_w \tag{2}$$

is readily evaluated with the above assumptions for the probability densities of the tornado threat and the warning time. For a given value of LT, the decay constant "b" for the tornado warning time distribution is defined by equation 2. Warning time probability densities corresponding to the "current" and "with LMS" LT assumptions described above are shown in Figure 10.

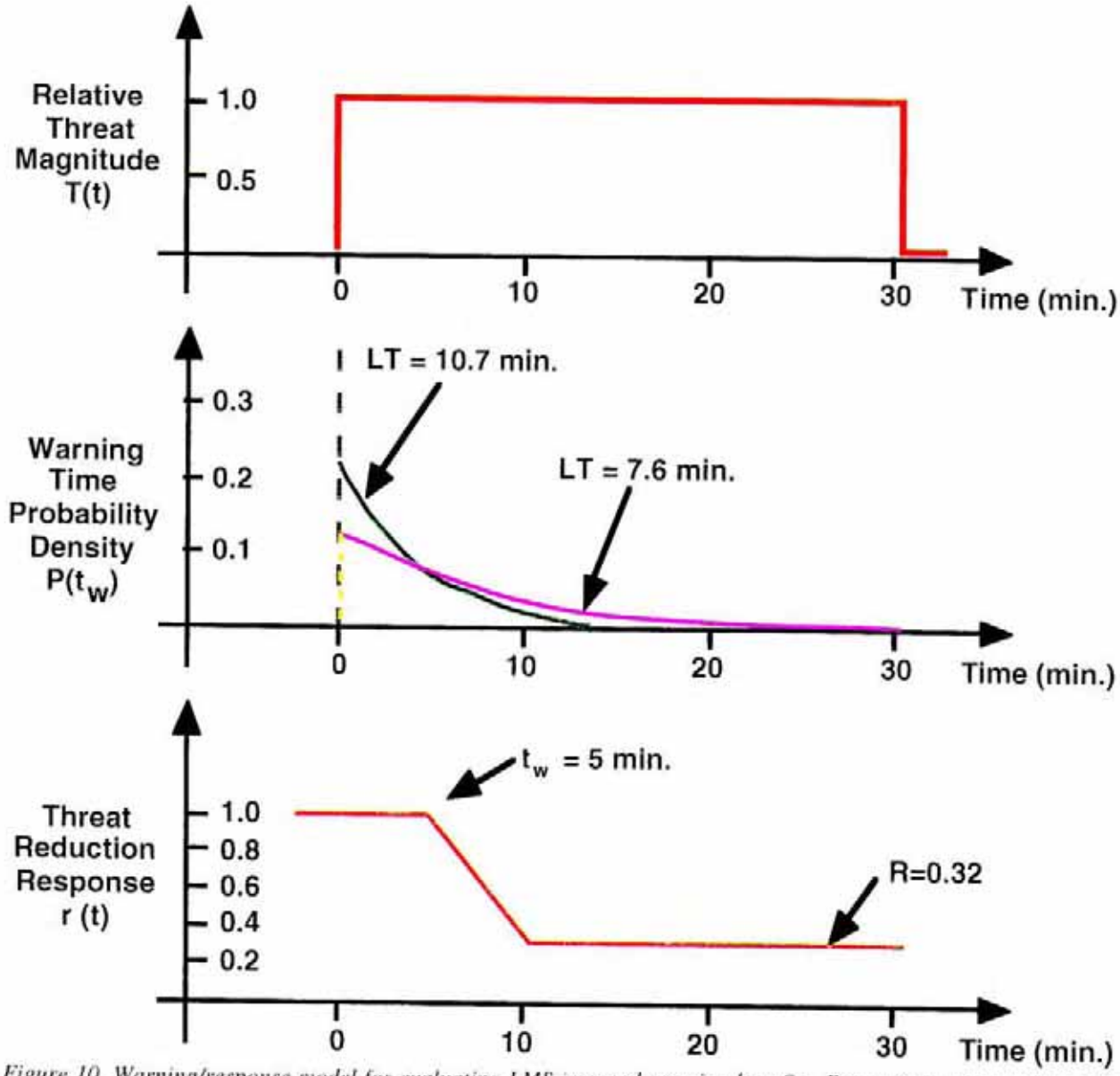

Figure 10. Warning/response model for evaluating LMS imposed warning benefits. Parameters are specific to the evaluation of tornado fatality reduction.

The bottom part of this same figure shows our model for the response "r(t)" individuals undertake to reduce their exposure to the tornado threat once a warning is received. We assume that over a five minute period following reception of the alarm, individuals reduce their average threat exposure linearly from full value (r(0) =1) to a (subsequently constant) residual level "R". The assumption of a relatively rapid response is plausible given the seriousness of the threat, and (in most cases) a presumably limited set of options for refuge. We assume a relatively optimistic value for the residual threat level "R" of 0.32; this is based on the assumption that 75 percent of the threatened public is made aware of the warning (Burgess, 1997) and that in 90 percent of cases, efforts at seeking shelter are effective in eliminating fatality.

Given the assumed distributions of warnings and subsequent responses, the fractional residual tornado threat is

$$FT = \int p(t_w)\ dt_w \int r(t - t_w)\ T(t)\ dt \Big/ \int T(t)\ dt \tag{3}$$

which through straightforward integration can be shown to equal approximately

$$FT = \frac{1}{30}\left\{[2.5 + 27.5R] + \frac{1}{b}[1 - R]\right\}. \tag{4}$$

Terms in the first square brackets on the right capture, respectively, the response transition time and the threat "pedestal" R which is present throughout the threat period in spite of the warnings. The second term captures the additional threat incurred during the initial period (1/b minutes) when the probability of having received a warning is relatively low. It is readily shown that this time constant for the warning probability distribution is approximately:

$$\frac{1}{b} = 15 - LT \tag{5}$$

for the case under consideration. Exact evaluation of fractional threat (FT) (for R=.32) gives values of 0.50 and 0.46 with the 7.6 min and 10.7 minute average lead times assumed without and with LMS, respectively.

Given the value of FT for current warnings and the 0.58 probability of detection for current tornado warnings it is straightforward to work backwards from current tornado deaths to what would be expected in the absence of warnings. This is shown in the first row of Table 6, given a current average tornado fatality toll of 44 per year. Forty-two percent of the tornadoes affecting this "baseline population" of victims will be missed with current detection technology; the numbers of fatalities for the remaining 58 percent are reduced by FT (0.5) for the current casualty tabulation (row 2). Application of the somewhat lower FT value calculated assuming LMS reduces fatalities only slightly if the probability of detection is unchanged (row 3). If however, we assume that probability of detection will rise with LMS implementation then a more substantial reduction in casualties is possible. The fourth row of Table 4 is calculated assuming that the LMS results in an increase in probability of tornado detection to 0.8.

In Table 7, we apply the same methodology to estimate tornado injury reductions that would result from improved warning timeliness and detection probability. The assumptions and modeling are identical to that described above except that a higher value for residual threat "R" is assumed, corresponding to greater likelihood that an injury (as opposed to a fatality) will occur in spite of an individual's responding to a warning. Here we set R equal to 0.55, corresponding to the previous assumption that 75 percent of the threatened population receives a warning and, in this case, that their actions are effective 60 percent of the time in preventing injury.

Table 6.
Tornado Fatality Reduction Calculations for Current Warning System and for Improved Lead Times and Probability of Detection Based on Use of LMS

		Fatalities		
Scenario	Fractional Threat Reduction (FT)	Missed Tornadoes	Detected Tornadoes	Total
Baseline (No Warnings)	–	26	36	62
Current ($P_d = 0.58$)	0.50	26	18	44
Current+LMS ($P_d = 0.58$)	0.46	26	17	43
Current+LMS ($P_d = 0.8$)	0.46	12	23	35

Table 7.
Tornado Injury Reduction Calculations for Current Warning System and for Improved Lead Times and Probability of Detection Based on Use of LMS

		Injuries		
Warning Scenario	Fractional Threat Reduction (FT)	Missed Tornadoes	Detected Tornadoes	Total
Baseline	–	520	718	1238
Current ($P_d = 0.58$)	0.67	520	480	1000
Current+LMS ($P_d = 0.58$)	0.63	520	451	971
Current+LMS ($P_d = 0.8$)	0.63	248	622	870

3.3.3. Severe Weather Warnings

As noted previously, severe weather warnings (other than tornado warnings) are aimed not only at preventing loss of life from wind-driven projectiles and falling trees, but at reducing property damage. In estimating the magnitude of this benefit, we apply the modeling

methodology discussed above, with modified parameters to capture expected differences in threat duration and the effectiveness of the response. We set the threat period equal to 1 hour under the assumption that hail and damaging straight line winds generally occur over larger areas and for longer duration than tornadoes on the ground. Lead time assumptions for severe weather warnings are, as described above, set at 16 minutes for the current system and 22.5 minutes with the addition of LMS. With respect to death and injury prevention, we again assume a 5 minute response period following reception of a warning and presume in both cases that the simple act of going indoors largely eliminates possibility of casualty. Thus we set "R" equal to 0.25 under the assumptions that 3/4 of the threatened population will receive the severe weather warning and that their responses, when completed, will be completely effective in reducing the possibility of casualty. Tables 8 and 9 summarize these calculations in the format described above. In the fourth column of each table, we treat the case where LMS data are assumed not only to increase the timeliness of the warning but also to increase the overall probability of a warning being issued from 0.8 to 0.9.

Table 8.
Thunderstorm Wind Fatality Reduction Calculations for Current Warning System and for Improved Lead Times and Probability of Detection Based on Use of LMS

		Fatalities		
Warning Scenario	Fractional Threat Reduction (FT)	Missed Severe Weather	Detected Severe Weather	Total
Baseline	–	10	41	51
Current ($P_d = 0.8$)	0.41	10	17	27
Current+LMS ($P_d = 0.8$)	0.37	10	15	25
Current+LMS ($P_d = 0.9$)	0.37	5	17	22

Table 9.
Thunderstorm Wind Injury Reduction Calculations for Current Warning System and for Assumed Lead Time and Probability of Detection Improvements with Use of LMS

		Injuries		
Warning Scenario	Fractional Threat Reduction (FT)	Missed Severe Weather	Detected Severe Weather	Total
Baseline	–	166	666	832
Current ($P_d = 0.8$)	0.41	166	274	440
Current+LMS ($P_d = 0.8$)	0.37	166	245	411
Current+LMS ($P_d = 0.9$)	0.37	83	276	359

Comparison of Tables 8 and 9 to the tornado casualty results discussed previously illustrates one of the model's sensitivities. In the case of the thunderstorm winds threat, the assumption that more effective responses to warnings are possible (i.e., "R" and "FT" are lower) results in a larger benefit for incremental improvements in the warning lead time and/or probability of detection.

Finally, we apply the model to estimation of property damage reduction that would result from earlier actions to remove cars, boats, livestock, etc. from the full force of hail and/or thunderstorm winds. The tornado-related property damage tabulated in Table 1 is not included in our "current total" under the assumption that it is largely unavoidable. For hail and thunderstorm winds, we assume that reduction of property exposure to severe weather requires a greater time period (20 minutes) than protecting oneself, and that the residual threat level "R" is high owing to the fact that the majority of exposed property cannot be removed from harm's way. We have assumed again that 75 percent of the public receives issued severe weather warnings and that their responses eliminate damage risk to 10 percent of exposed property. Thus, we set R equal to 0.925 for the calculations summarized in Table 10.

Table 10.
Hail and Thunderstorm Wind Property Damage Reduction Calculations for Current Warning System and for Improved Lead Times and Probability of Detection Based on Use of LMS

		Property Damage ($M)		
Warning Scenario	Fractional Threat Reduction (FT)	Missed Severe Weather	Detected Severe Weather	Total
Baseline	-	215	858	1073
Current ($P_d = 0.8$)	0.950	215	815	1030
Current+LMS ($P_d = 0.8$)	0.946	215	812	1027
Current+LMS ($P_d = 0.9$)	0.946	107	914	1021

3.4. Discussion

Overall, our analysis indicates that total lightning data provided by LMS may provide a valuable input for NWS severe weather warning responsibilities, and that the associated benefit to the public in terms of reduced fatalities, injuries and property damage would be worthwhile. Depending on whether or not LMS is assumed to produce improvements to the probability that warnings will be issued (P_d) , the aggregate incremental yearly benefits are modeled to vary from 3 to 14 fatalities, 58 to 211 injuries, and $3M to $9M in property damage. Interviews with cognizant researchers at the WSR-88D Operational Support Facility, the National Severe Storms Laboratory and other organizations, as well as the operational experience using total lightning data at the Melbourne, FL WFO were consistent with this generally optimistic view towards potential benefits.

Additional investigations of several technical issues are key to placing this assessment on more solid ground. Crucial to our benefits assumptions is the capability of LMS to detect and resolve the extremely high-rate lightnings observed in thunderstorms that subsequently produced severe weather at our Florida LISDAD site. Lightning rates exceeding 400 per minute imply flash durations of roughly 100 milliseconds or less, with large duty cycles. It is reasonable to ask whether these fall within the normal range of lightning luminosities, and whether the multiple individual flashes that would occur within the time interval normally spanned by a single flash will be resolved by LMS. We recommend that resolution of this question be a key objective for measurements using the LMS prototype currently flying on the Tropical Rainfall Measuring Mission (TRMM).

"Lightning jumps" (i.e., large derivatives in lightning rate) are viewed as a key signature in supporting better severe weather warnings. These are presumably part-and-parcel of the episodic updraft dynamics that cause thunderstorms to transition from non-severe to severe status. The

physics of these jumps needs to be placed on solid footing in order to reliably infer severe weather based on their occurrence. Continued, in-depth analysis of the LISDAD cases identified here, supplemented by storm dynamic and electrical modeling, is recommended to address this issue.

Benefits increased significantly with the assumption that LMS could not only improve average lead time, but could result in measurable improvements in the probability (P_d) that warnings would be issued for severe weather outbreaks. A significantly greater database and more operational experience than we have been able to acquire in just two years of operational testing at Melbourne, FL are required to resolve this issue. It is reasonable to speculate that lightning rate "jumps," or very high absolute rates, could cue forecasters to issue warnings for cells where radar indications might not put them over the "decision threshold". Balancing this optimism, however, is the concern that false alarm rates might be excessive for severe weather warnings issued primarily on the basis of the lightning data.

Recent statistics from NWS Weather Forecast Offices in locales where severe weather is frequent suggest that increasing skill in utilization of the WSR-88D and other new technology has increased the detection probability and lead time for tornado warnings at these stations. For example, Dodge City, KS, Houston, TX and Tulsa, OK all report probability of detection for tornadoes of 0.8 or greater for 1995-1996, the last two years for which statistics are available. Corresponding tornado warning lead teams for these stations vary from 11 to 17 minutes. While these samples are clearly too small to infer a national trend, we recognize that enhancements to existing severe weather sensors (for example, improved WSR-88D algorithms and scanning strategies), and increasing forecaster skill in interpreting their data may well improve warning statistics over the coming years. Such improvements to the lead time and detection probability of the "current system" may reduce the incremental benefit attributable to LMS.

4.0. THUNDERSTORM FLOOD

4.1. Current Costs to Society

The 1990-1995 average for National Weather Service statistics on thunderstorm ("flash") flood casualties and damage is shown in Table 11. Table 12's decadal averages for total flood fatalities (of which flash flood victims constitute the majority) do not show a clear trend: population growth in areas subject to flood hazard is likely off-setting the benefits of improved education, stream monitoring and warning functions.

Table 11.
Flash Flood Casualties and Property Damage, from NWS Natural Hazards Statistics, 1990-1995 Averages

Fatalities	Injuries	Property Damage
63	41	$ 555 M

Table 12.
Average Annual Flood Fatalities by Decade, from 1940-1991

Years	Flood Fatalities (per year)
1940-1949	144
1950-1959	79
1960-1969	121
1970-1979	182
1980-1989	110
1990-1991	102
Average Annual Fatalities (51 years)	114

In the context of LMS benefits, an important question is the proportion of the toll that is incurred in mountainous terrain where radar coverage may be inadequate for warning generation owing to beam blockage, necessity of siting the radar on elevated terrain, etc. Figure 11 shows the breakdown of flash flood fatalities by state for the above period. About 15 percent of the fatalities occurred in the Western Mountain states, where beam blockage is most likely to be a significant issue. Other portions of the country (e.g., the Appalachians) also may be subject to radar beam blockage, albeit over more limited areas.

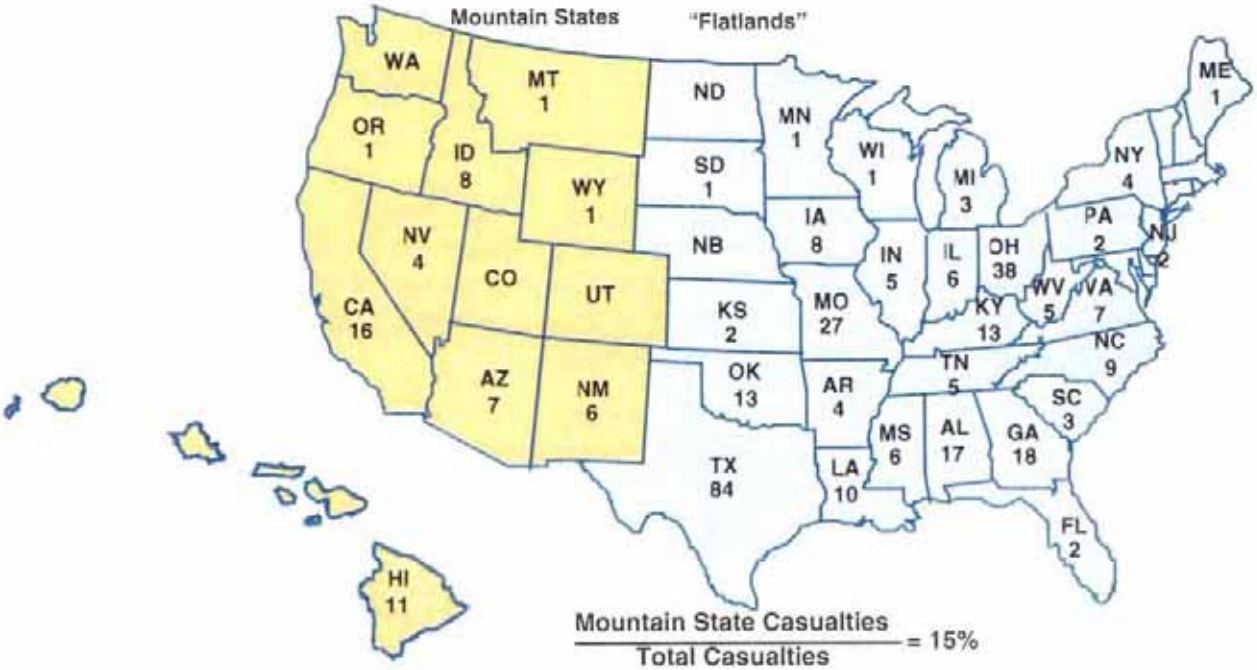

Figure 11. Fatalities attributed to flash floods during the period 1990-1995.

4.2. Technical Basis for Benefit

In principle, the NEXRAD S-band radar network should be capable of providing accurate areal rainfall measurements needed for flash flood forecasts with sufficient lead time for the evacuation of people and property. In practice, the mountainous terrain characteristic of the Western U.S. can cause radar beam blockage at low elevation angles and substantial underestimates of the areal rainfall. Interviews with Western Region National Weather Service personnel as part of this study emphasized the importance of this issue. The Tucson, AZ WFO for example, has significant radar beam blockage and/or low-altitude coverage gaps over 35 percent of its area of responsibility. To a person, the WFO personnel interviewed expressed enthusiasm for use of lightning data as a "gap filler" in fulfilling their operational responsibilities. Many, however, have only recently received capable real-time displays of data from the NLDN via a Western Region headquarters initiative; as a result, the forecasters indicated that the data were not currently being used in a quantitative manner. A NOAA Technical memo by McCollum, et al., (1996) provides a good overview of NLDN usage at the Tucson WFO.

Quantitative evidence for the importance of beam blockage in estimating rain rate has recently surfaced in an extensive comparison of NEXRAD-radar measured precipitation and rain gage totals across the U.S. by S.J. Vollrath in the Parsons Laboratory in MIT's Department of Civil and Environmental Engineering. Table 13 shows the results on radar/rain gage bias (in percent) for comparisons in four major time zones for the Spring months of 1994. Negative bias indicates that the radar reads low in comparison to the gages.

Table 13.
Percentage Bias of Radar Versus Rain Gage Estimates of Precipitation

Region	Percent Bias
Eastern	6.2
Central	0.4
Mountain	-60
Pacific	-67

The average negative bias in the time zones with mountainous terrain is an order of magnitude greater than for the Eastern and Central zones, suggestive of beam blockage effects.

The use of lightning flash counts as a proxy measure for rainfall has been explored in numerous studies (Battan, 1965; Kinzer, 1974; Grosh, 1978; Maier, et al., 1978; Piepgrass, et al., 1982; Goodman and Buechler, 1990; Buechler, 1990, 1994; Williams, et al., 1992; Petersen and Rutledge, 1996; and Tapia, et al., 1997). These studies have demonstrated consistent proportionality constants between rainfall and lightning flash counts for convective weather (of the kind responsible for flash floods). All but two of the above studies have made use of ground flash data, and the currently operational National Lightning Detection Network is available to fill radar gaps for precipitation measurement.

Is there an additional benefit to using total lightning measurements from space to achieve this goal? Almost certainly, from the standpoint that intracloud lightning is the more prevalent lightning type, but this additional benefit is difficult to quantify. Few studies have been done that compare ground flashes and total flashes as a proxy for rainfall (Grosh, 1978; Goodman and Buechler, 1990; Chèze and Sauvageot, 1997). The excellent study of Piepgrass, et al., (1982) uses total lightning as measured with an extensive network of field mills and rainfall with a similar distribution of rain gages. The rainfall/flash rate comparisons are very tight even on one minute time scales, but there are no comparisons with the ground flashes alone. In the storms in the West responsible for flash floods, it is likely that both intracloud lightning and ground flashes will be prevalent, leading to only marginal additional benefit from the total lightning observations.

4.3. Benefits Model for Thunderstorm Flood

The major benefit for LMS in this category is taken as its "gap-filling" capability in areas of poor radar coverage. Using digital terrain data and WSR-88D locations, we estimated that approximately 25 percent of the area of the high-plains and west coast states would experience sufficient beam blockage to call into question the ability to issue reliable flash flood warnings based on the radar data alone. Although such areas are often remote from population centers (i.e. the percentage of the western states' population not well covered by WSR-88D may be smaller), the ability of water to move quickly through drainage basins in steep terrain makes this fraction a reasonable estimate for the proportion of flood-inducing thunderstorms that may elude the radar

net. If we assume a 0.8 probability for issuing a flash flood warning when radar coverage is adequate, the overall flash flood warning P_d for this portion of the country is 0.75 x 0.8 = 0.6.

In areas not adequately covered by radar, we assume that some fraction of flood-inducing thunderstorms could be warned for based on monitoring of lightning from either the current NLDN, or from LMS. Although comparisons of CG versus total lightning-based rainfall estimates have not been decisive (see above), it is reasonable to speculate that the "richer" signature provided by the total lightning measurements could yield a higher effective P_d. An incremental benefit for LMS in flash flood warning will be estimated using the somewhat arbitrary assumptions that the "stand alone" flash flood warning P_d's for NLDN and LMS are respectively 0.5 and 0.7. With these, the overall P_d for flood warnings in the mountainous states becomes 0.75 x 0.8 + 0.25 x 0.5 = 0.73 with NLDN and 0.75 x 0.8 + 0.25 x 0.7 = 0.78 with LMS.

The 1990-1995 flash flood casualty data discussed above indicated that 15 percent of the fatalities occurred in states where radar beam blockage may be an issue. We will use this fraction in reducing the initial casualty and property damage base for estimating the incremental benefits of NLDN- and LMS-based "gap filling."

The benefits estimation approach is that discussed previously in the context of severe weather warnings (see Figure 10 and associated discussion). Parameters necessary for the model were set based on discussions with Western Region NWS personnel and through analysis of media accounts of flash flood casualties in Albuquerque, NM where one of the authors maintains an FAA sponsored weather radar field site. Flash flooding may begin following 20 to 30 minutes of sustained heavy precipitation over a suitable drainage region. The duration of the multi-cell thunderstorms responsible is typically about 1 to 1-1/2 hours and subsequent run-off times may span an additional 1/2 to 1 hour. Thus, it is reasonable to set the overall threat period as two hours. Average warning lead time was taken as 30 minute, whether issued based on radar or lightning data.

Flood warnings are typically issued through local television stations, some commercial radio stations (we estimate 50 percent) and by public service personnel. Relative to severe weather warnings, the fraction of threatened individuals who receive warnings is probably lower and some may not recognize that their current location and/or intended travel path place them in harm's way. For these reasons, we set the threat residue level "R" relatively high–0.5–although we again assumed that when threat avoidance responses were initiated, they could be completed within the five-minute period assumed in the severe weather context.

Tables 14 and 15 summarize estimated annual national flash flood fatalities and injuries for the various warning scenarios, using the 1990-1995 tabulations for the current totals. The format is similar to that used previously in discussing severe weather warning benefits, except that an additional column ("Fatalities/Injuries Non-Western States") has been inserted to make explicit that 85 percent of the current casualties are assumed to occur in areas where the lightning-sensor gap-filling role is not applicable and are therefore excluded from the benefit analysis.

Property damage estimates are shown in Table 16. The assumptions are as above except that the residual threat "R" has been set to 0.57. This value is based on Figure 12. The figure shows that 87 percent of flash flood fatalities during our 1990-1995 reference period occurred in vehicles or boats; that is, property that can be moved out of harm's way. We will use this fraction as an estimate for the percentage of flash flood property damage that is avertible, although we

recognize that the circumstances leading to human casualties from flood may differ on average from those leading to property damage. Combined with our previous estimate that half of affected individuals are aware of issued warnings, we arrive at the stated value for "R."

Table 14.
Annual Flash Flood Fatalities for Current Warnings, Warnings Supplemented by NLDN and Warnings Supplemented by LMS

		Fatalities			
Warning Scenario	Fractional Threat Reduction (FT)	Non-Western States	Western States (Flood Warning Not Issued)	Western States (Flood Warning Issued)	Total
Baseline	–	83	5	7	95
Current (P_d = 0.6)	0.60	54	5	4	63
Current+NLDN (P_d= 0.73)	0.60	54	3	5	62
Current+LMS (P_d=0.78)	0.60	54	3	5	62

Table 15.
Annual Flash Flood Injuries for Current Warnings, Warnings Supplemented by NLDN and Warnings Supplemented by LMS

		Injuries			
Warning Scenario	Fractional Threat Reduction (FT)	Non-Western States	Western States (Flood Warning Not Issued)	Western States (Flood Warning Issued)	Total
Baseline	–	54	3	5	62
Current (P_d = 0.6)	0.60	35	3	3	41
Current+NLDN (P_d = 0.73)	0.60	35	2	4	41
Current+LMS (P_d=0.78)	0.60	35	2	4	41

Table 16.
Annual Flash Flood Property Damage ($M) for Current Warnings, Warnings Supplemented by NLDN and Warnings Supplemented by LMS

Warning Scenario	Fractional Threat Reduction (FT)	Property Damage Non-Western States	Property Damage Western States (Not Warned)	Property Damage Western States (Warned)	Total
Baseline	–	667	42	63	772
Current (P_d = 0.6)	0.66	472	42	41	555
Current+NLDN (P_d = 0.73)	0.66	472	28	51	551
Current+LMS (P_d=0.78)	0.66	472	23	54	549

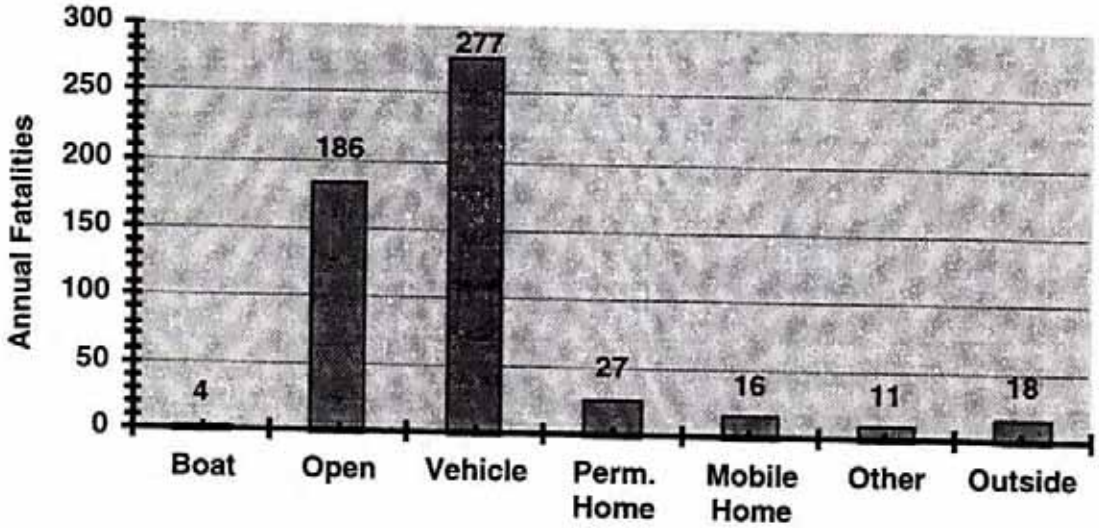

$$\frac{\text{vehicle + boat}}{\text{vehicle+boat+perm. home+mobile home}} = 87\%$$

Figure 12. Annual Flash flood fatalities by location of victims, 1990-1995.

4.4. Discussion

Incremental benefits for LMS in reducing casualties and damage from flash flooding were estimated to be relatively low. This is a result of:

1. Assumptions that led to a relatively low estimated proportion of total flash flood casualties and damage that could benefit through the filling of radar coverage gaps; and

2. The assumed partial capabilities of the existing NLDN which claim much of this already reduced "benefits pool".

Several of our assumptions could be refined through a more thorough investigation of casualty/damage statistics, radar coverage patterns and flash flood scenarios than could be accomplished within the scope of this study. Equally important in improving this benefits analysis would be quantitative comparisons of rain rate estimation from total lightning versus NLDN ground strike measurements and continued mesoscale model lightning assimilation studies of the type pioneered by Alexander, et al. (1997). Solid estimates of the differential warning P_d and/or lead times realized through measurements of total lightning would be invaluable. The analysis presented emphasizes, however, that the improvements must be shown to be large if a significant operational benefit in the flash flood warning area is to be realized.

5.0. AVIATION WEATHER

5.1. Introduction and Existing Sensor Description

In this section we examine the potential benefits to aviation of the Lightning Mapping Sensor. Three natural benefits categories are considered: Terminal, Enroute, and Oceanic. Terminal and Enroute both refer to operations over the continental United States, and Oceanic refers to international operations of U.S. air carriers, both over ocean and over other countries (e.g., through Central and South America).

We first examine the coverage of convective storms by existing sensors. Coverage of the storm volume and tops is most relevant to enroute flight, and coverage of low-altitude wind shear hazards (e.g., microbursts) is most relevant to terminal operations.

5.1.1. NEXRAD

Not all parts of the continental United States have equal coverage by the NEXRAD network (National Research Council (NRC), 1995). To provide accurate indications of storm structure required to determine the severity of a storm, the NEXRAD algorithms must have good "three-dimensional" coverage in a region. Figure 13 shows schematically our assumed coverage requirements.

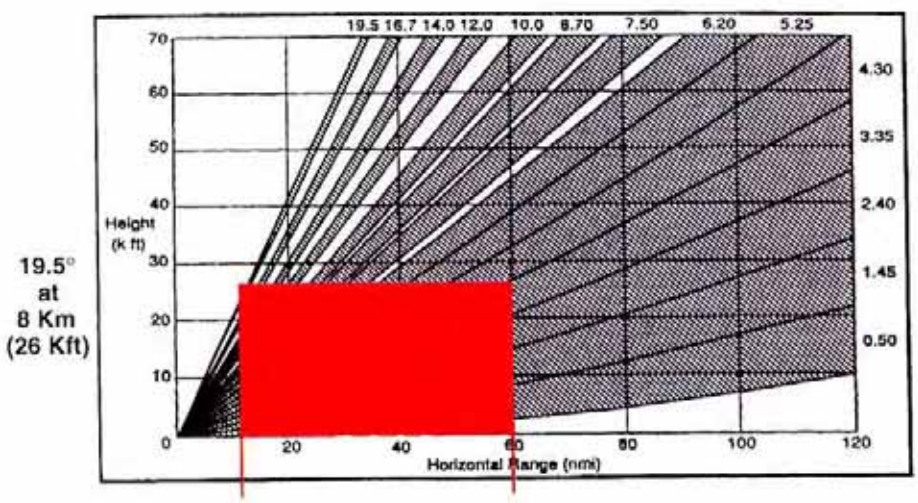

Figure 13. Schematic showing the NEXRAD Severe Weather Mode scan and our adopted definition of "three-dimensional" coverage: coverage by at least 4 different beams to 8 km altitude. At short range, the "cone-of-silence" will prevent 3-D coverage, and at long range, with curved earth calculations, fewer than 4 beams will provide coverage below 8 km (adapted from Howard, et al., 1997).

For a region to have good three-dimensional coverage, we require it to have vertical coverage to 8 km by at least the 4 lowest radar beams, which provide contiguous coverage to 3.5°. This definition leads to a gap in coverage over the radar in the cone-of-silence, where the top angle (19.5°) intersects 8 km altitude. It also leads to a maximum range of coverage defined by the intersection of the 3.5° beam (or the fourth beam from the bottom) with 8 km altitude. Figure 14 shows a map of this "three-dimensional" coverage to 8 km for the continental U.S. Our calculations show that **61 percent** of the CONUS is covered under these requirements.

Figure 14 . NEXRAD three-dimensional coverage envelope as described in text.

NEXRAD radars could also be used for low-altitude wind shear protection (e.g., microbursts and gust fronts), but the FAA-developed algorithms for detecting and predicting these phenomena have never been added to the NEXRAD system. The NWS meteorologists can usually spot the phenomena, but the volume update rate of 5-6 min precludes very timely detections of microbursts needed for aviation. It should be possible to use NEXRAD to predict microbursts by identifying precursory features aloft.

5.1.2. TDWR and ASR-9

The FAA TDWRs and ASR-9 radars provide additional storm coverage for the nation's top terminal areas. The ASR-9 radars with their fan beams provide a vertically-integrated measure of storm reflectivity with a rapid update rate of 30 s. A Doppler processor (Weather Systems Processor or WSP) will be added to approximately 35 ASR-9s. The TDWR scans the volume over the airport in 2-3 min. The TDWR and ASR-WSP provide Doppler radar coverage of low altitude wind shear at 1 min or better update rate over the airport. Figure 15 shows the location of all the FAA weather radars, compared with the region of NEXRAD 3-D coverage.

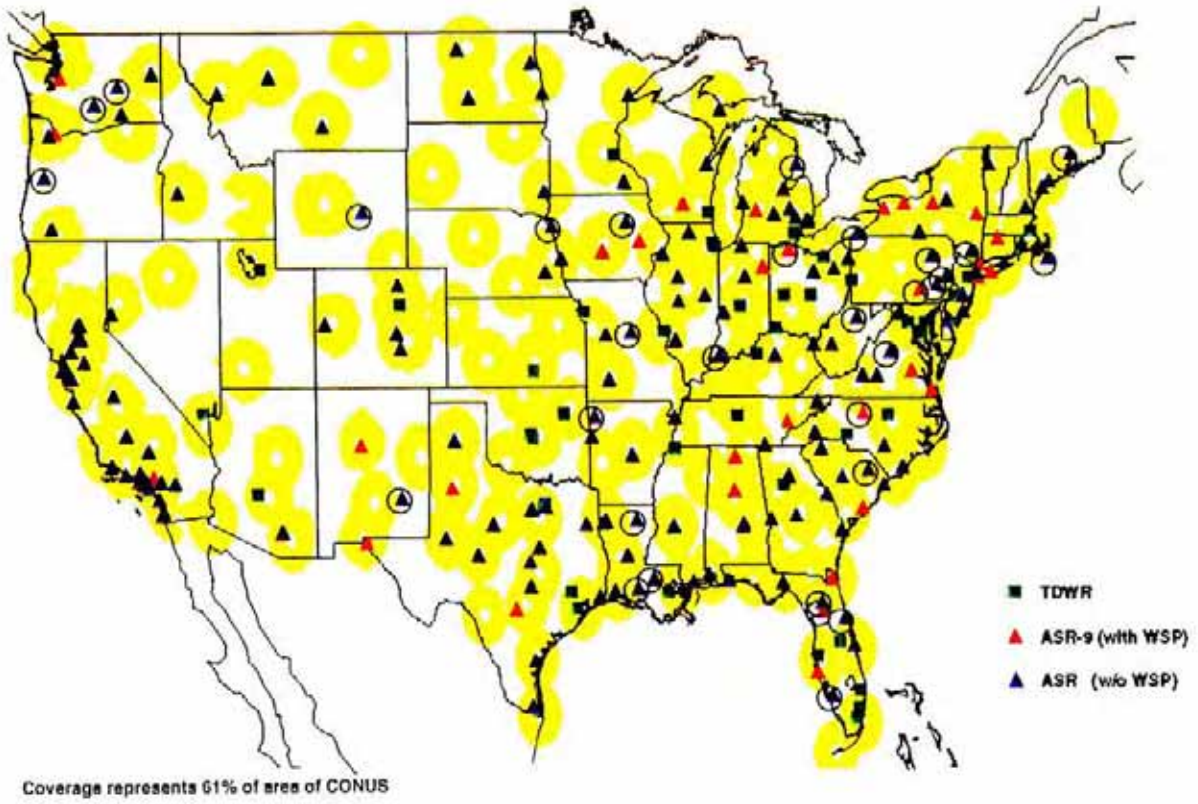

Figure 15. Locations of FAA wind shear detection radars (TDWR and ASR-9 with WSP) and weather reflectivity radars (ASR without WSP) relative to NEXRAD three-dimensional coverage envelope.

5.1.3. NLDN

The NLDN coverage is shown in Figure 16. Near uniform coverage exists over the lower 48 states, and extends 400 km offshore. Because of diurnal variations in the propagation of the signal, oceanic coverage at night can extend out to 4000 km offshore (Mosher, 1997), but the detection efficiency falls off sharply with range from the coast.

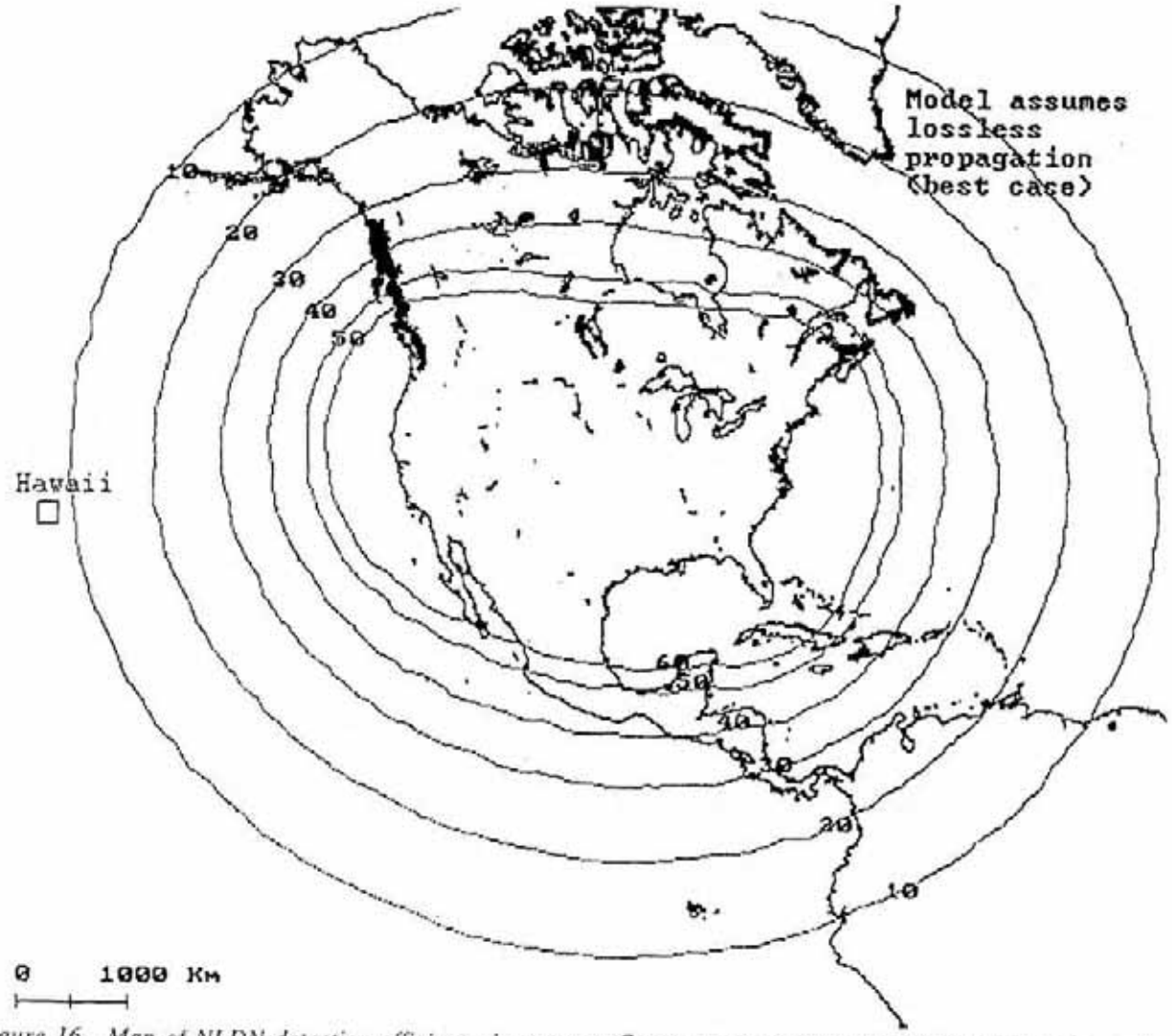

Figure 16. Map of NLDN detection efficiency in percent. Contours are in intervals of 10 percent (figure from Global Atmospherics, Inc.).

5.1.4. Geostationary Satellite

Geostationary satellite coverage is very helpful in determining broad regions of convective weather. However, since the highest cloud layer is sampled by the imager, convection below upper level clouds (e.g., anvil blow-off) cannot be seen. The GOES satellites do provide oceanic coverage, and constitute the primary means by which weather over the oceans is monitored today.

5.1.5. Airborne Weather Radar

Almost all air carrier flights are equipped with some kind of on-board weather radar capable of being scanned. Pilots use these data extensively in picking their way around storms enroute. The radars are typically capable of looking ahead over 150 miles, but attenuation from intervening heavy rain can cause severe underestimation or complete blockage of the signal from storms at longer range.

5.1.6. Visual Detection

One final method for aviators to determine the location and extent of convective weather is through visual cues. During daylight hours, storm tops can readily be seen, as can the storm cores as long as they are not embedded.

5.2. Technical Basis for LMS Benefits to Aviation

5.2.1. Proxy for Radar Reflectivity

Forecasters at the Aviation Weather Center (AWC) in Kansas City that create the Convective SIGnificant METeorological (SIGMET) product claim the National Lightning Detection Network (NLDN) ground strike data are perhaps their most valuable, ranking the national mosaics of NEXRAD data a close second (McCann, 1996). The ground strikes clearly indicate the storm regions AWC feels are significant for enroute flight and ultimately places under Convective SIGMET advisories. Many of the airlines use lightning information to alert flight crews of weather in advance of their picking it up on their airborne radars, allowing dispatchers to suggest efficient reroutes. Qualley (1997) suggested that the NLDN data are the most widely used weather tool in the domestic Flight Dispatch area at American Airlines.

Aviation users of NEXRAD data receive their information from private vendors in the form of national mosaics. "Composite Reflectivity" made by mapping the largest reflectivity value found at any altitude in a column is commonly used, but it is susceptible to contamination from ground clutter, AP, etc., and under-represents large, tall storms. The surface (or 1 km) reflectivity mosaic does not give pertinent information for altitudes above 18 Kft. We believe the best choice for mosaic is Vertically Integrated Liquid Water (VIL), derived by converting the effective radar reflectivity to its liquid water equivalent, and then summing the water content in each column. VIL provides a two-dimensional representation of the entire three-dimensional storm water mass. VIL has been shown to be highly correlated with total flash rate.

The other radar-based product of key importance to aviators is the Echo Tops map. The Echo Tops field is particularly important to national enroute flights, since areas of high echo tops define regions which commercial air carrier flights must either fly over or deviate around. The national mosaic of Echo Tops is subject to ring-shaped artifacts stemming from the NEXRAD scan strategy, and is only accurate where the radar coverage actually "tops" the storms. The discussion and figures in Section 3.2.1. emphasize these limitations of the NEXRAD echo tops field and identify the very strong correlation between cloud top height and total lightning flash rate for storms with tops above about 5 km.

We chose to clarify the applicability of lightning data as a proxy for radar reflectivity (or derivative parameters of reflectivity) by performing a two-dimensional image analysis over time. We selected three cases from LISDAD for study: one case from 1996 containing air mass storms typical of Florida summers, and two springtime cases from 1997 containing severe storms. The dates and times analyzed are given in Table 17.

Table 17.
Dates, Times, and Description of LISDAD Cases Analyzed

DATE	Time	Description
August 16, 1996	1840 - 2200 Z	Air mass storms over KSC w/ little motion
March 29, 1997	1625 - 2245 Z	Fast ESE-moving severe storm cluster
April 23, 1997	1200 - 1800 Z	SW - NE oriented line storm moving SE

The results of the image analysis are shown in Figures 17-22. (Details on the two-dimensional processing of lightning data are given in Appendix B.) For each case, we present a single snapshot when the weather is very close to Kennedy Space Center, and a six-panel time series plot to give an overview of the same case. LDAR's positional accuracy degrades with range from KSC, giving rise to a distinct radial alignment of the data beyond about 60 km.

For the airmass storm on August 16, 1996 (Figure 17), only LDAR recorded a large number of flashes for the storm SW of KSC in regions of low VIL , but both LDAR and NLDN recorded a large number in the high-VIL core of the storm. Neither lightning system measured any activity in the low VIL storms offshore with 30 Kft tops. Figure 18 shows the comparison of LDAR, VIL, Echo Tops and NLDN for the airmass storm on August 16, 1997.

VIL in the severe storm cluster on March 29, 1997 was better represented by LDAR at the time shown in Figure 19, again especially at low values of VIL, but the NLDN also nicely delineated the VIL in the storm cores with high echo tops. Figure 20 is the same comparison for the severe storm cluster on March 29, 1997.

The similarity between the Echo Tops map and LDAR is striking for the line storm on April 23, 1997 (somewhat less so for NLDN; Figure 21 and Figure 22). While the VIL shows almost a solid level 3 line over KSC, the lightning flash rate peaks in the tallest storms. Notice the arc-shaped artifacts in the radar-based Echo Tops data. These, of course, are completely absent in the lightning data.

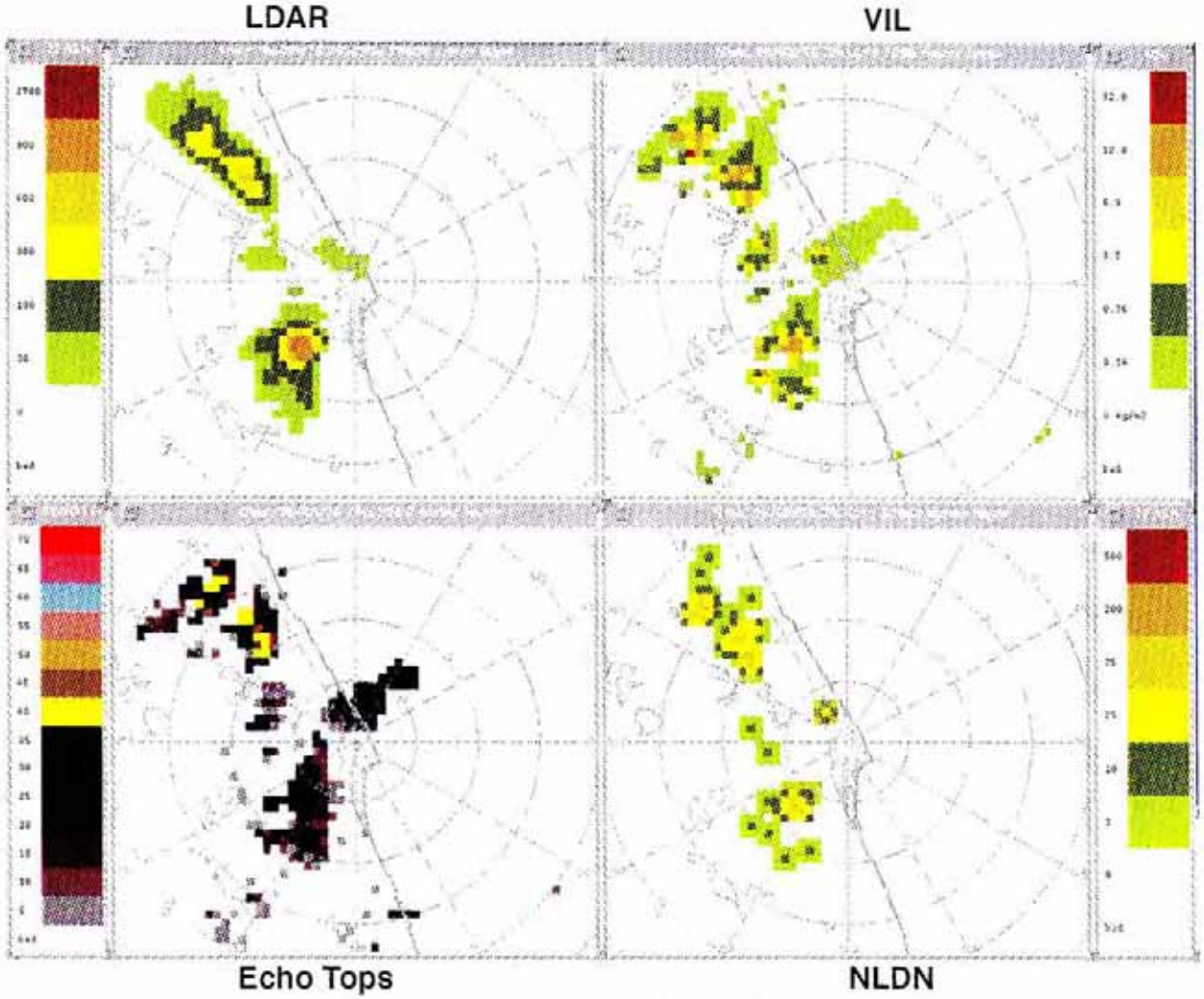

Figure 17. Four-panel plot showing LDAR, VIL and Echo Tops from NEXRAD, and NLDN data at 2034 UT on August 16, 1996. The lightning data has been mapped to two dimensions according to the procedure described in Appendix A. Lightning units are flashes per 5 min. x 48.8 (kernel weighting was not normalized). VIL units are kg/m^2, and Echo Tops are in kft.

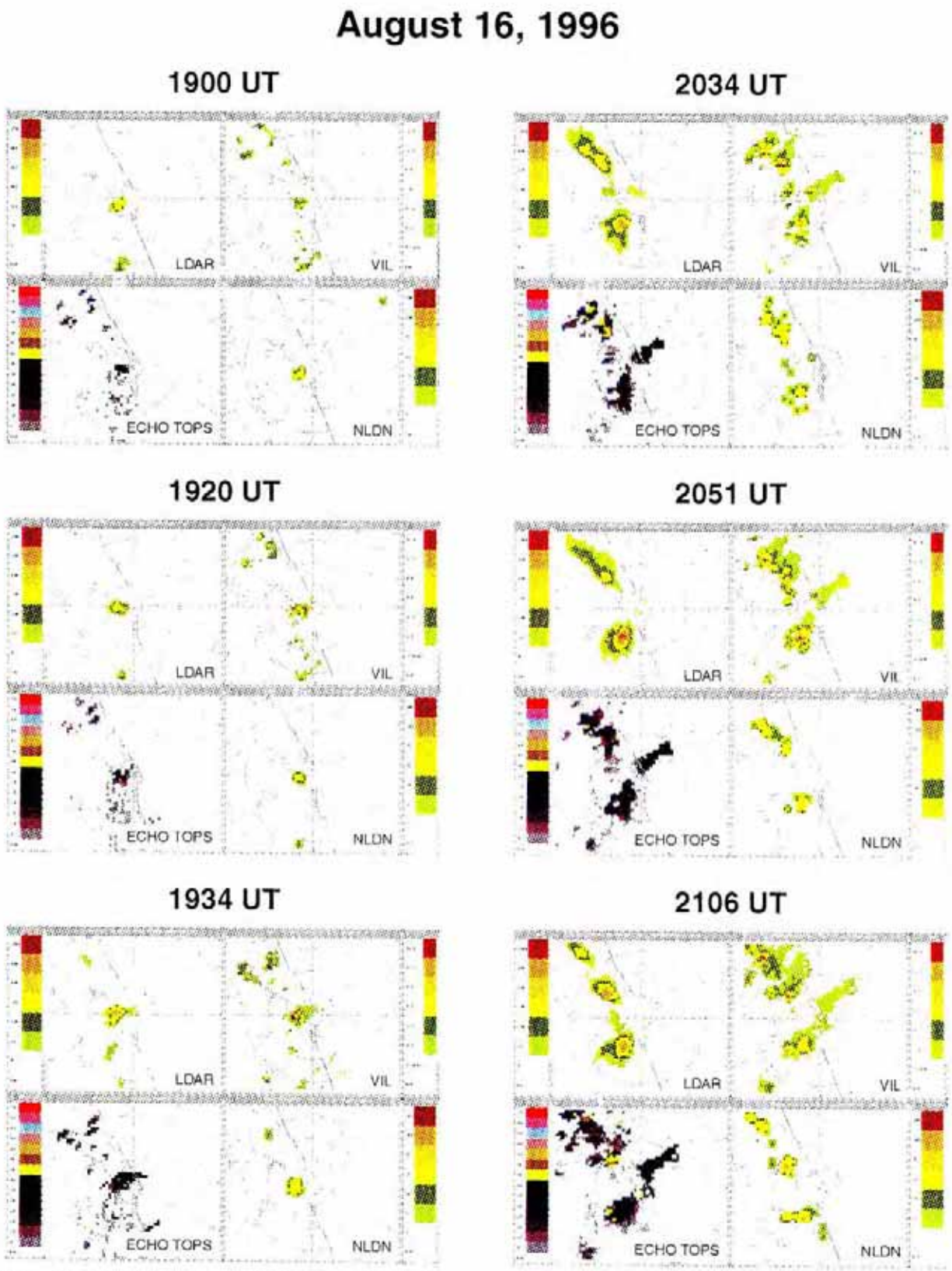

Figure 18. Six of the four-panel plots described in Figure 17 are shown for August 16, 1996. Images for every scan in the time interval shown in Table 17 are available from the authors at Lincoln Laboratory.

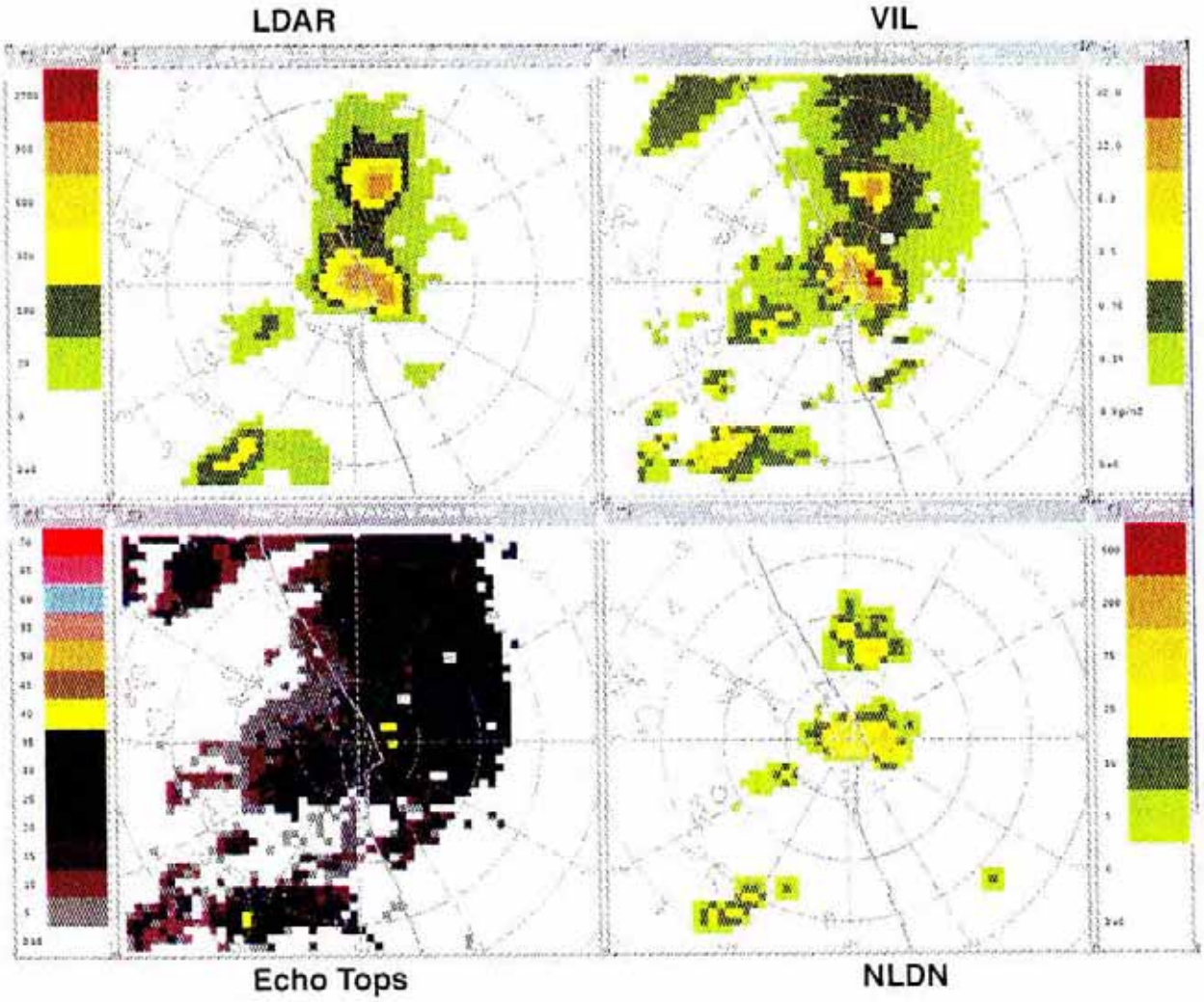

Figure 19. Four-panel plot showing LDAR, VIL and Echo Tops from NEXRAD, and NLDN data at 1941 UT on March 29, 1997. The lightning data has been mapped to two dimensions according to the procedure described in Appendix B. Lightning units are flashes per five-min. x 48.8 (kernel weighting was not normalized). VIL units are kg/m^2, and Echo Tops units are in kft.

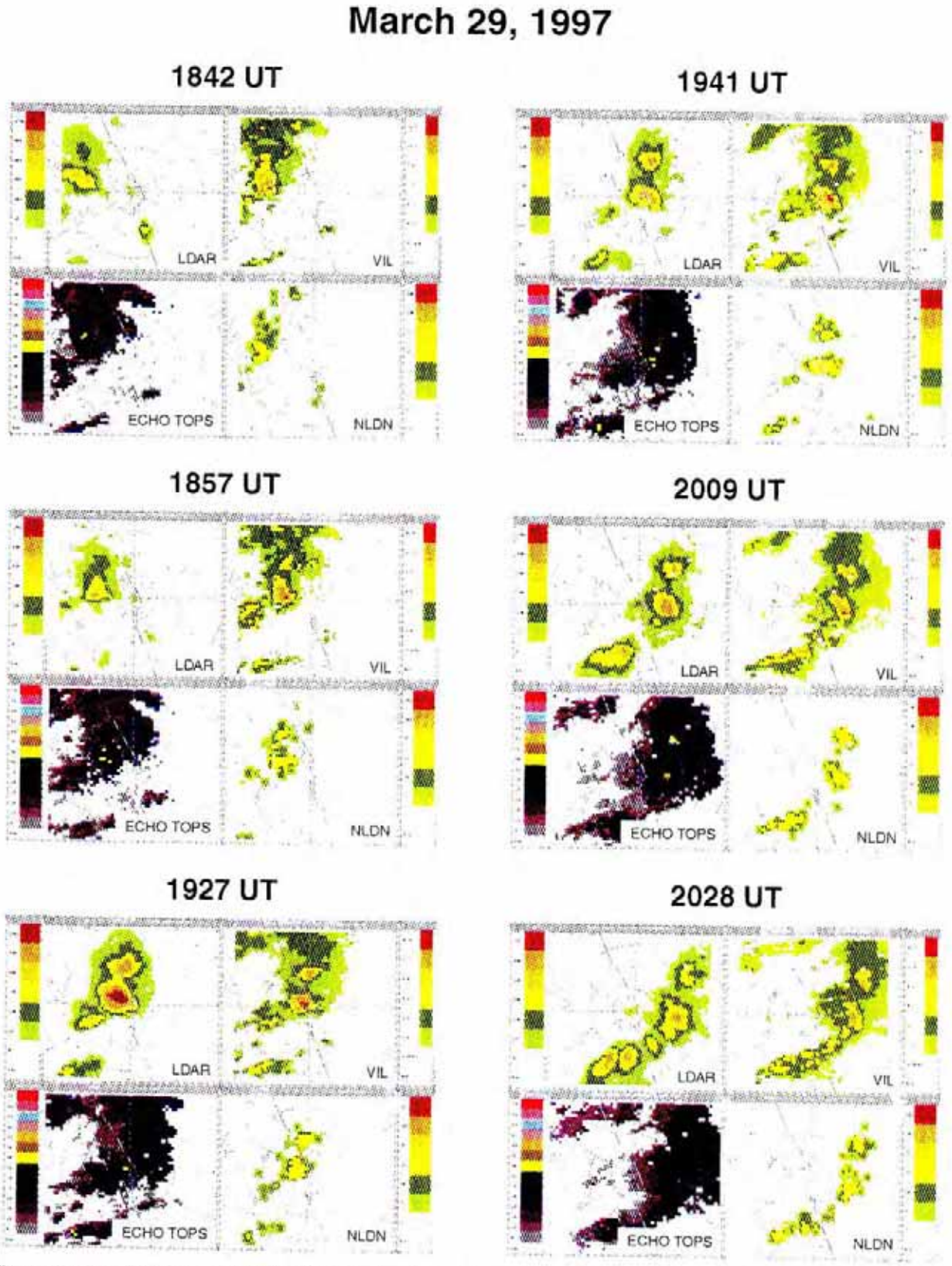

Figure 20. Six of the four-panel plots described in figure 19 are shown for March 29, 1997. Images for every scan in the time interval shown in Table 17 are available from the authors at Lincoln Laboratory.

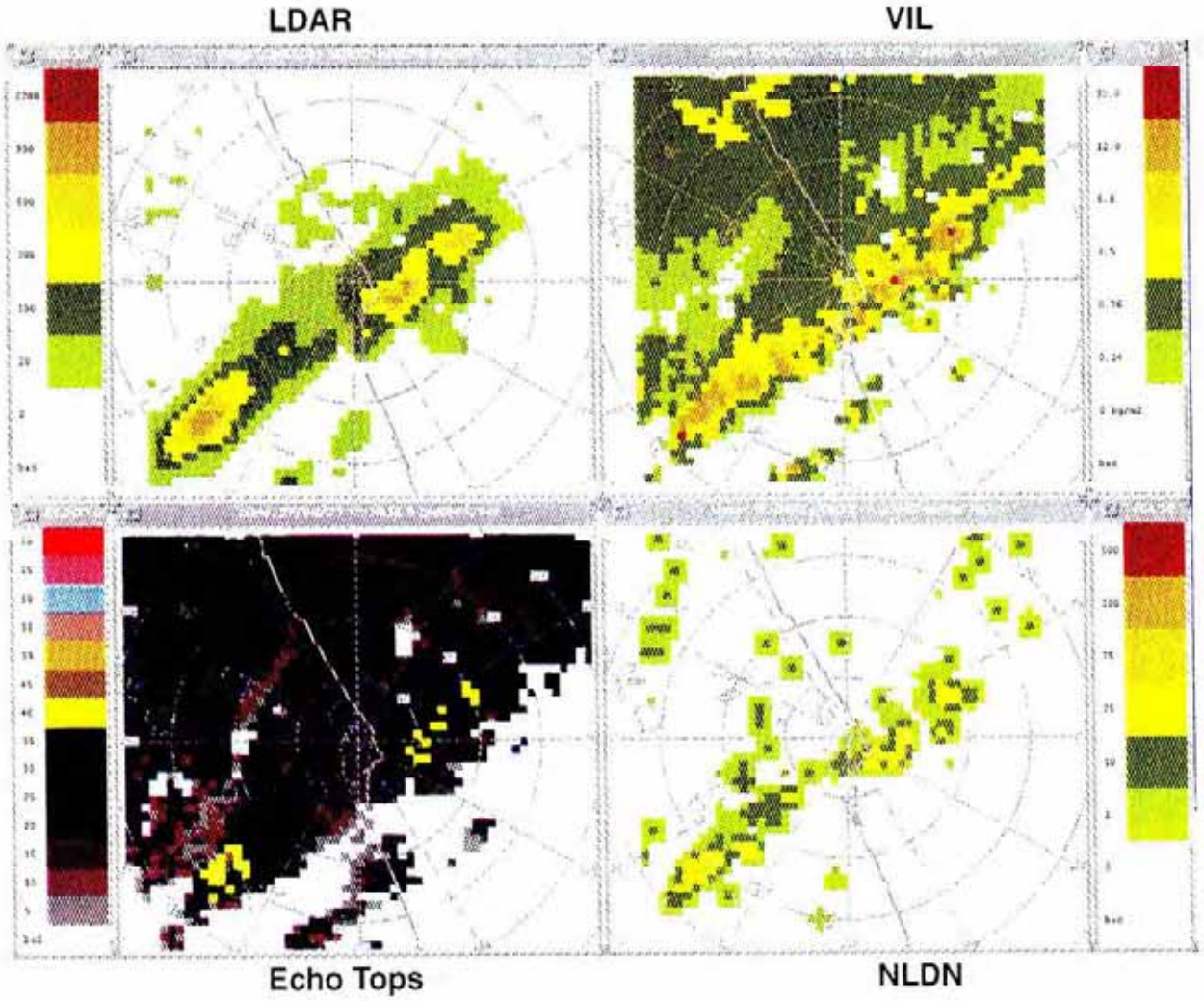

Figure 21. Four-panel plot showing LDAR, VIL and Echo Tops from NEXRAD, and NLDN data at 1638 UT on April 23, 1997. The lightning data has been mapped to two dimensions according to the procedure described in Appendix B. Lightning units are flashes per five-min. x 48.8 (kernel weighting was not normalized). VIL units are kg/m^2, and Echo Tops units are in kft.

April 23, 1997

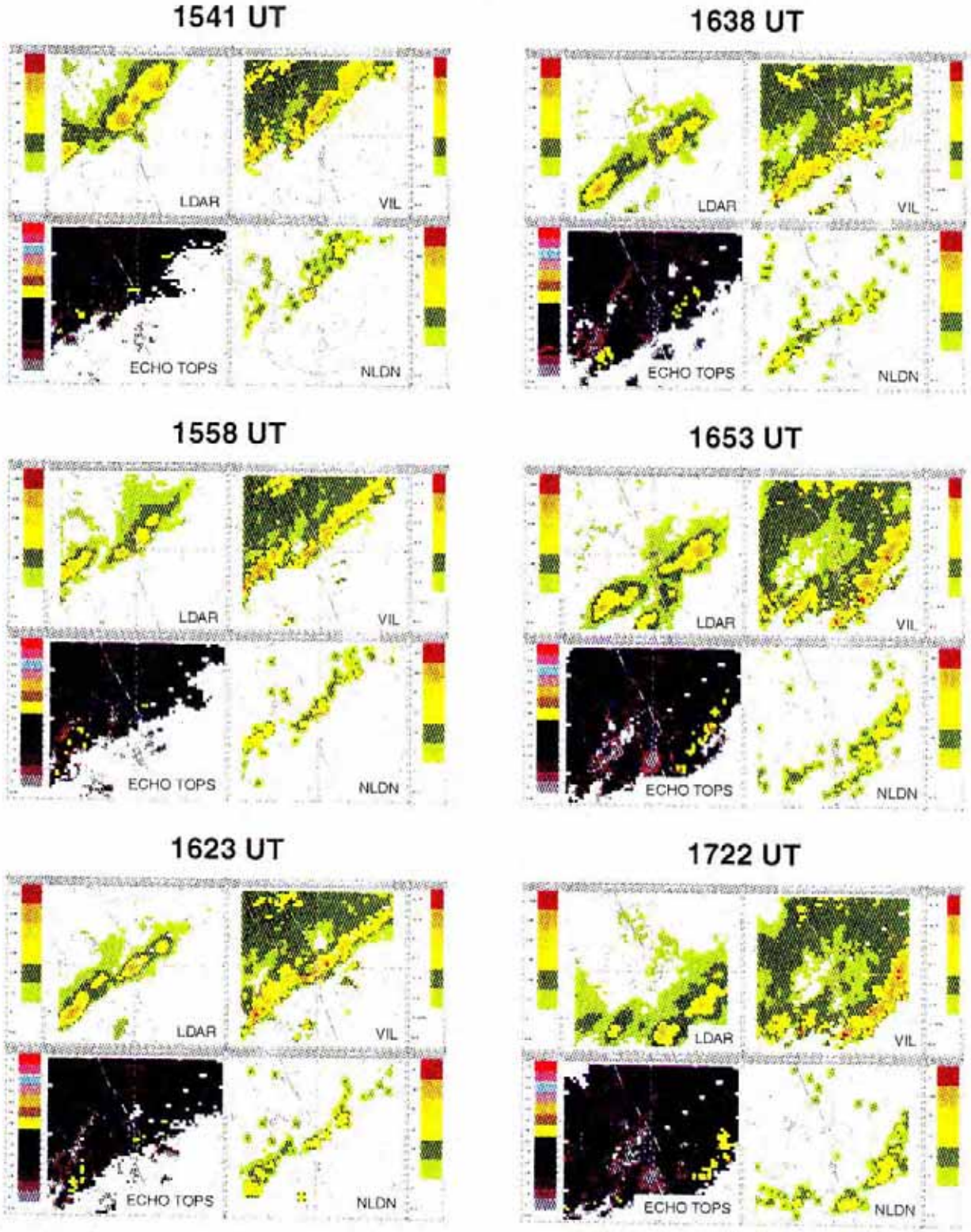

Figure 22. Six of the four-panel plots described in figure 21 are shown for April 23, 1997. Images for every scan in the time interval shown in Table 17 are available from the authors at Lincoln Laboratory.

Boldi (1997) performed a regression of VIL, sampled in 4 km pixels, versus LDAR lightning within a 20 km radius around KSC for the three cases described in Table 17. The lightning strikes were accumulated over 3 min in 4 km pixels for comparison (see Figure 23). The VIL-LDAR regression showed a correlation of **0.63**. A similar regression for NLDN showed a correlation with VIL of **0.25**.

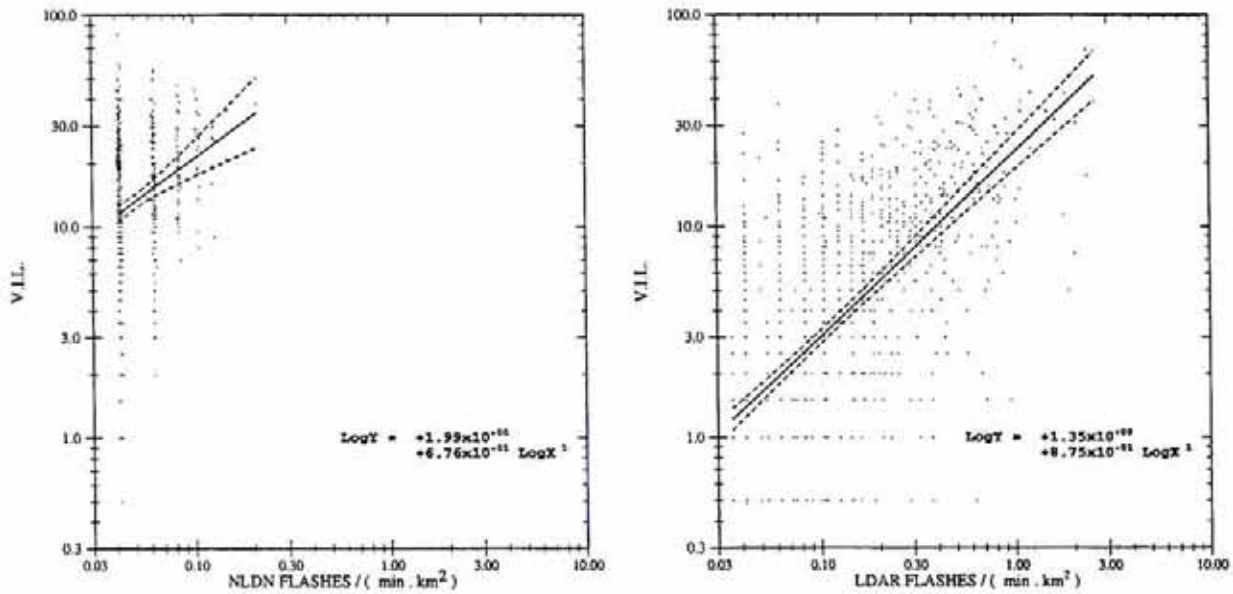

Figure 23. Linear regression between vertically integrated liquid water (VIL) pixel values and lightning flash rate densities.

The lightning data from both the LDAR and NLDN systems provide a useful synthesis of the radar-based VIL plus Echo Tops measurements. (This may well be why AWC and the commercial airlines find NLDN so useful.) The data could therefore provide benefit in filling gaps in the NEXRAD volume coverage indicated in Figure 14. However, the LDAR total flashes are more closely correlated with radar VIL than the NLDN data.

5.2.2. Microburst Prediction

In the airport terminal areas, it is important to avoid the hazardous microburst wind shear that has caused serious accidents in the past. It is not anticipated that lightning data could be used to detect microbursts, but it may be useful in predicting and/or inferring them. Microbursts can be predicted by automatically monitoring the growth and subsequent decay of the storm water mass in three dimensions as long as a relatively current temperature sounding can be constructed to determine the environmental potential for microbursts. An algorithm using this approach to predict microbursts has been specified as part of the ITWS system at the airports protected by TDWRs (Wolfson, et al., 1994). Williams, et al. (1995) have shown that total lightning is usually present prior to the onset of the downdraft that causes the microburst (90 percent of Orlando microburst cases, with a median lead time of 4 min). Only in a small number of cases (20 percent) did the peak in total flash rate precede the *onset* of the microburst, but in 90 percent of cases the peak total flash rate did lead the *peak* outflow strength (median lead time 6-7 min). Total lightning (and its trends) could potentially be used to discern the phase of microburst

parent-storm development, and thus to predict microburst wind shear. Total lightning does not serve as a robust precursor of microbursts in storms with a low total flash rate, such as dry microbursts and a minority of wet microbursts. CG flash rate does not provide a reliable precursor to microbursts (Goodman, et al., 1988; Williams, et al., 1989).

5.2.3. Aircraft Lightning Strike Prevention

Another potential application of total lightning data for enroute flight is to maintain separation between aircraft and lightning. Our conversation with one pilot at American Airlines (Midkiff, 1997) indicated that the addition of lightning information to the onboard weather radar display would be very useful. When aircraft are hit by lightning, they are primarily in flight (Qualley, 1997). The resulting actions are minimal in most cases (inspection of aircraft), but if the aircraft suffers damage it must be taken out of service and repaired. Here the LMS has a clear advantage over NLDN, because it indicates IC lightning directly. (Since aircraft are usually not on or near the ground when struck by lightning, the prediction of CG lightning using total lightning is of negligible benefit.)

5.3 Benefits Categories

5.3.1. Summary of Aviation Benefits Categories

Table 18 summarizes the preceding discussion of aviation benefit categories. The Terminal category is subdivided into Large, Medium, and Small Terminals. Microburst prediction is not a relevant quantity in Enroute or Oceanic flight.

Table 18.
Aviation Benefits Categories and Existing Sensor Coverage

	Large Terminals (ITWS, TDWR)	Medium Terminals (ASR with WSP)	Small Terminals (ASR w/o WSP)
Proxy for VIL	NEXRAD, TDWR, ASR	ASR	ASR
Proxy for Echo Tops	NEXRAD	none (could use NEXRAD [88%], NLDN, &/or GOES Sat.)	none (could use NEXRAD [79%], NLDN, &/or GOES Sat.)
MB Prediction	TDWR	none (could use NEXRAD [88%])	none (could use NEXRAD [79%])
Aircraft Lightning Strike Prevention	NLDN (CG only)	none (could use NLDN [CG only])	none (could use NLDN [CG only])

	Enroute	Oceanic (away from coasts)
Proxy for VIL	NEXRAD [61%], NLDN, On-board Weather Radar	On-board Weather Radar (avoidance possible with visual cues)
Proxy for Echo Tops	NEXRAD [61%], NLDN, On-board Weather Radar, visual determination	GOES Sat., On-board Weather Radar, visual determination
Aircraft Lightning Strike Prevention	NLDN (CG only)	none

Entries are color coded as follows:
Green all category needs met by existing sensors.
Blue some category needs met by existing sensors,
Red no category needs met by existing sensors or information systems.

5.4 Benefits Calculations

5.4.1 Assumptions

In every category listed in Table 18 for which LMS might provide benefit, the existence of the new data source implies the development or enhancement of an appropriate system to deliver the information to the users. The associated costs are different in every case and very difficult to estimate. In the calculations that follow, we do not include this "utilization" cost. The reader should keep in mind that an investment in delivery of the LMS information will offset potential benefits for some period of time.

For the calculation of benefits, we make the following specific assumptions. Unless otherwise noted, the costs given are appropriate for the year 1996 [or *estimated* 1996 by DOT (1997)]. The assumptions will be referred to as "A#" in the text that follows.

1. Perform calculations for US Commercial Air carrier only (no International carriers, US Air Taxi or US General Aviation).

2. International flights are divided into Atlantic, Latin America, and Pacific regions. We will assume no convection in the Atlantic region based on discussions with airlines. (The Caribbean is included in Latin America).

3. Savings in passenger wait time will not be quantified.

4. Revenue Passenger Enplanements per year: ((M) Tables 11 & 13; DOT 1997)

DOMES:	555.6
INT'L:	50.3
Atlantic	15.8
Latin America	19.2
Pacific	15.3

5. Avg. # of Passengers/Plane = Avg. # Seats/Plane x 1996 Estimated Load Factor: (Tables 7, 9, 14 & 15; DOT 1997)

DOMES:	(142) x (.68) = 97
INT'L:	(248) x (.73) = 181
Atlantic	(237) x (.76) = 180
Latin America	(181) x (.63) = 114
Pacific	(327) x (.75) = 245

6. Avg. # of Flights/Year (M) = Rev.Pass.Enplan. (M) / # of Passengers/Plane:

DOMES:	5.728
INT'L:	0.278
Atlantic	0.088
Latin America	0.168
Pacific	0.062

7. Avg. # Flight Hours/Year (M) = [Avg # Flights/Year (M)] x [Avg. Flight Duration in hours]. The duration of flights is [Avg. Passenger Trip Length in miles (Table 8; DOT, 1997)] / [Avg. Speed of Aircraft in miles/hour]. We will assume an average speed for domestic flights of 300 kts or 345 mph, and 460 kts or 529 mph for international flights.

DOMES:	5.728 x 799.4 / 345 = 13.27
INT'L:	0.278 x 3003.6 / 529 = 1.58
Atlantic	0.088 x 3003.6 / 529 = 0.50
Latin America	0.168 x 3003.6 / 529 = 0.95
Pacific	0.062 x 3003.6 / 529 = 0.35

8. US mix of aircraft (Table 16, DOT 1997):

Narrowbody:	2 engine	60%
	3 engine	18%
	4 engine	5%
Widebody:	2 engine	6%
	3 engine	7%
	4 engine	4%

9. Cost per flight hour per seat on aircraft (Table 1.2, Volpe 1996):
Avg cost = Cost of (Crew + Fuel + Maint)/No. of Avail. Seats

Narrowbody:	2 engine	$10.02
	3 engine	$12.12
	4 engine	$12.15
Widebody:	2 engine	$10.19
	3 engine	$11.90
	4 engine	$12.23

10. Based on these Tables, we assume the following airline costs per seat per hour, and cost per plane per hour (multiply by seats/plane) [Table 7, 8 & 16 (guidance); DOT, 1997]:

DOMES:	$11 x 142 =	$1562
INT'L:	$12 x 248 =	$2976
Atlantic	$12 x 237 =	$2844
Latin America	$12 x 181 =	$2172
Pacific	$12 x 327 =	$3924

11. The cost for an inspection is calculated by assuming that it takes about 1 hour, and is equal in personnel & material costs to 1 hour of maintenance. Thus, using statistics in Table 1.2 (Volpe, 1996) and guidance from Tables 7, 9, & 16 (DOT 1997):

DOMES:	$350
INT'L:	$620
Atlantic	$590
Latin America	$400
Pacific	$880

12. We estimate that geostationary coverage by LMS amounts to the following percentage of flight areas:

CONUS	100%	
Latin America	90%	**
Pacific	60%	

** Actual 90-100% based on newly proposed Field of View (FOV) (Figure 4).

13. We estimate that the NLDN covers the following area percentages of the geostationary satellite coverage regions:

CONUS	100%
Latin America	5%
Pacific	5%

14. We assume two thirds of flights occur during daylight, and one third during darkness.

5.4.2 More Efficient Routing by Providing a Proxy for VIL and Echo Tops

Terminal

Coverage of VIL and Echo Tops in the nation's airport terminals is, for the most part, excellent. VIL is measured well in Large, Medium, and Small Terminals (refer to Table 18) by the existing FAA and NWS radars. Echo Tops are used in the terminal area as an additional measure of storm severity and potential longevity, and are not a critical safety-enhancing or delay-reducing bit of information. This parameter is satisfactorily sampled in all Large Terminals by neighboring NEXRADs, and the information is available to aviation users through the ITWS display. In Medium and Small Terminals, no systems exist currently for the display of Echo Tops. A combination of NEXRAD, NLDN and/or GOES satellite data could be used to create such a product if a display mechanism existed. Given the above, we ascribe no terminal area benefit in this category to LMS.

Enroute

Over the nation's enroute airspace, coverage of VIL and Echo Tops is also, for the most part, excellent. These two pieces of information are used in conjunction by controllers and airline dispatchers to maintain separation of aircraft from hazardous weather, and to suggest a more efficient rerouting of flights than could be selected by pilots through use of visual cues and airborne radar alone. The existing sensors are NEXRAD, GOES satellite, and NLDN. The deficiencies in NEXRAD coverage (61 percent of CONUS according to our three-dimensional requirement) can be made up through the use of the NLDN. Satellite estimates of cloud top heights are notoriously difficult, so the key contender for LMS benefits is the combination of NEXRAD and NLDN.

To determine the benefit of LMS, we need to determine the incremental benefit NLDN provides over NEXRAD, and then quantify how much better LMS would be than NLDN for determining VIL and Echo tops.

NLDN could provide estimates of VIL and Echo Tops in the 39 percent of the CONUS not under NEXRAD three-dimensional coverage (Figure 14). To compute the incremental benefit of NLDN over NEXRAD, we will make the following assumptions:

1. NLDN provides enroute aviation benefits similar to those provided by NEXRAD in the ratio 39:61 by providing a proxy for the radar-based VIL and Echo Tops. NOAA (1985) has calculated the NEXRAD benefits as $143.6M. *

2. The efficacy will not be the same as NEXRAD, however. We will estimate the relative efficacy to be **0.25** based on the correlation between NLDN and NEXRAD VIL.

3. Commercial flight routes uniformly cover the CONUS.

4. The relative amount of convective weather in the uncovered region is 20 percent. This was estimated by visually "convolving" the NEXRAD coverage map in Figure 14 with the average annual lightning ground strike maps from four consecutive years, shown in Figure 24. The lightning ground strike maps represent the annual distribution of convective weather. NEXRAD coverage was purposely designed to be more dense in areas of frequent convective weather.

---

* The NOAA NEXRAD cost-benefit study included both safety and delay in its calculation of enroute benefit. The safety benefit dealt primarily with avoidance of hazardous low-altitude wind shear, and thus was inappropriate for reference in this category. The benefit from reduction in enroute delay was based on "maximum strategic and tactical use of Doppler radar data to minimize delays, which should result in a 25 percent reduction in weather related delays." Thus, in a fairly ad-hoc fashion (two storms studied by NCAR were used as examples to justify the assumptions), the delay benefit was broadly assumed to be 1/4th of the annual delay costs. While this number ($143.6M) represents annual benefits in 1983 dollars, there can be no real basis for increasing it to reflect more recent valuations, since it could only have been correct to within a factor of 2 or 3 at the time of publication.

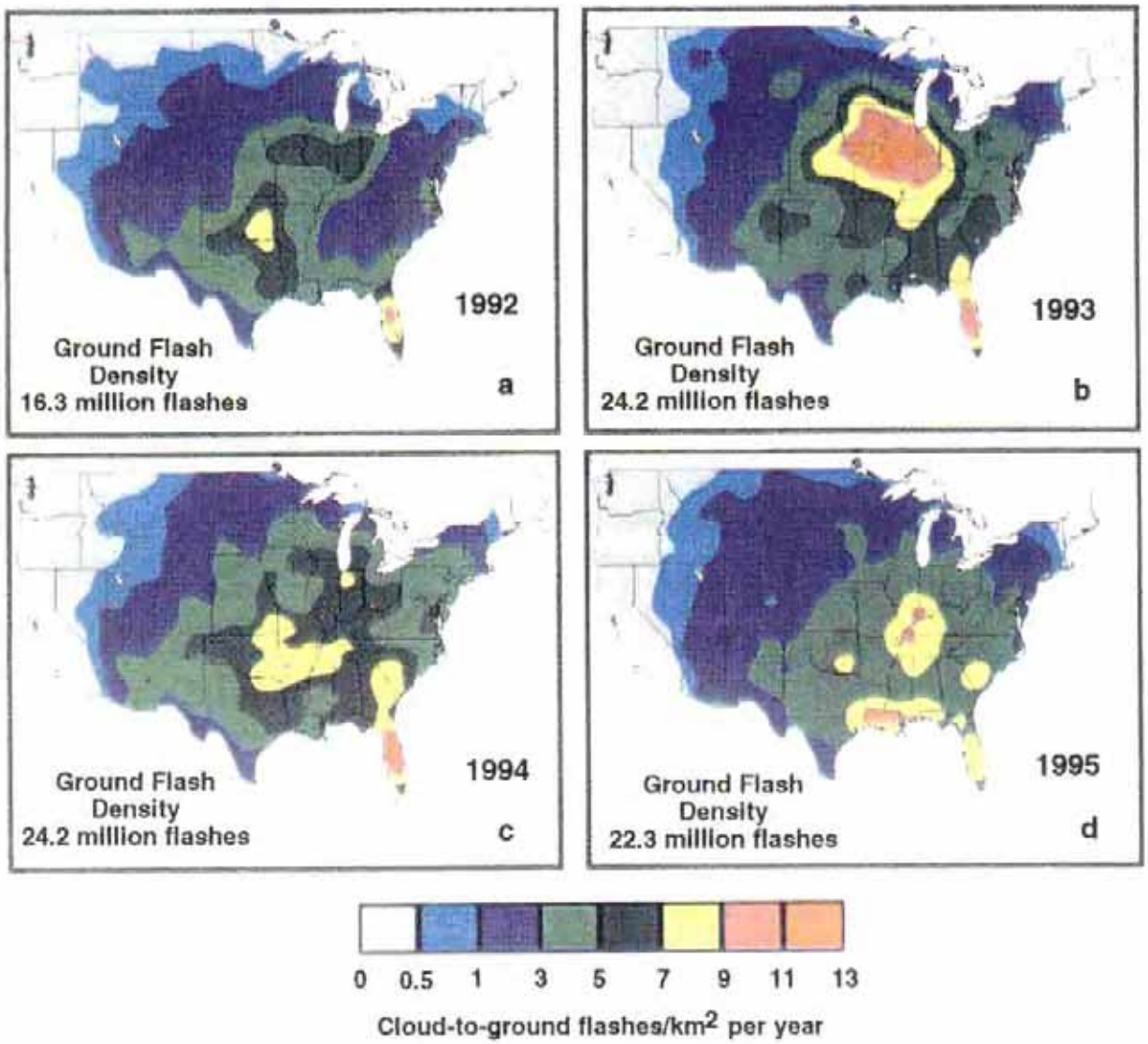

Figure 24. Lightning ground flash density for the years 1992-1995 are shown in panels (a) through (d), respectively. Measured values have been multiplied by 1.4 to correct for the assumed 70 percent detection efficiency in the NLDN (figure from Orville and Silver, 1997).

The benefit of NLDN relative to NEXRAD is:

$$\text{NLDN benefit} = [39/61] \times [0.25] \times [20\%] \times [\$143.6\text{M}] = \$4.6\text{M} \quad (6)$$

The benefit of LMS over NLDN can be calculated by using the ratio of the correlation of the two lightning data types to the NEXRAD VIL product (0.63 vs. 0.25). We calculate the relative benefit of LMS, and subtract the computed NLDN benefit to arrive at the incremental value.

$$\text{Enroute Benefit} = [(63/25) - 1] \times \$4.6\text{M} = \mathbf{\$7.0M} \quad (7)$$

Oceanic

The summary of existing sensor coverage in Table 18 shows that VIL and Echo Tops are detected on oceanic routes only by GOES satellite and airborne weather radar. Oceanic regions not covered by NLDN represent regions in which there is high potential benefit to aviation of the LMS.

Before computing the benefits, it is useful to understand how the oceanic traffic management takes place. Airlines are always trying to select the most efficient and comfortable routes, so that their costs are minimized and passenger safety maximized. The "best" oceanic routes are picked based on global numerical model output 3 or 4 times each day. Pre-flight planning rarely considers weather (other than winds); the exception is for routes near hurricanes or tropical storm systems. Once a flight route is determined it is rarely changed, although there have been some recent efforts at dynamic rerouting based on satellite data. In certain oceanic regions the routes cannot change due to political considerations.

Unlike the practice over the US, airline pilots do not communicate often with their dispatchers or with controllers once they are enroute over ocean. They can be reached via HF radio, commonly accomplished via a patch through a commercial aviation data link vendor (ARINC). When dispatchers do call pilots to have them change routes based on weather, it is often the existence of severe turbulence (not in storms) on the existing route that is the impetus. The pilots are more often making tactical deviations to avoiding tropical convection based on the information provided by their own airborne radars, on visual cues, and on news from other pilots flying a similar route (via air-air VHF communications).

Another factor making the tropical (oceanic) flights around convection different from those in the CONUS is the type of convection that occurs. The tropical thunderstorms are usually very tall, have well-defined edges, and are less frequently embedded in broad cloudy regions than many U.S. storms. Pilots have the most difficulty with line storms (especially those oriented parallel to the line of flight; Midkiff, 1997), and these are less common in the tropics than in mid-latitudes. So, while pilots may have to deviate around tropical convection more often because of its frequency (it is rarely possible to fly over tropical convection because the storms are tall and the heavily loaded planes cannot achieve the altitudes required), the deviations are easier and less time consuming than those over the continental U.S. The short delays incurred from the tropical deviations can often be made up enroute, so the flights are not necessarily late. However, some additional fuel cost is incurred.

If LMS data were available, it would be utilized by the airlines much the same way NLDN data are used today. Dispatchers would use the data to make strategic decisions for their enroute pilots. The method of communication from dispatcher to international pilot would probably have to be improved (e.g., by digital data link) for much of the LMS benefit to be realized. Perhaps a text message directing a rerouting and a graphic showing the long range weather situation could be "pushed" to the cockpit of the affected flights. In any event, we assume a system is in place that can utilize the new information.

We will first calculate the delay benefit of LMS for oceanic flight. All the airline meteorologists we interviewed agreed that convection in the North Atlantic does not occur often enough to be listed as a significant operational concern. Convection is a common occurrence on

Latin American and Pacific routes. Estimates of delay caused by oceanic convection are given below in Table 19.

Table 19.
Estimates of the Percentage of International Flights Deviating due to Convection and the Delay (in minutes) Incurred per Deviating Flight

Destination	Airline	Flights Deviating due to Convection (%)	Average Delay due to Convection (min)
Asia	Northwest (Fahey, 1997)	25	0
	United (Gregory, 1997)	50-60	5
Australia	United (Gregory, 1997)	90	5 (up to 15)
South America	United (Gregory, 1997)	90	5 (up to 15)
Caribbean	American (Qualley, 1997)	90 (high exposure)	–
	American (Midkiff, 1997)	–	5-10

Based on this input, we will assume the following average delay statistics:

Latin America	90%	5 min
Pacific	45%	5 min

Using A6 to determine the average number of flights per year, we can calculate the total number of delay minutes per year for each region.

Latin America: (0.168M) x (90%) x (5 min) = 756,000 min **(8)**

Pacific: (0.062M) x (45%) x (5 min) = 139,500 min **(9)**

To determine the benefit of LMS in reducing oceanic delay, we make the following assumptions.

1. Knowing where a storm will be while still upstream can allow a more efficient flight route to be selected, but sometimes an additional delay will be incurred as a safer route is sought. We will not account for the potential increase in delay.

2. The efficacy of LMS in detecting storms to be avoided is high in these regions, since tall tropical storms are virtually all highly electrified. We will assume the efficacy is **80 percent.**

3. Even if more efficient flight routes are chosen, not all of the delay will be mitigated. We estimate the delay savings will equal **50 percent** of the total delay.

4. The coverage by LMS for these routes is not complete because of the geostationary satellite field of view (A12).

5. In a limited region off the coast (**5 percent**), the incremental coverage of LMS over NLDN must be considered (A13). Geostationary coverage of these coastal regions is 100 percent.

The number of delay minutes saved by LMS over NLDN is:

Latin America:

$$(80\%) \times (50\%) \times (756{,}000) \times \{(100\%) \times (5\%) \times [63/25 - 1] + (90\%) \times (95\%)\}$$

$$= 281{,}534 \text{ min} = 4692 \text{ hours} \qquad \textbf{(10)}$$

Pacific:

$$(80\%) \times (50\%) \times (139{,}500) \times \{(100\%) \times (5\%) \times [63/25\text{-}1] + (60\%) \times (95\%)\}$$

$$= 36{,}047 \text{ min} = 601 \text{ hours} \qquad \textbf{(11)}$$

Using the cost per plane per hour from A10, we can calculate the annual benefit:

Latin America: ($2172) x (4692) = **$10.2M** **(12)**

Pacific: ($3924) x (601) = **$2.4M** **(13)**

The safety benefit of LMS for the oceanic regions will be in delineating growing cells. Qualley (1997) and Gregory (1997) both discovered that many turbulence encounters around convection are actually due to thunderstorms growing up into the path of flight. It is difficult to "paint" the onboard radar downward with any regularity. United estimates 5-6 occurrences of "extreme discomfort" on international flights each year, where passengers are injured. American estimates 5 such encounters per year in the Western Atlantic (Caribbean), to which it operates 160 round trip flights per day. This amounts to severe turbulence events on 0.004 percent of flights. Again using A6 to determine the average number of flights per year, we can estimate the total number of severe turbulence incidents per year:

Latin America: (0.168M) x (0.004%) = 7.2 **(14)**

Pacific: (0.062M) x (0.004%) = 2.7 **(15)**

For a case to be categorized as extreme, usually at least one person is severely injured. Volpe (1996) lists the cost of a serious medical injury at $520,000. We will use the same assumptions for the ultimate efficacy, and coverage of LMS relative to NLDN as we did in the delay calculation, but we will assume the entire cost of the turbulence incident was saved when the event was avoided. The safety benefit is:

Latin America:

$$(80\%) \times (\$520{,}000) \times (7.2) \times \{(100\%) \times (5\%) \times [63/25 - 1] + (90\%) \times (95\%)\}$$

$$= \mathbf{\$2.8M} \qquad \textbf{(16)}$$

Pacific:

$$(80\%) \times (\$520{,}000) \times (2.7) \times \{(100\%) \times (5\%) \times [63/25-1] + (60\%) \times (95\%)\}$$

$$= \mathbf{\$0.7M} \qquad \textbf{(17)}$$

From equations 12, 13, 16, and 17, the oceanic aviation benefit for LMS is therefore estimated to be **$16M** per year in more efficient routing and reduction of injury from turbulence encounters. Adding in the CONUS en route benefit (equation 7), the total benefit from LMS in determining the location, severity, and extent of thunderstorms in Terminal, Enroute, and Oceanic flights is estimated as **$23M** per annum.

5.4.3 Microburst Prediction

The potential microburst prediction capability of LMS affects only the airport terminal areas; microbursts do not pose a hazard to enroute or oceanic flight. Existing coverage in this benefit category is provided by TDWR/ITWS at the nation's largest airports. For all other airports, we suggest that volume coverage by the nearest NEXRAD radar could provide some prediction capability if the FAA chose to develop and deploy an algorithm and system to deliver this information to the end users. The 5-6 min volume update rate of the NEXRAD (twice as long as that of the TDWR) will limit the ultimate efficacy of any such system. Given the efficacy of the TDWR-based microburst prediction algorithm was estimated at 75 percent (Rhoda, 1997), we will estimate the efficacy of a NEXRAD-based algorithm to be half that, or 38 percent.

As an alternative, especially for airports outside the NEXRAD three-dimensional coverage region, an algorithm based on LMS could be similarly deployed. The prediction of microbursts based on the total lightning signal is far from mature; the literature describes only a handful of case studies from limited climates. However, these are convincing enough that we should assign some potential benefit to this area. There is no evidence NLDN could be used for microburst prediction. LMS would have advantage over a NEXRAD in the important area of update rate since integration periods of one minute or less are appropriate for the total lightning data. However, given all the uncertainties and the fact that no automated algorithm to predict microbursts based on lightning data has ever been developed and tested, we will assume the efficacy is no better than the NEXRAD-only prediction system (**38 percent**), and count benefit only for those airports not fully covered by NEXRAD. In reality, a microburst prediction algorithm would use any and all available data, including the ASR weather channel itself, and the LMS might add some improvement at sites within the NEXRAD coverage regions.

Figure 15 shows the existing FAA TDWR and ASR radars overlaid on the NEXRAD three-dimensional coverage map. Small circles have been placed around the radars that are outside the NEXRAD coverage regions. We find that 4 out of 33 ASR-WSP airports (12 percent) and 27 of 131 ASR "reflectivity channel only" airports (21 percent) are "uncovered." To estimate the safety benefit of having a microburst prediction algorithm at these airports, we will use the ITWS

method (Rhoda, 1997). ITWS used the original TDWR microburst safety benefit numbers for the top 100 airports based on each airport's specific microburst wind shear exposure (Martin Marietta, 1985), counted 10 percent of this as potentially undetectable because the outflow reached microburst strength in a period shorter than the radar's one-minute microburst detection update interval and then assumed that ITWS could predict a percentage (75 percent was chosen) of those 10 percent of events. ITWS also updated the 1984 cost numbers to 1994 numbers using a factor of 3.7 (includes cost of lives, injuries, and damages). We will not further update the 1994 numbers.

Only two of the four circled ASR-WSP sites, and four of the circled ASR "reflectivity channel only" sites, are in the top 100 airports used in the TDWR study. The uncovered WSP sites in the top 100 airports and the corresponding Safety benefit in 1984 dollars are:

59. Greensboro NC	$146,579
93. Toledo OH	$79,006

The uncovered ASR sites in the top 100 airports, and the corresponding Safety benefits in 1984 dollars are:

64. Daytona Beach FL	$124,803
68. Fort Myers FL	$124,470
80. Baton Rouge LA	$101,082
86. Lafayette LA	$105,423

To estimate the safety benefit at the circled sites not in the top 100, we note that the safety benefit at the 100th site in 1984 dollars is:

100. Akron, OH	$70,702

We will take half of the value of the 100th site (**$35,351**) as the average safety benefit for the remaining uncovered sites.

The safety benefit at the circled ASR-WSP sites is then:

WSP 1984 safety benefit:

Greensboro + Toledo + 2 x ($35,351) = $296,287

LMS WSP sites 1994 safety benefit = 3.7 x 10% x 38% x $296,287 = **$0.04M** **(18)**

The safety benefit at the circled ASR sites is then:

Daytona Beach + Fort Myers + Baton Rouge + Lafayette + 23 x ($35,351) = $1,268,851

LMS ASR sites 1994 safety benefit = 3.7 x 10% x 38% x $1,268,851 = **$0.18M** **(19)**

Thus, the total annual LMS benefit assessed for its potential to provide microburst predictions at smaller U.S. airports is **$0.2M**.

5.4.4. Lightning Strike to Aircraft

Enroute and Oceanic Benefit

Statistics on aircraft lightning strikes gathered over several years in the 1970s and early 1980s were described by Plumer, et al., (1985). To determine the relative benefit of LMS over NLDN for indicating the aircraft lightning hazard, we need to discern the type of lightning typically striking aircraft. Even though 87 percent of the aircraft were struck at altitudes below 16 Kft, 96 percent of aircraft reported their location "in cloud" (not below cloud base) when struck by lightning. What percentage of these clouds were *not* producing CG strikes? Williams (1985) shows that CG strikes are very infrequent (less than 1 per 10 min) in storms with cloud tops less than 5 km (16.4 Kft). Plumer, et al., (1985) show that 43 percent of the aircraft lightning strikes occurred in storms with cloud tops 15 Kft and below. (He also showed that aircraft were mostly struck in springtime storms, leading to the conclusion that aircraft were effectively avoiding well-defined, tall, highly electrified summer thunderstorms.) We will assume that **40 percent** of the lightning strikes were associated with storms that produced no CG strikes, and thus could not have been detected by NLDN.

Further, only 40 percent of pilots observed any other lightning activity at the time they were hit, suggesting that possibly 60 percent of the lightning strikes could have been triggered by the aircraft itself in marginally electrified clouds that were not producing any natural lightning (and thus would not have been detected by LMS). Because of the difficulty seeing IC lightning while flying in-cloud during daylight, we can guess that other lightning activity was actually present more than the observed 40 percent of the time. Assuming 2/3 of the flights were in daylight (very few flights between midnight and 4 am; A15), and half the solo daytime strikes were actually triggered (all at night were triggered), we can calculate that (2/3)(1/2)(60%) + (1/3)(60%) = 40% of the strikes total were triggered by the aircraft itself. This implies that only 60 percent of the strikes could have been detected by LMS.

Based on airline maintenance reports, Plumer, et al., found that a typical aircraft is struck by lightning once every 2,500 hours. Our assessment suggests that LMS could have detected, and thus incrementally aided in avoidance of, the lightning in: (40 percent not detectable by NLDN) x (60 percent naturally occurring lightning) = 0.24 strikes every 2,500 hours, or roughly **1 strike per 10,000 flight hours**. In areas where there is no NLDN, LMS could have detected 0.6 strikes per 2,500 hours or roughly **1 strike per 4,200 flight hours**.

The additional number of aircraft lightning strikes that could be detected per annum by LMS can be calculated by factoring in the total annual flight hours for each region, and the geostationary coverage of each region (A7, A12, A13):

Domestic:	[(13.27 M) / (10,000)]x [100%] = **1327**
Latin America:	(0.95 M) x {[5% x 100%] / (10,000)} + [95% x 90%] / 4,200} = **198**
Pacific:	(0.35 M) x {[5% x 100%] / (10,000)} + [95% x 60%] / (4,200)} = **49**

Every one of these strikes must be reported, which leads to a brief (1 hr) inspection of the aircraft. Very few of these strikes lead to any damage to the aircraft. Only 11 percent of aircraft lightning strikes resulted in outages requiring either repair or replacement of equipment, and only three percent resulted in any impact to the electrical/electronic systems. None of the strikes

resulted in engine flameout. Thus, the benefit of LMS is in the area of delay reduction (avoiding inspections), and not significantly in safety.

We will assume 89 percent of strikes lead to inspection, which implies 1 hr down time plus the maintenance costs. We will use A11 in this calculation for estimates of the inspection costs. Although there is a missed opportunity to create profits for the airlines during the 1 hr lost time, we will take a conservative approach and not evaluate this. We have assumed that passenger time will not be counted (A3), and airline crew are not paid for wait time. The cost per lightning strike for each region is:

Domestic:	\$350
Latin America	\$400
Pacific	\$880

For the 11 percent of strikes that cause outages, we will assume that the cost is above that for a simple inspection. We have information from our conversations with the airlines that the repair costs are usually under \$10,000 for severe strikes. We do not have enough information to differentiate repair costs between types of aircraft, and aircraft mix for the various regions. Thus we will assume an average repair cost of \$5000 per aircraft.

The total benefits are:

$$\left.\begin{array}{lll} \text{Domestic:} & (1327)\,[(89\%) \times (\$350) + (11\%) \times (\$5000)] = & \mathbf{\$1.14M} \\ \text{Latin America:} & (198)\,[(89\%) \times (\$400) + (11\%) \times (\$5000)] = & \mathbf{\$0.2M} \\ \text{Pacific:} & (49)\,[(89\%) \times (\$880) + (11\%) \times (\$5000)] = & \mathbf{\$0.1M} \end{array}\right\} \qquad (20)$$

summing to **\$1.4M** per annum as the estimated reduction in airline costs that would occur through reduced in-flight lightning strikes.

Terminal Benefit

There is a serious terminal lightning hazard due to cloud-to-ground lightning striking objects or people on the ground at the airport. (All effects of in-flight strikes were included under the enroute calculation.) Airline ground operators take the threat of lightning very seriously, and take action based on the NLDN ground strike information. The primary benefit of the LMS sensor here is the additional lead time warning of CG strikes that would presumably be gained. There are benefits of this lead time in saving lives due to CG strikes on the airport, but they have been accounted for along with other civilian ground strike occurrences elsewhere in this report. We note but do not count the potential increase in delay caused by moving people indoors sooner with the LMS system. The aircraft themselves can be struck while parked at the airport, but it appears this is very infrequent. We will therefore not assign a benefit in this category for terminal operation.

5.5 Summary

We have evaluated how total lightning data would be useful to aviation, and have calculated the benefits that could be expected if an operational GOES LMS were deployed. We must remind the reader that we have calculated the benefit only for US Commercial Air carrier operations, have not included the cost of any system to utilize and provide LMS data to the end

user, and have not accounted for potential increases in delay at the expense of safety and comfort that might result from avoiding the electrified storms. Table 20 summarizes our results.

Table 20.
Summary of Annual LMS Aviation System Benefits ($M)

	Terminal	Enroute	Oceanic	Total
Proxy for VIL + Echo Tops	0	7.0	16.1	23.1
MB Prediction	0.2	N/A	N/A	0.2
Lightning Strike to Aircraft	0	1.1	0.3	1.4
Total	**0.2**	**8.1**	**16.4**	**24.7**

6.0 GROUND STRIKE WARNING

6.1. Personal Injury, Death and Property Damage

The Lightning Mapper Sensor's capability to detect IC lightning provides a mechanism for earlier identification of thunderstorms and thus a basis for potentially more timely warnings of ground strike hazard. Assuming that these were of sufficient reliability to be heeded, earlier threat-avoidance actions by exposed people could reduce casualties and damage. The magnitude of this benefit is assessed in the following subsections.

6.1.1. Current Costs to Society

Table 21 lists NWS statistics on the annual toll CG lightning exacts in the United States in terms of injury/fatalities to people and property damage. Several authors (e.g., Lopez, et al., 1993) express the view that the Government tabulations that serve as the basis for most of these estimates, for example "Storm Data," may significantly underestimate casualties and damage owing to dependence on newspaper clipping services to provide reports of the incidents.

Table 21.
NWS Natural Hazards
Statistics Compilation for Storm Data, Annual Average for 1990-1995

	Fatalities	Injuries	Property Damage
Cloud-to-Ground Lightning	64	360	$35M

Clearly, much lightning-induced property damage (fire, building damage, tree damage) would not be avertible through better short term lightning warnings. Some reduction in power-surge induced damage to electronic equipment might be anticipated, however. Although most large, vulnerable Government and commercial sector facilities are protected by stand-by generators, these may not always be turned on early enough to eliminate the threat. Discussions with consumer computer repair personnel indicated that widely used surge protectors are effective in protecting against most power spikes, and that prevention of damage in the event of large spikes caused by nearby lightning would require disconnection of power cords and modems. Provision of reliable warnings of lightning threat might induce a fraction of owners to disconnect their computers during the storm. Although we were not able to obtain an estimate of the yearly costs of potentially avertible lightning strike damage to electronic equipment, we acknowledge that the total might be significant, given that such equipment is ubiquitous in our society.

Our subsequent evaluation estimates the potential benefit of preventing fatalities and injuries through the provision of more timely lightning warnings. We note that the benefit evaluation methodology we use would apply to property damage as well, should avertible property damage subsequently be found to comprise a significant total.

6.1.2. Technical Basis for LMS Benefit

Figure 25 plots a distribution of time lags between the first cloud flash in thunderclouds and the first ground flash. Data from the Melbourne, FL WSR-88D were used to identify storm cells. The Lightning Detection and Ranging (LDAR) system at Kennedy Space Center and the National Lightning Detection Network (NLDN) were used to detect and localize cloud and ground flashes respectively. These analyses were performed as part of the LISDAD effort described previously.

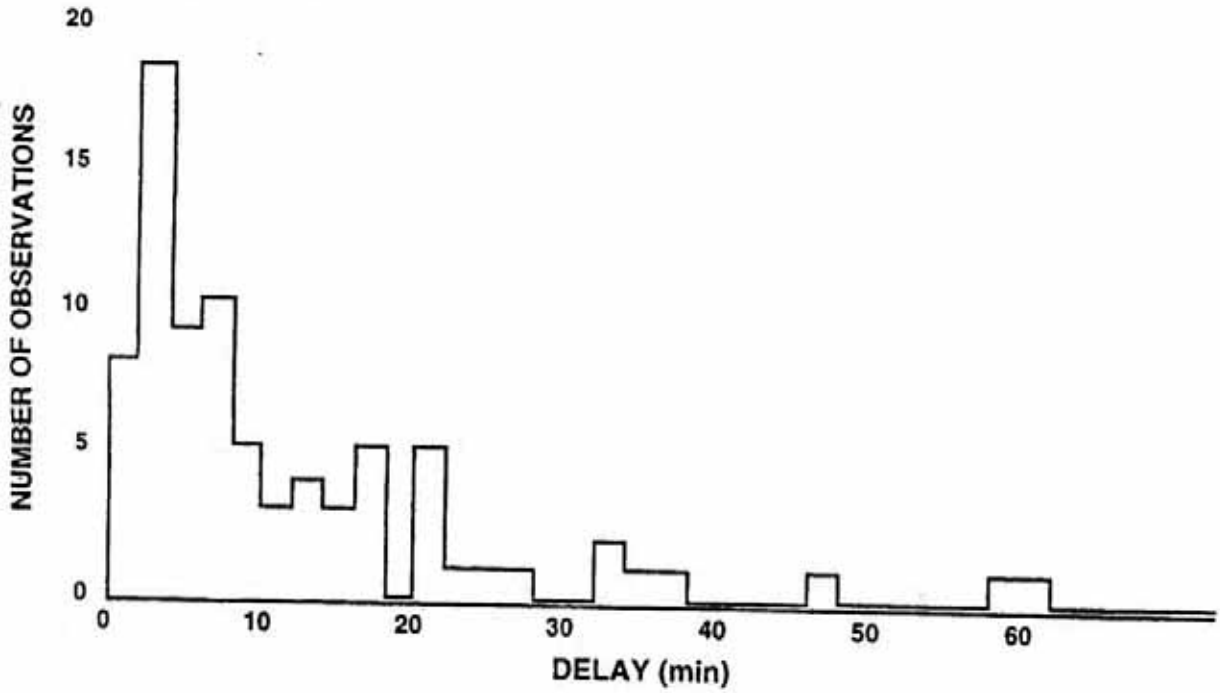

Figure 25. Distribution of delay between first intracloud and first cloud-to-ground flash in Florida thunderstorms.

In all cases, the first lightning flash in the storms observed was intracloud. The median of the distribution, a number which will be invoked in subsequent benefit calculations, is about six minutes.

Measurements of the ratio of intracloud to cloud-to-ground lightning vary widely, depending on the geographic location of the measurement, the type of thunderstorm (e.g., severe/non-severe) and the thundercloud life-cycle phase. Where reliable measurements of both lightning types have been available, IC to CG ratios of 10:1 are typical of recent measurement programs. For the severe weather cases listed in Table 3, IC to CG ratios of 10:1 to 40:1 are evident.

Both the precedence of cloud flashes and their higher overall rate support the contention that–in storms where a significant fraction of the overall ground strike exposure occurs during the developing phase of the storm–LMS' capability to detect intracloud lightning would allow for an earlier warning of ground strike hazard. We expect that the incremental benefit is small for "line storms"–synoptically-organized, long-lived thunderstorm systems where ground flashes occur at a significant rate for a major fraction of the storm's life cycle. Reliable ground strike warnings for such storms could presumably be generated using NLDN detections of CG lightning, in

combination with radar detection and tracking of the storms. Air mass or "pulse" thunderstorms, by comparison, have significantly shorter durations and typically move more slowly; thus the initial minutes of ground strike hazard constitute a significant fraction of the overall threat, and are likely to begin "on top of" potential victims. For this class of storm several minutes of threat anticipation based on IC lightning monitoring may provide a significant reduction in risk exposure.

A major dependency for realizing this benefit is the warning infrastructure required to rapidly alert affected individuals of the lightning threat. As shown in the following subsection, LMS' incremental benefits hinge on providing warnings only a few minutes earlier than might otherwise be possible. Data from the satellite would need to be quality controlled, clustered into "lightning cells" and/or merged with radar depictions of storm cells and used to generate alerts with very small latency. More challenging still would be dissemination to the large number of locations where lightning casualties are possible. The United States, for example, has roughly 15,000 golf courses, an equal number of municipal parks, numerous school grounds, swimming pools, etc., a significant fraction of which would need to be covered in order to accomplish a major reduction in threat. It is possible that this could be accomplished via cable TV and/or computer systems inter-connectivity (e.g., World Wide Web), although data latency issues need to be considered and software to generate site-specific warnings would be required.

Interviews with cognizant researchers and vendors/users of current NLDN data provided insights into this data dissemination issue. Our understanding is that Global Atmospherics, Inc. (GAI), the corporation that collects and disseminates NLDN data, has had difficulty in tapping this distributed market for ground strike warnings. Costs for access to and display of NLDN data (several thousands dollars per year) apparently dissuade many potential customers. Litigation concerns in the event that a lightning strike casualty occurred in the presence of an advertised warning capability were also apparently an issue. We did, however, find that some outdoor recreation and employment facilities are subscribing to NLDN-generated warning services. Examples are the Robert Trent Jones golf courses in Alabama (seven courses), a "traveling" system used during the Professional Golfers Association (PGA) tournaments, several entertainment parks in central Florida (Disney World and Wet and Wild) and airports (e.g., Orlando International Airport). Given the limited effort we were able to put into this search for NLDN users, we expect that a much larger subscriber-base exists.

Reactions to the possibility of NWS Weather Forecast Offices (WFO) providing lightning ground strike alerts were mixed. A number of forecasters expressed enthusiasm for this concept, provided that adequate data feeds to the WFO were in place. An approximately equal number however, expressed skepticism that such alerts were practical and stated that this class of threat would best be handled through better education of the public.

6.1.3. LMS Ground Strike Warning Benefit Model

Figure 26 depicts "data" that were input to the ground strike benefits model described in this section. Holle, et al., (1993) examined NLDN data in proximity to documented lightning casualties in Florida. They report that 41 percent of the casualties occurred during "infrequent" lightning, defined as an average CG rate of less than 1 per 4 minutes within a 16 x 16 nmi box surrounding the strike point. Although total lightning rates may have been significantly higher during such periods (e.g., 2 to 3 per minute, assuming a 10:1 IC to CG ratio), we will assume that generation of automated ground strike hazard warnings would be problematic in these conditions, owing to the likelihood that they would be perceived as false alerts. Thus 41 percent

of current casualties are assumed to be the result of "bolts from the blue" and are excluded from subsequent benefit modeling. An alternate approach, not pursued here, would be to construct a different threat reduction response for this segment of the exposed population–presumably with a higher residual exposure level since a smaller fraction of warned individuals would react.

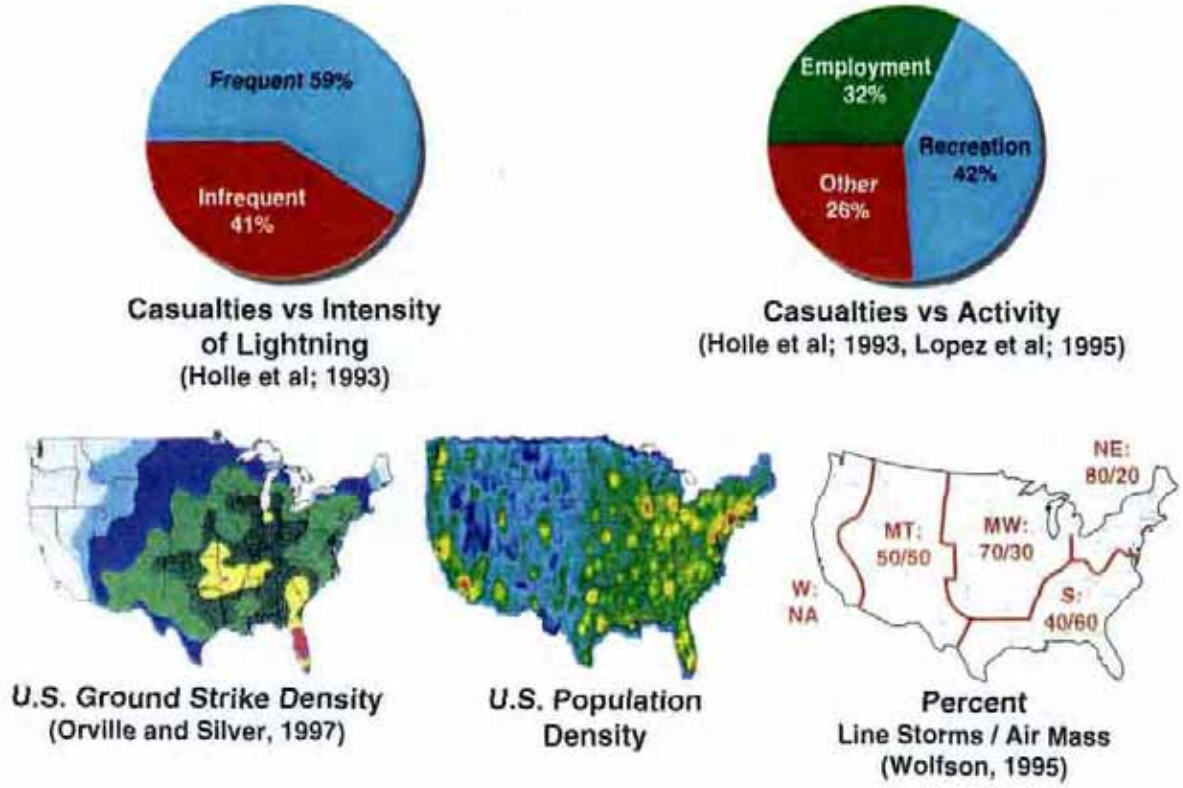

Figure 26. Data used in estimating LMS benefit for human warnings of lightning ground strike.

Lopez, et al. (1995) and Holle, et al. (1993) published information on the activities of Colorado and Florida lightning strike victims at the times of the incidents. As discussed below, these are used in modeling the responses individuals undertake to reduce their exposure when they become aware of a lightning threat. We took the average of the above two papers' reported fractions of victims involved in recreational activities (42 percent) and employment related activities (32 percent). An additional 26 percent of victims were listed as engaged in "other" activities. Lacking better information, we assigned one-half of these to the "recreational" category and one-half to the employment category for subsequent analysis.

The exposures of potential lightning victims to "line" and "air mass" thunderstorms were estimated using a Lincoln Laboratory study of the relative frequencies of these two broad thunderstorm types at a number of U.S. locations. This involved manual analysis of radar composite images, surface observations and other pertinent data sources during the summer months (April - September, 1994). The analysis was performed for Dallas-Ft. Worth, Atlanta, Chicago, and New York City and results were generalized to the regional fractions shown in Figure 26. Weighting these estimates by the U.S. regional distributions of population and ground strike density (the latter from Orville and Silver, 1997), we estimate that approximately 55 percent of U.S. CG lightning exposure occurs in association with line thunderstorms.

Figure 27 illustrates the model–similar to that in Section 3–used to assess the benefits of an earlier lightning threat warning. For simplicity we assume that the threat is of constant level for a period of 20 minutes, a typical duration for both the passage of a line-storm and for the electrically active phase of an air mass thunderstorm. When individuals become convinced that a threat is present (this time is designated "t_w"), they act so as to reduce the probability of a strike according to the linear functions shown in the lower part of the figure. We assume that, on average, individuals involved in recreational activities require a significant period of time (10 minutes) to reach shelter and that a constant residual level of exposure remains (0.25 of their initial exposure). Golfers completing their current hole and moving to shelter, boaters steering their vessels to shore, hikers seeking a sheltered spot are examples of the responses modeled here. In the case of individuals at work, we expect that buildings or vehicles will be available for shelter at or near the job site; thus our model assumes that risk is reduced to negligible levels by two minutes after the time that the threat is perceived.

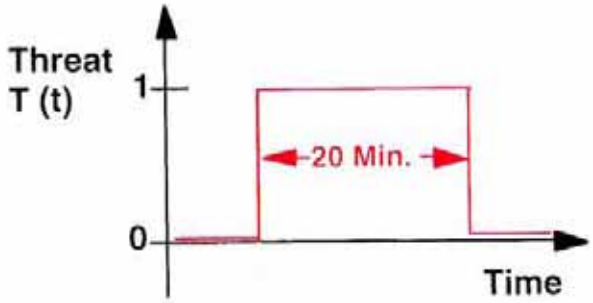

$$\text{Residual Threat} = \frac{\int T(t)\,R(t)\,dt}{\int T(t)\,dt}$$

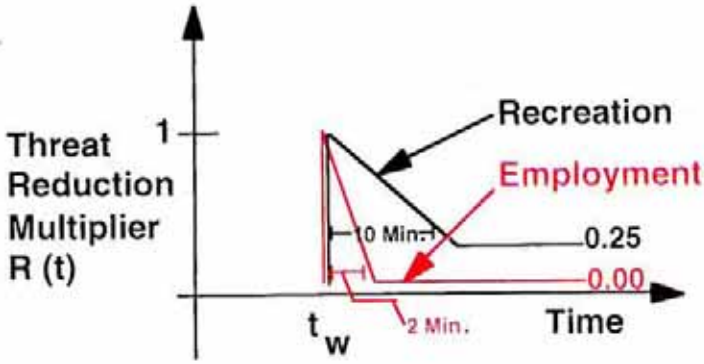

Figure 27. Model for estimating LMS benefit for human warning of lightning ground strike.

Assumptions on the time of warning, t_w, are shown in Table 22 for three warning system scenarios. The first models the current situation where perception of lightning exposure relies primarily on the eyes and ears of threatened individuals. We assume that individuals become aware of lightning in approaching line storms at a range of approximately 5 nmi–a typical audible range for thunder. Assuming an average storm propagation speed of 20 kts, this corresponds to 15 min. Allowing for 10 minutes of "integration time" for the individual to determine that the lightning is sustained and that the storm is indeed approaching his position, we set t_w equal to -5 minutes for this case. For air mass thunderstorms, we assume that five minutes

are required following the first proximate ground strike for the individual to perceive that sustained lightning is occurring and to initiate his avoidance response.

Table 22.
Lightning Warning Time t_w, Relative to Beginning of the Threat Period

Scenario	Line Storm	Air Mass
1. No warning system (current situation)	-5 minutes	5 minutes
2. Real-time warning system–no new sensors	-10 minutes	2 minutes
3. Real-time warning system–LMS	-10 minutes	-4 minutes

Scenario 2 assumes that an automated, real-time lightning warning system has been put in place using existing sensors (e.g., WSR-88D for storm identification and tracking; NLDN for CG lightning detection). For both storm types, the ability to view the storm and its lightning macroscopically and to track movement could presumably lead to earlier average lead times. For line storms, we assume that at least 10 minutes lead time for CG lightning warnings would be feasible (further improvement is irrelevant with the response models shown in Figure 27). For air mass storms, the required warning system integration time following the first CG flash is taken as two minutes, corresponding to perhaps 2 to 5 NLDN flash detections.

LMS' capability for IC lightning detection is included in scenario 3. This is assumed to move the warning time for air mass thunderstorms 4 minutes prior to the first ground flash. We estimate this value for t_w using the median lag between the first IC and CG flash from Figure 25, and again the assumption of a requisite 2 minute warning system integration time.

The fractional residual threat (FT) for combinations of individual activity, storm type and warning system scenario are tabulated below in Table 23. These are calculated in straightforward fashion according to the definition shown in Figure 27. Note that, as in Section 3, these capture the residual threat relative to that which would be present if no avoidance activity whatsoever were undertaken.

Table 23.
Fractional Residual Threat (FT) for Cloud-to-Ground Lightning

Scenario	Line Storm–Employment	Line Storm–Recreation	Air Mass–Employment	Air Mass–Recreation
1. No warning system (current situation)	0	0.30	0.30	0.63
2. Real-time warning system–no new sensors	0	0.25	0.15	0.51
3. Real-time warning system–LMS	0	0.25	0	0.32

Conclusions from the model can now be presented using the constraints imposed by the input data and the tabulated residual threat. Partitioning of current casualties into the categories indicated by the columns of Tables 24 and 25 are consistent with the fractions of low flash rate storms, employment versus recreation activity, and line versus air mass storm exposure described above. The residual threat tabulations of Table 23 are then used to extrapolate current casualties to:

1. That which would occur in the absence of any avoidance response by threatened individuals;

2. The reduced casualty rates that could be achieved if **all** threatened individuals were covered by the assumed warning systems.

Table 24.
Annual Lightning Fatalities vs. Warning Scenario

	"Bolts from the Blue"	Line Storm, Employment	Air Mass, Employment	Line Storm, Recreation	Air Mass, Recreation	Total
No Avoidance	26	Undetermined	57	26	20	129
No Warning System (Today)	26	0	17	8	13	64
Warning System (Current Sensors)	26	0	8	6	10	50
Warning System (LMS)	26	0	0	6	6	38

??

.45 x .45

.55 x .55

Table 25.
Annual Lightning Injuries vs. Warning Scenario

	"Bolts from the Blue"	Line Storm, Employment	Air Mass, Employment	Line Storm, Recreation	Air Mass, Recreation	Total
No Avoidance	148	Undetermined	320	144	115	727
No Warning System (Today)	148	0	97	43	72	360
Warning System (Current Sensors)	148	0	47	36	58	289
Warning System (LMS)	148	0	0	36	36	220

Several comments on Tables 24 and 25 are warranted. At least one of the assumptions of the model can be checked using these tabulated results. Our assumptions imply that "common sense" avoidance actions by individuals today alleviates the line-storm related threat for individuals at a job site who can move quickly to shelter. This in turn, implies that employment-related lightning casualties should be minimal for those regions of the U.S. (northeast and midwest) where lines storms are the predominate convective structure. Examination of "Storm Data" reports of the circumstances surrounding lightning casualties could be performed as a "sanity check."

The tables assumed that all current lightning victims would receive alerts from the envisioned warning systems. Realistically, a sizable fraction of individuals exposed to lightning would likely not be reachable; the incremental savings of life would be reduced in proportion to the fraction of the exposed population that is "out of earshot" of the warning. As an example, if we assume that 25 percent of exposed individuals receive warnings from the envisioned automated systems, the "total" columns of Tables 24 and 25 are modified as shown in Table 26.

Finally, the factor of two reduction in casualties that we model to result from today's "common sense" avoidance procedures reinforces the intuitive notion that better education of individuals to the lightning threat, and to appropriate avoidance actions, could significantly reduce casualties even in the absence of technology-based warning systems.

Table 26.
Annual Lightning Casualties vs. Warning Scenario, Assuming that only 25 Percent of Exposed Individuals Receive Automated System Warning

	Fatalities	Injuries
No Avoidance	129	727
No Warning System (Today)	64	360
Warning System (Current Sensors)	61	342
Warning System (LMS)	58	325

6.1.4. Discussion

Our fact-finding interviews indicate that, at least in situations where concentrated populations of individuals are exposed to lightning threat, interest in remote-sensing based warning systems (currently primarily NLDN) is real. A number of commercial sector warning systems are currently in use, although considerations of cost and litigation exposure are apparently slowing deployment.

Our simple model suggests that if implemented widely, such real-time lightning warning systems, even using current storm monitoring technology, would result in an economically significant reduction in loss of life, using the value of life assumptions discussed previously. The practicality of such a system reaching a major fraction of threatened individuals is, of course, a point of debate. Introduction of the capability to monitor total lightning activity from LMS doubles the incremental benefit according to this model.

6.2. Economic Disruptions Due to Ground Strike Threat

6.2.1. Overview

In the interest of safety, a variety of outdoor work places routinely suspend employee activity when the threat of lightning ground strike is deemed significant. Obvious examples are construction, agriculture, recreational facilities and airfield ground operations. Other industries, for example the electric power distribution industry, must significantly alter their normal mode of operation during ground strike threat, often at substantial cost. In the absence of positive information on the lightning threat, many such suspensions are longer than necessary. Widely used activity-suspension criteria are ominous clouds and/or thunder. Visually impressive cumulus congestus clouds may, however, develop well in advance of strong electrification and certainly before ground strike danger is imminent. Likewise, thunder may be heard from storms well removed from the listener and may confuse his perception of the threat posed by nearby clouds.

Even the more advanced CG threat assessment technologies such as weather radar, ground electric field "mills" and NLDN are imperfect. Radar–particularly the "composite" reflectivity widely available from commercial vendors of WSR-88D products–cannot reliably identify which storms are producing lightning unless reflectivity and vertical development are well in excess of the "threshold values" typical of newly electrified storms. Ground electric field mills are subject to long false-alert periods due to electrified stratiform precipitation and/or thunderstorm debris clouds. Explicit detection of CG lightning from NLDN is probably the most effective means for assessing the threat and has seen widespread application in large, lightning sensitive industries. However, NLDN's inability to provide precursory information in all situations requires either accepting some level of risk from the initial lightnings in a storm, or the use of other criteria/technologies (i.e., those discussed above) in initiating the lightning threat response.

It is plausible that LMS' capability to detect the IC lightning that systematically precedes the first ground flashes from a storm would facilitate initiating work-suspensions or changed operation modes closer to the time at which the actual ground strike threat begins. The amount by which the "alert" period could be reduced is difficult to estimate owing to the near absence of operational experience with total lightning data. The following sub-section describes an analysis (Madura, 1997) of work-suspension reductions achievable at Kennedy Space Center using the LDAR system described previously. His analysis indicates a yearly alert-period reduction of 560 hours at KSC, although it is not clear that reductions that could be achieved in the absence of total lightning data (using, for example, operational weather radar and NLDN) are fully accounted for. In the assessment of electric power industry potential savings in sub-section 3, we assume an average alert-period reduction of 5-10 minutes. An argument for this assumption is that the typical duration of the initial "IC-only" lightning phase–0 to 10 minutes (Figure 25)–is 5 to 10 minutes shorter than the "radar-ambiguous" storm phase where peak reflectivity and echo height transit the range of values (30-50 dBz, 6-10 km MSL) typical for the onset of strong electrification (Dye, et al., 1989; Henry and Wilson, 1993).

Incremental benefits in this area may not be attributable to LMS for moving line storms, where, as described in the preceding sub-section, weather radar and NLDN provide data sufficient to reliably define the ground-strike threats in advance of the storm's arrival. We previously estimated that such storms are responsible for 55 percent of CG lightning exposure in the United States.

6.2.2. Lightning Advisories at the NASA Kennedy Space Center

Benefit Areas

Lightning activity and severe weather in the vicinity of the NASA Kennedy Space Center (KSC) and Cape Canaveral Air Station (CCAS) have an enormous impact on Space Shuttle and unmanned launch vehicle preparations. An estimated 2000-3000 cloud-to-ground lightning strikes per year occur within 5 nm of any of the dozen space launch, processing, and support sites located here. Lightning warnings and advisories are issued for a 5 nm radius area surrounding any of these sites, four of which are Space Shuttle related. Accurate lightning hazard advisories increase safety by keeping personnel (primarily those people working outdoors) out of danger and improve productivity by reducing unnecessary labor down time. Despite the location of KSC/CCAS in the lightning capital of the US, and the suddenness with which thunderstorms develop locally, no ground operations personnel have been injured by lightning.

Lightning advisories at KSC are currently issued as a two-phase process. The Phase 1 advisory is intended to provide a 30 minute lead time and is issued when the potential for lightning exists within 5 nm of a specific site. This advisory provides lead time to ground crews requiring extra lead time to secure their operations. The Phase 2 warning is issued when lightning is imminent or observed. This warning is tailored to support ground operations requiring minimal time to react. The end result is that unnecessary labor down time is minimized without compromising safety. At the Titan launch complex alone, Phase 1 advisories were in effect for 314 hours in 1995 and 339 hours in 1996. Phase 2 warnings were in effect for only 118 hours in 1995 and 126 hours in 1996.

Total lightning data from the KSC LDAR system have increased the forecasters' confidence about when to issue lightning advisories/warnings. This increases both safety (fewer warnings with zero lead time) and decreases the amount of lost ground time (fewer false alarms). Knowing exactly if, when, and where any and all lightning is occurring allows forecasters to be much more site and time specific. Total lightning data uniquely enable the Phase 1-2 advisory process to be more precisely implemented.

Canceling the advisory or warning is as important as issuing with respect to ground operations safety and productivity, but more difficult because radar and field mills are less useful. LDAR has significantly increased the forecasters' confidence that the danger has passed and has reduced the length of time between the last lightning strike and the time the Advisory/Warning is canceled.

Finally, LDAR and total lightning information are important in evaluating Rule F (debris clouds) of the lightning launch commit criteria (LCC). Thunderstorm debris clouds must be greater than three hours old before they are considered safe to launch through. When a thunderstorm decays, there can be a large uncertainty as to when to begin the three-hour clock–especially for distant storms. If the Launch Weather Team has total lightning information available, the team can much more precisely determine the beginning time of the thunderstorm's demise as a charge producer and start the clock. Reducing this uncertainty and resulting ultra-conservatism increases launch availability. This is so important, KSC is researching the feasibility of extending the LDAR range to the west coast of Florida, to improve their ability to begin the clock on upstream thunderstorms whose debris cloud may advect over the launch path. Total lightning data are also extremely helpful for evaluating debris clouds coming from the data void ocean area to the east.

Value Analysis

The analysis assumes that if no forecast support were available, operations managers would implement lightning precautions whenever they perceived threatening weather. The duration of such "threatening weather" episodes can be estimated by the number of hours an advisory for lightning within 25 nm was valid prior to the implementation of LDAR as an operational support tool (1307 hours in 1992–the only year complete data were available at the time of the analysis).

Following implementation of LDAR, the availability of Phase 1 advisories and Phase 2 warnings allowed lightning-sensitive ground operations to continue. People continued working longer, well beyond what might be perceived as threatening or hazardous weather if no other weather support was available. (From April 1994 to March 1995, Phase 1 advisories were valid for 476.5 hours and Phase 2 warnings for 270.5 hours).

As shown in Table 27, the approximate number of base personnel impacted by lightning advisories in Shuttle Launch Complex (SLC)-39 and Industrial areas is 700. An additional 75 people are affected at the Shuttle Landing Facility (SLF), Vehicle Assembly Building (VAB), and Orbital Processing Facility (OPF) areas. However, not all are on duty simultaneously.

Table 27.
Breakdown of KSC Personnel Affected by Lightning Advisories

Shift	# People Affected	% of Advisories	Equivalent # People
1st	550	60	330
2nd	175	40	70
3rd	50	< 1	0

Therefore, it is assumed that 400 people are affected by each advisory. The average cost for an employee affected is assessed at $46/hour.

The savings from Phase 1-2 advisories is equal to the labor hours lost if lightning sensitive work ceased too early under threatening weather (25 nm advisories) minus labor hours actually lost because work is allowed to continue until the Phase 1-2 advisory is issued. Under the previous "25 nmi threatening weather" warning criteria, yearly lost labor costs were:

$$\begin{aligned} C1 &= (\text{\# hours 25 nm advisories valid}) \times (\text{\# people affected}) \times (\$46/\text{hour}) \\ &= 1307 \times 400 \times \$46 = \$24.1\text{M} \end{aligned} \tag{21}$$

With current warning criteria, the cost if lightning sensitive work stops only while Phase 1 advisories are valid is:

$$\begin{aligned} C2 &= (\text{\# hours Phase 1 valid}) \times (\text{\# people affected}) \times (\$46/\text{hour}) \\ &= 476 \times 400 \times \$46 = \$8.8\text{M}. \end{aligned} \tag{22}$$

Correspondingly, if lightning sensitive work stops only while Phase 2 warnings are valid, costs are:

$$\begin{aligned} C3 &= (\text{\# hours Phase 2 valid}) \times (\text{\# people affected}) \times (\$46/\text{hour}) \\ &= 270 \times 400 \times \$46 = \$5.0\text{M}. \end{aligned} \tag{23}$$

It is estimated that 20 percent of operations at KSC stop at Phase 1 and the remaining stop work at Phase 2. The yearly estimated savings realized through the total-lightning based Phase 1-2 advisory system is therefore:

$$\text{Total Savings} = (0.20) \times (C1\text{-}C2) + (0.80) \times (C1\text{-}C3) = \$18.3\text{M}. \tag{24}$$

Discussion

The value analysis for Phase 1-2 advisories illustrates the magnitude of the savings that can be achieved by one institution (NASA KSC) from one program element (Space Shuttle ground processing) by implementing a total lightning based advisory process. The savings cited here do

not include the considerable savings to Atlas, Delta, Titan, and other commercial and DOD launch programs. This savings is believed to come at no reduction in safety.

The analysis presented here does not include potential savings to KSC and CCAS space programs from an earlier termination of the end of storm threat. An earlier termination of an advisory can offer savings estimated to be as large as the savings from the initial issuance of the advisory (Madura, 1997). This call has proved to be difficult, yet is of great interest at other NASA field centers (MSFC, JSC, Stennis, Wallops) and contractor facilities (e.g., Thiokol facilities in Utah) where rocket launches, motor testing, and solid fuel manufacturing takes place.

6.2.3. Electric Power Generation and Distribution

Benefit Areas

Lightning is responsible for approximately 50 percent of the power failures in regions of the U.S. where thunderstorms are most active, costing U.S. electric utility companies as much as $1 billion per year in damaged equipment and lost revenue (Diels, et al., 1997). For Duke Power, a major electricity supplier in the southeastern U.S., lightning causes 90 percent of power outages during the summer (Keener, 1997). Based on 1990 "Outage System" data, the national average was 25 outage minutes per customer attributable to lightning. Lightning has caused at least one serious malfunction at a nuclear power plant (Angle and Hutchinson, 1994).

Through the use of real-time lightning location information from the NLDN, individual utility managers report having saved more than one half million dollars annually by quickly pre-positioning and dispatching repair crews to sites expected to be under the threat of lightning strikes or have already sustained damage. Duke Power (Keener, 1997) estimates savings of $200,000 annually. Approximately $60,000 or 1/3 of this savings is reduced labor costs (Bowden and Keener, 1993) and the remainder accrues from reduced outage time. The number of personnel involved in lightning outage responses is typically several dozen, comprised of customer service representatives ($10 per hour), dispatch center staff and contract line crews ($50 to $100 per hour). Repairs are often scheduled after normal working hours to handle storm related outages, yet service must be restored as quickly and safely as possible.

Con Edison ramps up more expensive in-city generation in preparation for the possible loss of overhead transmission lines due to lightning. This transition takes 15-20 minutes. Use of NLDN data makes it possible to reduce the length of the thunderstorm watch periods, enabling the utility to reduce unnecessary operating costs and take timely precautionary measures (Maffetone, et al., 1991). Con Edison estimates that NLDN data reduced the thunderstorm-watch time by 68 minutes on average for each storm during the period 1983-1986. During this period, 122 watches were issued with a 138 hour reduction in watch time or 35 hours per year. The cost of maintaining a watch is estimated at $6400 per hour in 1997 dollars. Thus, the 35-hour watch reduction saves an estimated $220,000.

A National Benefit Estimate for LMS Data

The Electric Power Research Institute (EPRI) estimates there are 3300 utility companies with 3400 plants within the U.S. Perhaps as many as one-third or approximately 1000 utility companies suffer the $200 million to $1 billion annually in damage and lost revenue due to lightning (Bernstein, 1997). Thus, the average cost per affected utility is at least $200,000 per year.

If we assume that 1000 utilities are affected by lightning as Duke Power and Con Ed are affected, then one estimate for the incremental benefit from total lightning is the reduction in the length of the watch period where more expensive generation or transmission modes are required. As discussed in Section 6.2.1, we have assumed that a 5 to 10 minute reduction in this period is possible using data from LMS. Using the figures reported by Con Ed, a ten-minute lead time produces a 15 percent (10/68) incremental savings beyond the watch time reduction realized through NLDN. Per annum, this would total 5.1 h per year (35 h x 10/68) in annual watch reduction and would save the utility industry $33 million per year (5.1 h x $6400 x 1000 utilities). More conservative assumptions of a five-minute average watch time reduction, and accounting for the above-mentioned likelihood that LMS' incremental benefit would be small for line storms, result in a yearly national benefit estimate of $ 7 million.

Discussion

The above calculation considers only one aspect of power company savings–reducing the duration of higher operating cost periods–and uses cost values appropriate for a specific company. A comprehensive analysis would assess whether LMS total lightning data could reduce customer outage time and/or repair crew costs and would consider the varying operating costs and revenues for utilities in different parts of the U.S. This analysis exceeds the scope of the present effort.

In addition to utility companies, users of back-up or emergency power who need to decide on using alternative, more expensive sources of power in the advent of a power outage could benefit from more reliable data on the onset and cessation of CG lightning threat periods.

7.0. SUMMARY, DISCUSSION AND RECOMMENDATIONS

7.1 Aggregate Benefits

Table 28 summarizes the benefit estimates from the previous sections. For the severe weather benefit, we have entered the average of the two estimates provided for each category considered in Section 3; that is, with and without the assumption that LMS data will improve warning detection probability as well as lead time. The casualty benefit entries for the ground strike category are from Table 26 where we assumed that 25 percent of exposed individuals would receive warnings from envisioned new warning systems that employ LMS data. The "operating costs" entry for this category reflects the more conservative of the two electric power utility benefit estimates in the second subsection under Section 6.2.3.

As a rough estimate for the aggregate dollar value of these benefits, we entered a value for human life of $1.5 million, $50,000 as the average costs of a serious injury and $5,000 for a minor injury. We assumed that 20 percent of the injuries averted would have been serious. In totality, the benefits estimated are substantial in relation to the projected costs of the LMS. MSFC estimates the sensor cost at approximately $10 to $15 million (Christian, 1997), which would be prorated over the GOES five-year operational lifetimes.

Table 28.
Summary of LMS Annual Benefits Estimates

Benefit Category	Fatalities	Injuries	Property Damage or Operating Costs
Severe Weather Warning	9	135	$6M
Flash Flood	0	0	$ 2 M
Aviation	–	–	$ 25M
Lightning Ground Strike	3	17	$7M
Total	12	152	$ 40M
Monetized Value	$60 M		

The methodology and data collected for evaluation of LMS severe weather, flash flood and ground strike casualty and property damage benefits allow for expression of these benefits as percentages of the overall toll of convective weather in the areas considered, and of the benefits that are already being realized through warnings generated using existing operational sensors. This representation of LMS aggregate benefits is given in Table 29. The LMS incremental benefit relative to that realized using existing sensors has been estimated as:

$$\text{Incremental Benefit} = [\text{Baseline} - \text{LMS}]/[\text{Baseline-Current}] - 1 \qquad (25)$$

where "Baseline," "LMS" and "Current" are aggregates from the corresponding rows of the appropriate benefit summary tables in Sections 3, 4 and 6.

Table 29.
LMS Benefits for Severe Weather, Flash Flood and Ground Strike Expressed Relative to Total Societal Toll and Relative to Current Warning System Benefit

	LMS Reduction relative to Current Societal Toll	LMS Incremental Reduction relative to Current System Reduction
Fatalities	6%	8%
Injuries	8%	15%
Property Damage	< 1%	3%

This scaling emphasizes that the estimated LMS benefits, while substantial in absolute terms, constitute a modest increment relative to the current societal toll of convective weather phenomena and indeed, relative to the benefits already being realized using existing operational sensors. The principal aviation benefit we ascribed to LMS–reduced operating costs to airlines–is likewise modest in relative terms. The FAA currently estimates that thunderstorms cost the airlines and U.S. public approximately $2 billion per year in operating costs and passenger delay. The FAA's Integrated Terminal Weather System–targeted primarily towards reduction of delay caused by thunderstorm activity in terminal airspace–is estimated to result in aggregate savings of $250 million per year.

7.2 Confidence in Assumptions

Overall, the authors believe that the assumptions employed in this study were not biased either towards or against the proposition that LMS provides operational "value." We freely admit the necessity of assigning numerical values to many important entries in the benefits calculations based on incomplete information. Estimates of LMS-based warning and/or operational decision-making enhancements were, in many cases, based on data and insights obtained from the Florida LISDAD demonstration. An example is the assumptions relative to severe weather warning lead-time enhancements. In other cases, interviews with technically and/or operationally cognizant personnel were conducted, and the technical literature was examined to ascertain whether justification for LMS-based incremental capability was present. We then used our best judgment in developing performance assumptions to establish the order-of-magnitude for LMS-produced operational capability improvements.

Examples of capability improvements which we estimated using our own best judgment are:

1. The flood-warning detection probabilities that would be achievable using CG or total lightning data in radar coverage gaps (Section 4);

2. The percentage of oceanic thunderstorms that would be detected using LMS (Section 5).

While the numerical values we used are certainly open to discussion, we believe that the qualitative results from the associated analyses–that the flood warning incremental benefit is small whereas that associated with aviation outside the CONUS is significant–are valid.

A second major element of the benefits calculations was models for the effect of warnings or operational decisions in reducing casualties, property damage or operating costs. The extent to which these can be disputed varies considerably. In the case, for example, of airline operating costs and associated benefits in more efficient flight diversions around weather, we believe that the major inputs are well established. Airline management tracks most of the relevant parameters routinely since they are critical to profitability. Conversely, our models of human reaction to convective weather warnings rely heavily on best judgment drawn from case studies and other anecdotal information. Obviously, the parameters input to these models can be questioned: indeed, the authors freely concede that additional effort in developing "sanity-checks" and discussing these assumptions with personnel familiar with public-warning issues would be very valuable. Overall, however we again believe that our assumptions are unbiased and capture the order-of-magnitude benefit sufficiently to draw conclusions as to the operational value of LMS.

7.3 Open Issues

Our generally positive conclusions as to the operational efficacy of LMS must be qualified with explicit consideration of their dependency on phenomenological relations, technical capabilities and infrastructure not fully demonstrated. Assumptions on the consistency of relations between lightning and other operationally relevant storm phenomena, on the existence of robust algorithms for reliably alerting operational personnel to appropriate lightning signatures and on the existence of appropriate data communications, processing and display facilities were intrinsic to many of our benefits estimates. These issues are considered further in the following paragraphs.

7.3.1 Phenomenology

Further observational data on the severe weather lightning signals discussed in Section 3 are needed. As mentioned there, the nature of the extraordinarily high-rate intracloud lightnings that occur prior to and during severe weather needs to be clarified, particularly in relation to the how their optical emissions will be detected from space. This question, in turn, relates to the lightning-rate and rate-derivative thresholds that will be applicable for severe weather detection using LMS. The lightning "jump" phenomena needs further study. Is an episode of extreme lightning rate derivative a necessary and/or a sufficient condition for severe weather or can a longer-duration, lower-derivative increase that produces the same peak rate also presage tornadoes, hail or damaging winds?

Aggressive integration of lightning with other sensor data is probably essential in achieving large gains in severe weather warning capability. Much research has been conducted on relations between NLDN-detected CG lightning and severe weather, often with intriguing–if inconsistent–findings. Effort is needed to determine how information on IC/CG lightning rate ratios and/or CG current polarity complement the total lightning signals considered here. Perhaps more importantly, the lightning signals need to be explicitly linked to corresponding severe weather indications in radar and satellite visible and infrared imagery.

Better understanding of total lightning as a quantitative measure for rainfall would aid in determining its benefits for flood warnings or water management in radar coverage gaps. Although we identified a corpus of technical literature dealing with relations between rainfall and the widely available NLDN CG lightning, corresponding studies for total lightning are largely absent.

Lightning prevalence and relations between rates and storm intensity in oceanic convection need to be confirmed since favorable assumptions on lightning as a robust indicator of operationally important convection were used in estimating aviation benefits.

7.3.2 Algorithms

Without exception, the benefits we ascribed to LMS presumed the existence of robust algorithms for alerting operational personnel or affected individuals to relevant lightning phenomena. Necessary algorithms, summarized in Table 30, encompass "preprocessing" operations such as clustering optical pulses into flash-rate histories for individual radar cells, temporal/spatial "image" processing to delineate storm location and intensity in radar coverage gaps from the often sparse lightning data (see Appendix B), and methods for effectively integrating data from LMS with radar, NLDN and other GOES satellite sensors.

Table 30.
Partial list of LMS Data Processing Algorithms Necessary for Realization of Operational Benefits

Application Area	Required Algorithms
Preprocessing	Flash Counting Lightning/Radar Cell Association
Severe Weather	Static or adaptive rate and derivative thresholds Integration with NLDN/radar/satellite VIS/IR
Flash Flood and Water Management	Total lightning - rainfall conversion
Aviation	Storm image synthesis
Ground Strike Hazard	LMS data integration with radar/NLDN Warning generation logic

The authors believe that appropriate algorithms, with performance consistent with the assumptions of this report, are achievable. Aggressive development and validation efforts will be necessary, however, to realize necessary algorithmic capabilities by the time of likely LMS initial sensor deployments (ca. 2000-2003). As noted in several places in this report, data sets and operational experience with total lightning measurements are extremely limited and are likely to remain so until deployment of LMS. Continued exploitation of the LISDAD total lightning demonstration system in Florida (and indeed, its replication in other significant U.S. storm environments) is strongly recommended as a means of pursuing necessary algorithm development.

7.3.3 System Architecture

All the benefits we ascribed to LMS require that the satellite sensor's lightning detections be appropriately processed and transmitted to the end user with very low latency. Delays of even five minutes in accomplishing this would essentially eliminate all convective weather warning benefits (Sections 3, 4 and 6). En route and oceanic aviation routing benefits would probably remain with somewhat longer latencies although even here, the value of the information would undoubtedly degrade rapidly with "data age." The distributed disposition of the major beneficiaries of LMS data–NWS Weather Forecast Offices throughout the nation's severe weather belts, perhaps one half dozen major airline operations centers and the NWS Aviation Weather Center, and innumerable recreation, outdoor activity and employment sites–complicates

the data distribution task. Indeed, with respect to LMS' potential for providing improved ground strike warnings, this communications issue raises major uncertainty as to the magnitude of what is potentially a very large benefit.

The authors recommend that a study be conducted as soon as feasible to identify requirements and appropriate mechanisms for LMS data communication to operational users targeted to receive data from initial LMS deployments.

A second system architecture issue is the distribution of data processing tasks required for dissemination of LMS-based "information" to operational users. LMS data quality control, flash detection and geo-registration will presumably be accomplished on the satellite or at the central ground receiving/data-dissemination facility. It is likely that processing appropriate for convective weather warning responsibilities at individual WFO's will be accomplished using the Advanced Weather Information Processing Systems (AWIPS) under procurement by NWS. Software modifications and incremental processor loading required to utilize LMS data in AWIPS should be determined.

Dissemination of LMS-based information appropriate for aviation system usage, and for the general public (exclusive of WFO-generated warnings) may occur by way of commercial providers analogous to the NEXRAD Information Distributors (NIDs). The Government would provide LMS data over specified ports to selected distributors. Alternately, the Government could make LMS data available to any suitably equipped external user–for example, on a "Web-site". In either case, a determination is needed as to whether "raw" lightning data or some set of derived products be provided. In the latter case, a processing configuration suitable for handling generation of products over the huge domain covered by LMS would be necessary.

The analysis in this report indicates that Lightning Mapper Sensors operating on GOES satellites could provide considerable value to the U.S. public. As the Government continues with development and deployment of this sensor, the authors strongly recommend that demonstrations and analysis such as those described above be aggressively pursued in parallel. This strategy will allow for early realization of full benefits from LMS data, and will maintain a clearly defined rationale for the sensor during the inevitable budgetary ups and downs that will occur during its development cycle.

REFERENCES

Adler, R.F. and D.D. Fenn, "Satellite Observed Cloud Top Height Changes in Tornadic Thunderstorms," Journal of Applied Meteorology, **20**, 1369-1375, 1981.

Alexander, G.D., J.A. Weinman, and M. Karyampudi, "The Impact of Assimilation of Rain Rates Derived from Lightning and Satellite Data on Forecasts of the March 1993 Superstorm," *Monthly Weather Review*, submitted, 1997.

Angle, C. W., and C. R. Hutchinson, "Entergy Uses Lightning Network to Improve Nuclear Plant Availability during Storms," EPRI Innovator IN-104103, available from EPRI, P.O. Box 10412, Palo Alto, CA 94303, November, 1994.

Battan, L.J., "Some Factors Governing Precipitation and Lightning from Convective Clouds," *Journal of Atmospheric Sciences*, **22**, pp. 79-84, 1965.

Bernstein, R., Personal communication, 1997.

Black, R. A. and J. Hallett, "On the Electrification of the Hurricane," *Journal of Atmospheric Sciences,* submitted, 1997.

Black, R. A., Personal communication, 1997(b).

Boldi, R., Personal communication, 1997.

Bowden, George, and Ronald N. Keener, Jr., "Duke Power Uses Lightning Network to Reduce Crew Dispatch Costs," EPRI Innovator IN-101090, available from EPRI, P.O. Box 10412, Palo Alto, CA 94303, December, 1993.

Buechler, D.E., P.D. Wright, and S.J. Goodman, "Lightning Rainfall Relationships During COHMEX," *Preprints, 16th Conference on Severe Local Storms,* American Meteorological Society, pp. 710-714, 1990.

Buechler, D.E., H.J. Christian, S.J. Goodman, "Rainfall Estimation Using Lightning Data," *Seventh Conference on Satellite Meteorology and Oceanography*," June 6-10, Monterey, CA, American Meteorological Society, 1994.

Buechler, D.E., R.J. Blakeslee, H.J. Christian, R. Creasy, K. Driscoll, S.J. Goodman, and D.M. Mach, "Lightning Activity in a Tornadic Storm Observed by the Optical Transient Detector," *Preprints 18th Conference on Severe Local Storms*, American Meteorological Society, San Francisco, CA, February, 1996.

Burgess, D.W. and L.R. Lemon, "Severe Thunderstorm Detection by Radar," *Radar Meteorology*, D. Atlas, ed., American Meteorological Society, pp. 619-647, 1990.

Burgess, Personal communication, 1997.

Byers, H.R. and R.R. Braham, *The Thunderstorm*, U.S. Government Printing Office, June, 1949.

Cammarata, M.E., E.W. McCaul, Jr., and D.E. Buechler, "Observations of Shallow Supercells During a Major Tornado Outbreak Spawned by Tropical Storm Beryl," *Preprints, 18th Conference. on Severe Local Storms*, San Francisco, CA, American Meteorological Society, pp. 340-343, February 19-23, 1996.

Carey, L.D. and S.R. Rutledge, "A Multiparameter Radar Microphysical Study of the Kinematic Evolution of a Lightning-Producing Storm," *Meteorology and Atmospheric Physics*, **59**, pp. 33-64, 1996.

Chèze, J.-L. and H. Sauvageot, "Area-Average Rainfall and Lightning Activity," *Journal of Geophysical Research*, **102**, 1707-1716, 1997.

Christian, H.J., R.J. Blakeslee, and S.J. Goodman, "The Detection of Lightning from Geostationary Orbit," *Journal of Geophysical Research*, **94** (D11), 13329-13337, 1989.

Christian, H.J., R.J. Blakeslee, S.J. Goodman, and D.M. Mach, "Algorithm Theoretical Basis Document (ATBD) for the Lightning Imaging Sensor (LIS)," NASA, 53 pp. 1996.

Christian, H.J., Personal communication, 1997.

Diels, Jean-Claude, Ralph Bernstein, Karl E. Stahlkopf, and Xin Maio Zhao, "Lightning Control with Lasers," *Scientific American*, pp. 2-6, August, 1997.

Donaldson, R.J., "Analysis of Severe Convective Storms Observed By Radar," *Journal of Meteorology*, **15**, pp. 44-50, 1958.

Donaldson, R.J., "Radar Observations of a Tornado Thunderstorm in Vertical Section," Severe Storm Project, Report #8, U.S. Department of Commerce, April 1962.

DOT-FAA, "FAA Aviation Forecast–FY 1997-2008," Report No. FAA-APO-91-1. Approx. 200 pp., 1997.

Driscoll, K., Personal communication, 1997.

Dvorak, V.F., "Tropical Cyclone Intensity Analysis and Forecasting From Satellite Imagery," *Monthly Weather Review*, **103**, pp. 420-430, 1975.

Dvorak, V.F., "Tropical Cyclone Intensity Analysis Using Satellite Data," NOAA Technical Report NESDIS 11, 47 pp., 1984.

Dye, J.E., W.P. Winn, J.J. Jones, and D.W. Breed, "The Electrification of New Mexico Thunderstorms, I: Relationship Between Precipitation Development and Onset of Electrification," *Journal of Geophysical Research*, **94**, 8643, 1989.

Fahey, T., Personal communication, 1997.

Frost, R. Cumulus and cumulonimbus cloud over Malaya, Meteorological Office Air Ministry, *Meteorological Report* No. 15, 1954.

Fujita, T.T., *Mystery of Severe Storms*, University of Chicago Press, 298 pp, 1992.

Goodman, S.J., D.E. Buechler, P.D. Wright, and W.D. Rust, "Lightning and Precipitation History of a Microburst Producing Storm," *Geophysical Research Letters*, **15**, 1185-1188, 1988.

Goodman, S.J. and D.E. Buechler, "Lightning-Rainfall Relationships," *Preprints, Conference on Operational Precipitation Estimation and Prediction*, Anaheim, CA, 7-8 February, American Meteorological Society, pp. 112-117, 1990.

Goodman, S.J. and R. Raghavan, "Investigating the Relation Between Precipitation and Lightning Using Polarimetric Radar Observations," *Preprints, 26th International Conference on Radar Meteorology*, 24-28 May, Norman, OK, American Meteorological Society, 1993.

Gregory, S., Personal communication, 1997.

Grosh, T., "Lightning and Precipitation: The Life History of Isolated Thunderstorms," *Preprints, Conference on Cloud Physics and Atmospheric Electricity*, Issaquah, WA, American Meteorological Society, p. 617, 1978.

Henry, S. and J. Wilson, "Developing Thunderstorm Forecast Rules Utilizing First Detectable Cloud Radar-Echoes," *Preprints: Fifth International Conference on Aviation Weather Systems*, Vienna, VA, American Meteorological Society, 1993.

Holle, R., R. Lopez, R. Ortiz, C. Paxton, D. Peeker, and D. Smith, "The Local Meteorological Environment of Lightning Casualties in Central Florida," *Preprints: Conference on Atmospheric Electricity*, St. Louis, MO, American Meteorological Society, pp. 775-784, 1993.

Howard, K.W., J.J. Gourley, R.A. Maddox, "Uncertainties in WSR-88D Measurements and Their Impacts on Monitoring Life Cycles," *Weather and Forecasting*, **12**, 166-174, 1997.

Johnson, J.T., P.L. Mackeen, A. Witt, E.D. Mitchell, G.J., Stumpf, M.D. Eilts, and K.P. Thomas, "Storm Cell Identification and Tracking Algorithm: An Enhanced WSR-88D Algorithm," *Weather and Forecasting*, June, 1998.

Josephson, W., Personal communication, 1997.

Keener, Ronald N., Jr., "The Estimated Impact of Weather on Daily Electric Utility Operations," Workshop on the Social and Economic Impacts of Weather, Boulder, CO, 2-4 April, 1997.

Kinzer, G.D., Cloud-to-Ground Lightning vs Radar Reflectivity in Oklahoma Thunderstorms, *Journal of Atmospheric Sciences*, **31**, 787-799, 1974.

Krehbiel, P.R., "An Analysis of the Electric Field Change Produced by Lightning," PhD. thesis, University of Manchester (England), 1981.

Laroche, P., C. Malherbe, A. Bondiou, M.E. Weber, C. Engholm, and V. Coel, "Lightning Activity in Microburst Producing Storm Cells," *25th International Conference on Radar Meteorology*, Paris, France, 24-28 June, 1991.

Latham, D., Personal Communication, 1997.

Lee, A.C.L., "An Operational System for the Remote Location of Lightning Using VLF Arrival Time Difference Technique," *Journal of Atmospheric and Oceanic Technology*, **3**, 630-642, 1986.

Lee, T., Personal Communication, 1997.

Lemon, L.R., New Severe Thunderstorm Radar Identification Techniques and Warning Criteria: A Preliminary Report," NOAA Technical Memorandum, NWS NSSFC-1, Department of Commerce, July, 1977.

Lennon, C. and L. Maier, "Lightning Mapping System," International Conference on Lightning and Static Electricity, Cocoa Beach, FL, 1991.

Lhermitte, R. and P.R. Krehbiel, Doppler radar and radio observations of thunderstorms, IEEE *Trans. Geosci. Electron.*, GE-17(4), 162-171, 1979.

Lhermitte, R.M. and E.R. Williams, "Thunderstorm Electrification: A Case Study," *Journal of Geophysical Research*, **90**, 6071-6078, 1985.

Lopez, R., R. Holle, and T. Heitkamp, M. Boyson, M. Cherington, and K. Langfond, "The Under-reporting of Lightning Injuries and Deaths in Colorado," *Bulletin of the American Meteorological Society*, **74**, pp. 2171-2178, 1993.

Lopez, R., R. Holle, and T. Heitkamp, "Lightning Casualties and Property Damage in Colorado from 1950 to 1991 Based on Storm Data," *Weather and Forecasting*, **10**, pp. 114-126, 1995.

MacGorman, D.R., "Lightning in Tornadic Storms: A Review," *The Tornado: Its Structure, Dynamics, Predictions and Hazards*, Eds., C. Church, D. Burgess, C. Doswell, and R. Davies-Jones, *Geophysical Monograph* **79**, American Geophysical Union, May, 1993.

Madura, J., Personal communication with W. Fuller, KSC/RT-A, April 1995.

Madura, J., Personal communication, 1997.

Maffetone, T., D. Mark, W. Montgomery, and R. Noberini, "More Accurate Lightning Data Reduce Utility's thunderstorm Watch Periods," EPRI Innovator IN-100026, available from EPRI, P.O. Box 10412, Palo Alto, CA 94303, September, 1991.

Maier, M.W., A.W. Boulanger and J. Sarlat, "Cloud to Ground Lightning Frequency over South Florida," *Conference on Cloud Physics and Atmospheric Electricity*, American Meteorological Society, Issaquah, Washington, July, 1978.

Maier, L., C. Lennon, P. Krehbiel and M. Maier, "Lightning as Observed by a Four-Dimensional Lightning Location System at Kennedy Space Center," *10th International Conference on Atmospheric Electricity*, 380-383, Osaka, Japan, 1996.

Malherbe, C., J. Pigere, P. Blanchet, O. Deste, A. Bondiou, and P. Laroche, "Relation Entre L'activité Electrique D'Orage et le Développement de Microbursts–Experience MIT/ONERA," Orlando, FL, 1991, RF ONERA # B0516154P4, June 1992.

Martin Marietta, "Terminal Doppler Weather Radar Report," Report No. ATC-85-1004, Rev. 1, 1985.

Mazur, V., E. Williams, R. Boldi, L. Maier and D.E. Proctor, "Initial Comparison of Lightning Mapping with Operational Time-of-Arrival and Interferometer Systems," *Journal of Geophysical Research*, **102**, 11011-11085, 1997.

McCann, D.W., "The Enhanced-V: A Satellite Observable Severe Weather Signature," *Monthly Weather Review*, **111**, 887-894, 1983.

McCann, D., Personal communication, 1996.

McCaul, E.W., Jr., "Observations and Simulations of Hurricane-Spawned Tornadic Storms," in *The Tornado: Its Structure, Dynamics, Productions, and Hazards*, C. Church, D. Burgess, C. Doswell, and R. Davies-Jones, Eds., *Geophysical Monograph* **79**, American Geophysical Union, 1993.

McCaul, E.W, Personal communication, 1997.

McCollum, D., D. Bright, J. Meyer, and J. Glueck, "Operational Applications of the Real Time National Lightning Detection Network Data at the NWSO, Tucson, AZ," NOAA Technical Memorandum NWS WR-241, September, 1996.

Midkiff, A., Personal communication, 1997.

Molinari, J., P.K. Moore, V. P. Idone, R. W. Henderson, and A. B. Saljoughy, "Cloud-to-Ground Lightning in Hurricane Andrew," *Journal of Geophysical Research*, **99**, No. D8, pp. 16665-16676, August, 1994.

Molinari, J., P. Moore, and V. P. Idone, "Convective Structure of Hurricanes as Revealed by Lightning Locations, *Monthly Weather Review*, submitted, 1997.

Molinari, J.P., Personal communication, 1997(b).

Mosher, F., Personal communication, 1997.

National Oceanic and Atmospheric Administration, "A report on NEXRAD: National Airspace System Cost/Benefits," Report No. FCM-R6-1983, 1983.

National Research Council, "Toward a New National Weather Service–Assessment of NEXRAD Coverage and Associated Weather Services," Prepared by NEXRAD Panel, National Weather Service Modernization Committee, National Academy Press, Washington, DC, 104 pp., 1995.

Negri, A.J., "Cloud Top Structure of Tornadic Storms on 10 April 1979 from Rapid Scan and Stereo Satellite Observations," *Bulletin of the American Meteorological Society*, **63**, 1151-1159, 1982.

Nisbet, J.S., T.A. Bernard, G.S. Forbes, E.P. Krider, R. Lhermitte and C.L. Lennon, "A Case Study of the Thunderstorm International Project Storm of July 11, 1978 1. Analysis of the data base," *Journal of Geophysical Research*, **95**, 5417-5433,1990.

Orville, R.E., and A.C. Silver, "Lightning Ground Flash Density in the Contiguous United States: 1992-95," *Monthly Weather Review*, **125**, No.4, 631-638, 1997.

Petersen, W.A. and S.A. Rutledge, "Characteristic Differences in Cloud-to-Ground Lightning Flash Densities and Rain Yields for Different Climate Regimes," *International Conference on Atmospheric Electricity*, Osaka, Japan, 1996.

Piepgrass, M.V., E.P. Krider and C.B. Moore, "Lightning and Surface Rainfall During Florida Thunderstorms," *Journal of Geophysical Research*, **87**, 11193,11201, 1982.

Plumer, J.A., N.O. Rasch, and M.S. Glynn, "Recent Data from the Airlines Lightning Strike Reporting Project," *Journal of Aircraft*, **22**, 429-433, 1985.

Qualley, W., Personal communication, 1997.

Raghavan, R., S. Goodman, P. Meyer, B. Boldi, A. Matlin, M. Weber, E. Williams, D. Sharp, S. Hodanish, J. Madura, and C. Lennon, "A Real-time Examination of the Incremental Value of Lightning Data in Diagnosing Convective Storm Characteristics," *Preprints, Seventh International Conference on Aviation, Range & Aerospace Meteorology*, Long Beach, CA, American Meteorological Society, 1997.

Rasmussen, E.N. and J.M. Straka, "Mobile Mesonet Observations of Tornadoes During VORTEX-95, *AMS Conference on Severe Local Storms*, 1-5, San Francisco, CA., American Meteorological Society, February, 1996.

Rhoda, D., Personal communication, 1997.

Sentman, D.D. and G. Wescott, "Red Sprites and Blue Jets," videotape prepared by the Geophysical Institute, University of Alaska, Fairbanks, AK, 1995.

Sharp, D., Personal communication, 1997.

Spratt, S.M., and A.J. Nash, "Central Florida WSR-88D Observations and NWSO Operations During Tropical Cyclones Alberto, Beryl, and Gordon," *Preprints, 17th Conference on Hurricanes and Tropical Meteorology*, Miami, FL, American Meteorological Society, 298-300, 1995.

Stanley, M., P. Krehbiel, and W. Rison, "Lightning as a Precursor of Outflow and Downbursts from Thunderstorms," *28th Conference on Radar Meteorology*, Austin, TX, American Meteorological Society, pp. 151-152, 1997.

Stolzenburg, M., "Observations of High Ground Flash Densities of Positive Lightning in Summer Thunderstorms," *Monthly Weather Review*, **122**, 1740-1750, 1994.

Tapia, A., J.A. Smith and M. Dixon, "Estimation of Convective Rainfall from Lightning Observations, *Journal of Applied Meteorology*, (in press), 1998.

Troxel, S.W. and C.D. Engholm, "Vertical Reflectivity Profiles: Averaged Storm Structures and Applications to Fan-Beam Radar Weather Detection in the US," *Preprints, 16th Conference on Severe Local Storms*, Kananaskis Park, Alberta, Canada, American Meteorological Society, 1990.

Vescio, M. D., S. J. Weiss, and F. P. Ostby, "Tornadoes Associated with Tropical Storm Beryl," *National Weather Digest*, **21**, 2-10, 1996.

Volpe National Transportation Systems Center, Operations Assessment Division, "Cost, Benefit, and Risk Assessment Guidelines for R,E,& D Investment Portfolio Development," 55 pp., 1996.

Vonnegut, B. and C.B. Moore, "Giant Electrical Storms," in *Recent Advances in Atmospheric Electricity*, L.G. Smith, Ed., Pergamon Press, 1958.

Vonnegut, B., "Some Facts and Speculations Concerning the Origin and Role of Thunderstorm Electricity, *Meteorological Monograph*, **7**, 1963.

Williams, E.R., "Large-Scale Charge Separation in Thunderstorms," *Journal of Geophysical Research*, **90**, No. D4, 6013-6025, 1985.

Williams, E.R., M.E. Weber, and R.E. Orville, "The Relationship Between Lightning Type and the Convective State of Thunderstorms," *Journal of Geophysical Research*, **94**, 13213-13220, 1989.

Williams, E.R., "The Tripole Structure of Thunderstorms," *Journal of Geophysical Research*, **94**, 132151-13167, 1989.

Williams, E.R., S.A. Rutledge, S.G. Geotos, N. Renno, E. Rasmussen and T. Rickenbach, "A Radar and Electrical Study of Tropical 'Hot Towers'," *Journal of Atmospheric Sciences*, **49**, 1386-1395, 1992.

Williams, E.R., M. Weber, R. Boldi, and P. Laroche, "The Use of Lightning for the Detection of Microbursts and Other Aviation Hazards," White Paper for Lightning, Location, and Protection, Tucson, AZ, 1995.

Williams, E.R., "Meteorological Aspects of Thunderstorms," in *Handbook of Atmospheric Electrodynamics*, H. Vollard, Ed., Boca Raton, FL, CRC Press, 1995.

Williams, E.R., "The Electrification of Severe Storms," *Severe Storms Monograph*, C.A. Doswell, III, Ed., (in prep), 1997.

Wolfson, M.M., R.L. Delanoy, B.E. Forman, R.G. Hallowell, M.L. Pawlak, and P.D. Smith, "Automated Microburst Wind Shear Prediction," *The Lincoln Laboratory Journal*, **7**, 399-426, 1994.

Wolfson, M.M., personal communication, 1995.

Workman, E.J. and S.E. Reynolds, "Electrical Activity as Related to Thunderstorm Cell Growth," Bulletin of the American Meteorological Society, **30**, 142-144, 1949.

APPENDIX A
STUDY PARTICIPANTS

1. Technical Review Panel

Fred Mosher (Aviation Weather Center)
Gary Ellrod (NESDIS)
Hugh Christian (MSFC)
Dave Helms (NWS)
Dave Sharp (NWS, MLB WFO)
Dave Pace (FAA)
Don Burgess (WSR 88D OSF)
Don MacGorman (NSSL)

2. Interviewees

NLDN Vendors

Ken Cummins (GAI)

Researchers

Ron Holle (NSSL)
Don Burgess (OSF)
Don Latham (BLM)
Bill McCaul (USRA)
Bob Black (Hurricane Center)
John Molinari (SUNY)
Walt Lyons (Lightning Researcher, Industry Consultant)
Don MacGorman (NSSL)
Bill Taylor (NSSL)
Glen Salo (MRC)
Erik Rasmussen (NSSL)
Steve Rutledge (Colorado State Univ.)
Ralph Markson (ARA)

Consultants

David Curtis (DC Consulting)
Rodney Bent (GAI)

Weather Service Provieders, Private Sector

Rich Kithil (National Lightning Safety Institute)
Maria Pirone (WSI)
John Traynor (Kavouras)

NWS Forecasters

Dave Sharp (MLB, FL)
Steve Hodanish (MLB, FL)
Skip Ely (Ft. Worth, TX)
Charlie Liles (ABQ, NM)
David Bright (TUS, AZ)
Doug Green (Phoenix, AZ)
Steve Keighton (Flagstaff, AZ)
Mike Foster (Ft. Worth, TX)
Bill Sammler (Wakefield, VA)

Department of Defense

Bill Bauman (USAF)
Tom Lee (USN)
Peter Roohr (USAF)

Aviation Systems

Tom Fahey (NW)
Warren Qualley (AA)
Fred Mosher (AWC)
Steve Gregory (UA)
Alan Midkiff (AA)
John Hansman (MIT)
Randy Wicken (MIT/LL)
Val Heinz (MIT/LL)

USDA

Don Latham
Wally Josephson

NLDN Users, Private Sector

Ronald N. Keener, Jr. (Duke Power)
Ralph Bernstein (EPRI)

NASA

John Madura (KSC)
James Weinman (GSFC)

APPENDIX B
TWO-DIMENSIONAL MAPPING OF LIGHTNING DATA

Our two-dimensional analysis included all the weather radar data within the vicinity of the LDAR system for the three cases listed in Table 17. Both VIL and Echo Tops were made from the NEXRAD Level II archive data at 4 km resolution. Maps of LDAR and NLDN lightning, for comparison with the radar fields, were made according to the following steps:

1. A grid was established that has the LDAR sensor at the center, which is located at KSC. The size of the grid elements was selected to be 4 km x 4 km to match the radar data products resolution. (Note: The NASA LMS is actually expected to have 8 km resolution.) Each grid represents the lightning activity during a five-minute interval of time.

2. A weighting kernel was defined to represent the spatial distribution (quasi-Gaussian) that is given to each lightning event. The kernel used is given in Table B-1, below.

Table B-1.
Default Kernel Weights for Spatially Distributing Lightning Strikes
Sum of Weights = 48.8.

	-2	-1	0	1	2
-2	0.5	0.6	0.7	0.6	0.5
-1	0.6	2.2	5.1	2.2	0.6
0	0.7	5.1	10.0	5.1	0.7
1	0.6	2.2	5.1	2.2	0.6
2	0.5	0.6	0.7	0.6	0.5

3. The values of the elements in the grid are incremented by the kernel for each lightning event. The center of the kernel is aligned with the grid element whose position corresponds to the location of the lightning event. Since the kernel weights are not normalized, the final number of lightning strikes in the grid will be (approximately) 48.8 times larger than the true number.

To determine standard NWS-level equivalent values for display purposes, we chose to color the lightning and VIL data according to the standard NWS 6-level reflectivity scale used for Airport Surveillance Radars. (Since the ASRs have a broad fan beam, they naturally provide a vertically integrated measure of the reflectivity.) The VIL-to-NWS level conversions were calculated using the curves presented by Troxel and Engholm ((1990) Figure B-1), and the lightning flash rate map conversions were derived by eye. The final correspondence between NWS-levels and the various parameters to be compared is presented below in Table B-2.

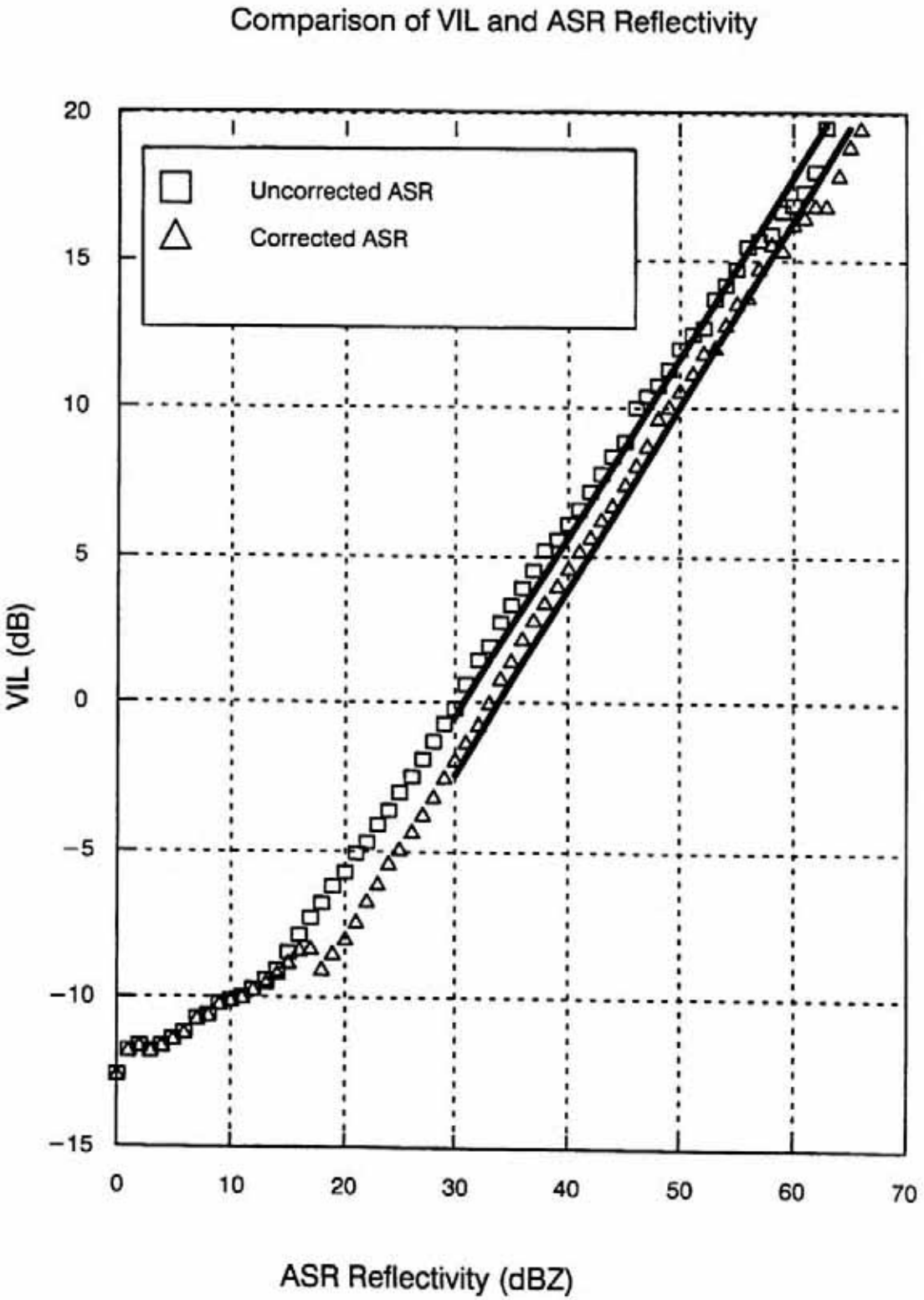

Figure B-1. Comparison of VIL and ASR reflectivity for uncorrected ASR reflectivity (boxes) and corrected ASR reflectivity (triangles), where the correction is applied only to reflectivities greater than 18 dBZ. (Troxel and Engholm, 1990.)

Table B-2.
Compilation of Color Bar Thresholds Used to Compare VIL, NLDN, and LDAR Data to NWS Levels. The NWS Level Correspondence to ASR Reflectivity is also Given

NWS level (ASR reflectivity)	VIL (Kg/m^2)	NLDN (flashes per 5 min x 48.8)	LDAR (flashes per 5 min x 48.8)
1 (18 dBZ)	0.14	1	20
2 (30 dBZ)	0.76	10	100
3 (41 dBZ)	3.50	25	300
4 (46 dBZ)	6.90	75	600
5 (50 dBZ)	12.0	200	900
6 (57 dBZ)	32.0	500	2700

APPENDIX C
POTENTIAL LMS BENEFITS FOR TROPICAL STORM FORECASTING/WARNING, FOREST FIRE MANAGEMENT, AND QUANTITATIVE PRECIPITATION FORECASTS

1. Tropical Storms and Hurricanes *

1.1. Introduction

1.1.1. Lightning and Hurricane-Spawned Tornadoes

It is now widely recognized that numerous tornadoes can be produced when tropical cyclones (TCs) move over land (McCaul, 1990). A comparison made between "Great Plains" tornadic supercells and tropical cyclone tornadic cells shows that while the average depth of rotation associated with the TC-tornado cells (3.5 km) was much less than their Midwest counterparts, the ratios of depth of rotation to storm top were comparable (Spratt and Nash, 1995). However, the shallower depth and weaker detectable rotation of the TC-tornadic mesocyclones greatly reduced the probability of detection with the current WSR-88D mesocyclone algorithm when compared to identification of traditional supercells.

From a recent study of the tornadoes produced by the 16 August, 1994 Tropical Storm Beryl and related observations of tropical cyclones (Cammarata, et al., 1996), it appears that the radar signatures of these tornadic storms are difficult to detect beyond ranges of about 100 km. In view of the fact that the average spacing of WSR-88Ds is on the order of a few hundred kilometers, this implies only some 10-15 percent of the Southeastern U. S. is close enough to a radar to make direct detection likely. Many investigators are coming to the conclusion that radar operators will need to use either modified radar algorithms or additional clues and data types in order to provide accurate warnings of mini-supercell tornadoes to the public (McCaul, 1997).

The Beryl outbreak was a good example of a major swarm outbreak of TC tornadoes. In this particular case, the CAPE was probably unusually large, perhaps in the 2000 J/kg class (Vescio, et al., 1996). The right-front quadrant rainband convection was correspondingly intense, but as with most TCs, the cells were small and somewhat shallow. However, the most intense storms, which were clearly mini-supercells, did produce moderate amounts of CG lightning (McCaul, 1997). Most TC tornado outbreaks, however, are weaker, and consist of only a handful of reports of brief, weak tornadoes. Tropical cyclone tornadoes tend to come from the most intense convective cells in the right-front quadrant of the cyclone, and such cells tend to be the most active electrically. Thus, McCaul suggests that the combined observation of higher VIL and electrical activity can help identify the most suspicious cells, regardless of their range from a radar. In addition, the lightning data exhibit temporal variations that may in some cases provide cues on the occurrence of tornadogenesis, although it is not yet feasible to issue warnings based on these temporal fluctuations alone.

---

* Sources: Robert Black, NCEP/Tropical Prediction Center; Bill McCaul, Universities Space Research Association; Tom Lee, NRL, Monterey, CA; John Molinari, SUNYA; Dave Sharp, NWS WFO Melbourne, FL.

Dave Sharp (1997) reports that individual tornadic cells within the outer rainbands of the 7 October, 1996 Tropical Storm Josephine were electrically active. Inferences could be made from the Melbourne NEXRAD regarding relative updraft strength and intensification (and subsequent vortex stretching) along with the presence of intrusions of cooler air aloft. In addition, some of these tornadic storms produced only intracloud lightning (as inferred from both the LDAR and NLDN data). This matter is regarded as significant by the National Weather Service in Melbourne. Total lightning activity could be used to assist in the detection of tornadic cells under similar situations with other tropical cyclones. This becomes very important at greater ranges from the radar since such severe cells are often compact in dimension. Nearly every tornadic storm associated with Josephine indicated LDAR-observed lightning.

Because the most dangerous cells within the tropical cyclone are also the strongest and deepest, it is possible that they may exhibit significant amounts of intracloud lightning in addition to their enhanced CG activity relative to other less dangerous cells. Although the actual amount of lightning activity in TC tornadic cells will likely be noticeably less than for midlatitude severe storms, there still may be enough activity to allow for improved identification of the most dangerous cells in areas far from radars.

1.1.2. Lightning and Hurricane Intensity Changes

Lightning activity in the vicinity of hurricane and typhoon eyewalls is usually infrequent. However, occasionally the lightning occurs as frequently as one flash per minute. Black and Hallett (1997) conclude (from airplane measurements) that the strong vertical motions and high liquid water contents that are needed for hurricane lightning are coupled to the general evolution of the hurricane. Further, they suggest that lightning may be a useful additional indicator of change in hurricane intensity and/or its track. A snapshot of eyewall lightning during Hurricane Linda is shown in Figure C-1. This image was observed by the NASA OTD just prior to a change in the storm track.

Molinari, et al., (1997) examined cloud-to-ground lightning data for eight Atlantic-basin hurricanes. They found a maximum of lightning occurring in the eyewall region and in the outer rainbands. The eyewall maximum occurred as a short-lived outbreak, typically 2.5 hours in duration, and it always occurred at the beginning of or during times of intensification. Sometimes it marked a major deepening event, such as Opal in the Gulf or Andrew before landfall (Molinari, et al., 1994; Williams, 1995). The eyewall signature is enhanced when intracloud lightning is available in addition to ground flashes (Williams, 1995). At other times, when the flash rate is lower, one of two things happens: either moderate deepening of the storm, or the imminent end to an extended period of deepening. The latter usually indicates the onset of an eye wall cycle. Molinari (1997(b)) suggests that it would someday be of great operational value to know of these events in real time. Knowing such information over open ocean would be of great scientific interest, and of value in understanding the genesis of hurricanes. The economic value of such forecasts would presumably involve shipping, aviation and any other operation that would want to know when a hurricane is forming.

A useful operational technique for estimating the intensity of hurricanes over ocean using only the shape and other characteristics of the storms on satellite images (because in situ data are usually not available) was developed by Dvorak (1975, 1984). The Dvorak scheme is a tropical cyclone classification system based on IR appearance. This procedure is considered unreliable (compared with direct aircraft reconnaissance) for intensity estimates in the case of rapidly intensifying storms, which often start with a completely obscured eye (Black, 1997(b)). The

Dvorak technique is not as important in the Atlantic basin because aircraft reconnaissance is conducted on every tropical disturbance that threatens a populated coast.

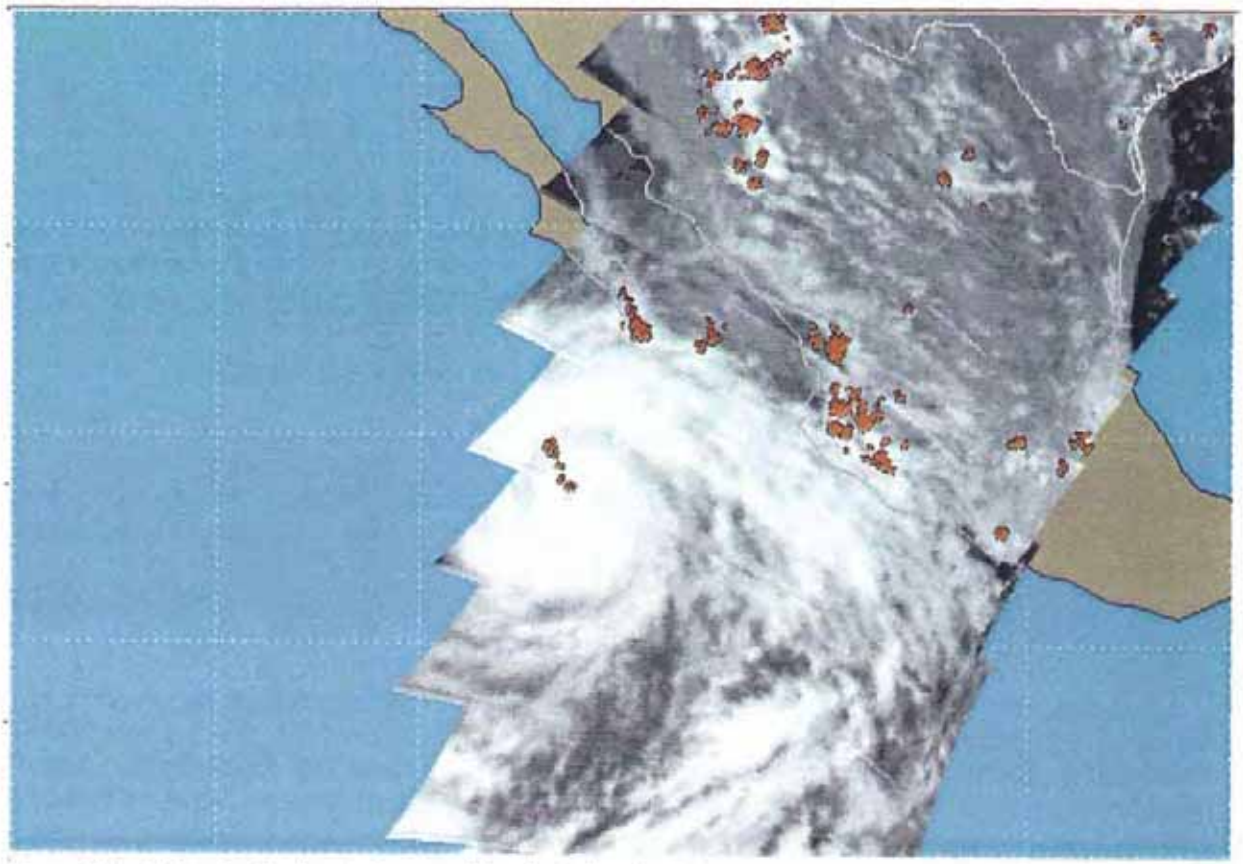

Figure C-1. Lightning flashes in the eyewall and rainbands of Hurricane Linda as observed by the NASA Optical Transient Detector on 12 September 1997. The flashes are superimposed on the OTD near-IR background images in the time interval 2115-2119 UTC. (Image courtesy of the NASA Global Hydrology and Climate Center, Huntsville, AL).

Both Black (1997(b)) and Molinari (1997(b)) thought the Dvorak method might be improved by incorporating continuous observations of total lightning. Although the Dvorak technique is not as necessary in the Atlantic as in the Pacific, an improved version may help avoid occurrences like Hugo on 15 September 1989, when one aircraft got into trouble because forecasters failed to pick up the rapid deepening prior to the arrival of the WP-3D's (Black, 1997(b)). Only transportation interests (and the occasional hurricane research operation) in the Atlantic need Dvorak-derived tropical cyclone intensity estimates. There is no other choice in all other ocean basins.

The Navy (and presumably commercial interests as well) routinely expends large sums of money moving ships, planes, and personnel away from the predicted path of these storms. A successful forecast generates savings of millions of dollars, whereas a failed forecast puts property and lives in danger (Lee, 1997). With the Air Force, the Navy maintains the Joint Typhoon Warning Center (JTWC) in Guam. The Navy is beginning a major research effort to improve the capability of JTWC, but is constrained by the limitations of current environmental satellite data. The Navy (as well as NESDIS) is currently attempting to diagnose storm properties such as rainfall, convective intensity, and tropical cyclone characteristics using the Special

Sensor Microwave/Imager (SSM/I) polar-orbiting data. The poor temporal sampling makes this mission more difficult (Lee, 1997).

2.0. Lightning and Forest Fires **

2.1. Introduction

Research at the Fire Sciences Laboratory, Missoula, MT, demonstrated that lightning-initiated wildland fires are caused by the continuing current component of the lightning flash to ground. Approximately one negative flash in five contains a lightning stroke with a continuing current. Approximately 95 percent of positive flashes to ground have a continuing current component. Continuing currents can be primarily characterized by their duration and their amplitude. Research shows that the NLDN-measured peak current is not an important factor in the ignition of fire. The current duration, on the other hand, is at least as important–or more so in some cases–as fuel characteristics such as moisture or bed depth (Latham, 1997).

NLDN data are presently available to the Forest Service. However, the NLDN data do not identify flashes with continuing current nor the duration of a continuing current. Research at the Intermountain Fire Sciences Laboratory has led to a methodology that enables the calculation of the probability of an individual ignition given the fuel state and the continuing current duration. Therefore, any technology that can provide both the location and the duration of a continuing current discharge will be a large improvement over knowledge of location and polarity alone (Latham, 1997).

Preliminary results from the NASA OTD sensor indicate a possible signature for long duration, continuing current discharges. A continuous output of optical pulses lasting for more than 100 milliseconds at the same pixel location has been correlated with positive cloud-to-ground flashes observed by the NLDN (Driscoll, 1997). If further research affirms the robustness of this signature, then the lightning mapper data can be used to better delineate the area of most probable ignition and perhaps allow fire fighting resources to be better used.

In a newly created program, the Department of Defense, in collaboration with USGS, will be releasing and evaluating high spatial resolution satellite products designed to support fire detection and fire perimeter mapping. Thermal hot spot detection is presently provided by infrared mapping from aircraft. Medium resolution 1-km Advanced Very High Resolution Radiometer (AVHRR) satellite imagery is used to assess decayed vegetation and soil moisture (fuel mapping). Although the new products are expected to be useful, they do not fully address the need for improved lead time that a value-added lightning detection scheme may offer. In addition, improved hot spot detection combined with long, continuing current flash detection may improve the probability of fire detection with reduced false alarms.

2.2. Fire Preparedness and Operations

DOI's FY97 preparedness funding is approximately $140 million. This dollar pool includes suppression equipment (aircraft, trucks, bulldozers, transport vehicles), prevention supplies, weather monitoring, lightning detection, supplies for suppression (shovels, hoses, pumps, radios,

---

** Sources: Don Latham/USDA Intermountain Fire Sciences Laboratory; Wally Josephson/ DOI, Office of Managing Risk and Public Safety.

etc.), dispatch operations, overhead costs (rental facilities, lights, heat, water) and salaries for permanent and temporary staff. Only a portion of the funded amount, perhaps as little as one to five percent, can be changed to improve the fire fighting resource efficiencies (W. Josephson, 1997). This assumes that funds are available to change to some other more efficient method and that start up and operational costs do not outweigh the benefits. Current funding does not allow for initial high cost projects. The agencies currently have a fire planning program that optimizes the use of various aircraft, fire engines, and crews to determine what mix of support is the most efficient and effective.

Getting to the fire faster does not necessarily guarantee a savings of dollars. There is a marginal return for each dollar spent at a given point towards trying to be more efficient. Another issue is that the 1995 Fire Management Policy and Program Review states that DOI must manage for the health of the land. The use of fire on the land is a natural occurrence and it is expected that additional acres will be burned to assist in managing the lands as resource managers have planned. This will include the use of prescribed fire and–given strict prescriptions–being able to monitor fires started by lightning which will probably increase the total acres burned. Therefore, getting to a fire before it "rages" does not define the potential of what will be burned. Even on the most severe burning days, some fires do not burn significant areas. The fire has to have nearly continuous fuels or high enough winds to overcome sparse fuels. If the fire is in a rocky secluded area the fire may never be attacked, but if it is next to a housing area, then it most definitely will be attacked. Thus, one can define the costs (potential savings) only after the fire, but not beforehand.

2.3. DOI Perspective on Satellite Lightning Mapping

The study team contacted and briefed a number of people involved in fire fighting operations. As a result of this inquiry, Wally Josephson responded with the following memo detailing their interests in an LMS capability.

From: Wallace Josephson, Department of the Interior, Office of Managing Risk and Public Safety

Subject: Wildland Fire Management Support for Continuous Total Lightning Observations

Date: 27 June, 1997

The wildland fire community has reviewed the proposed research and does support the mission of this project. Our community is always looking for more efficient ways to detect and suppress wildland fires.

An attempt to quantify the benefits of knowing where lightning will occur 30 to 60 minutes in advance is very difficult for our agencies. Expenditures on detection and prepositioning of resources are not identified separately within Department of the Interior agencies budgets. Therefore, they can not be extracted for analysis. Best estimates are that $2-300,000 (0.001-0.002 percent) of our preparedness funds are spent on actual detection and prepositioning of resources. A majority of these funds are spent in Alaska. It is believed that expenditures for current detection methods would equal that of any new detection method. Current

methods of detection use aircraft, vehicle, lightning data maps or lookout tower resources. With the additional knowledge of the location of possible lightning the local fire managers would still have to locate the fire and direct resources to that fire. If prepositioned resources are in the correct location, savings may be realized. If not, it may take two hours to move crews to the proper location. This would cost valuable time and dollars above normal expenditures, therefore, we believe it is a zero net sum gain until a field test can be conducted.

The 30-60 minute time frame can provide opportunities for early detection and prepositioning of resources, however, this is only beneficial for the first fire. For all subsequent fires, resources are generally limited and management must then determine the best resource distribution to reduce resource loss based on local fire management plans.

We believe that savings in dollars to the wildland fire program will be marginal as compared to the overall funding of the program. Only anecdotal evidence can support these statements; therefore, it is in our interest to support the project until such time it can be determined whether it can benefit the wildland fire management program.

One concern that must be addressed is the coverage of the sensor. The Wildland Fire program has responsibility for a large amount of land in Alaska. If this system proves to be of benefit, we would need coverage for Alaska as well as the rest of the U.S. Detection and prepositioning of resources in Alaska is more costly and therefore more beneficial than in the lower 48 states.

3.0 Total Lightning Assimilation and Quantitative Precipitation Forecasting

In a novel study by Alexander, et al. (1997), continuous lightning flash data were used to infer *convective* rain rates over the Gulf of Mexico during a rapid development phase of the 13 March 1993 Superstorm. Lightning data were obtained from two sources: the NLDN and the U.K. Meteorological Office (UKMO) long-range sferics detection system located in Europe (Lee, 1986). The continuously available lightning observations were blended with GOES IR and SSM/I rain rate estimates, which are not continuously available, and the resulting convective rainfall rate distribution was continuously assimilated into the mesoscale model 5 (MM5). They showed that lightning measurements could reveal convective activity at least six to nine hours before it was evident in GOES IR imagery. The assimilated rainfall distributions based on these data significantly improved the 12- to 24-hour forecast of intensity and precipitation patterns of the 1993 Superstorm compared to a forecast in which precipitation was not assimilated and a forecast that relied upon SSM/I and IR data only.

Figure C-2 shows the evolution of the surface pressure as a function of time both during the assimilation period and the prediction period (from Alexander, et al., 1997). The SSM/I data interpolated with GOES IR data alone did not improve the forecast produced from conventional meteorological data. However, the introduction of lightning data did significantly improve the 0000 UTC 14 March minimum surface pressure forecast. Because the 1993 Superstorm

deposited unusually heavy precipitation along the U.S. east coast, the predicted distribution of precipitation is of special interest.

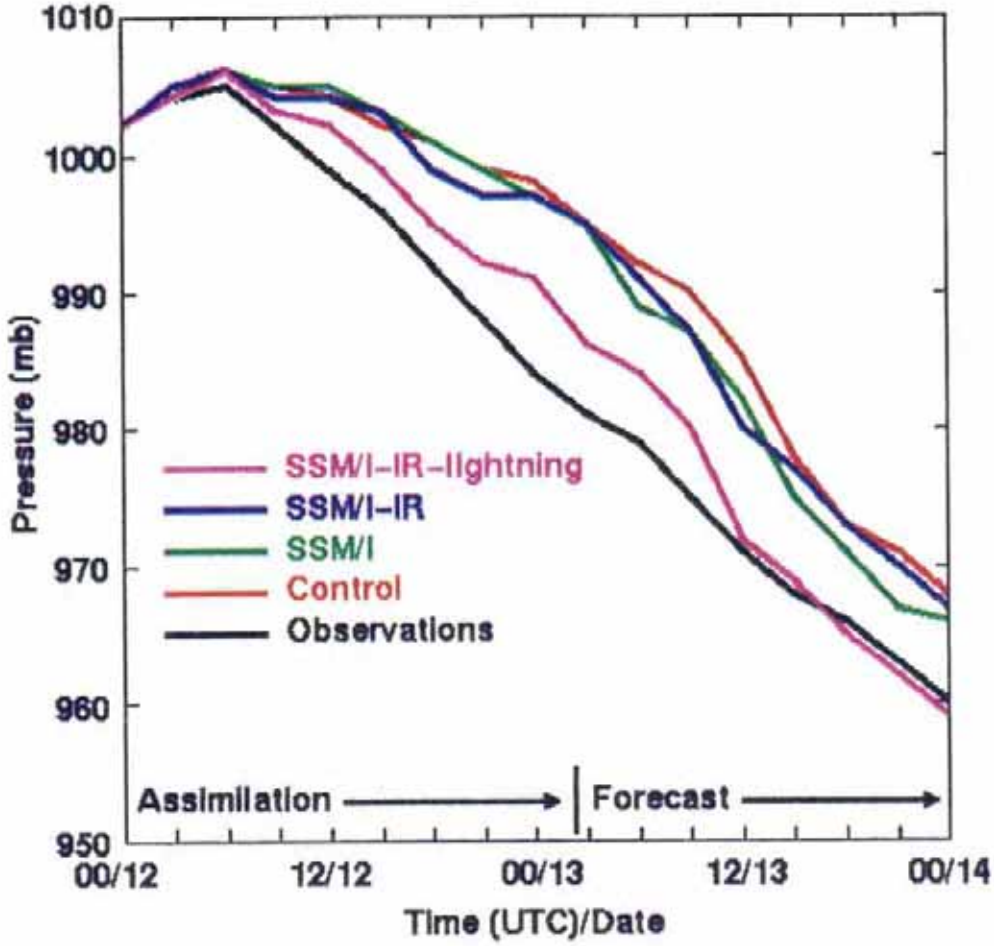

Figure C-2. Evolution of surface pressure of the 13 March 1993 Superstorm as a function of time, both during the assimilation period and the prediction period (Alexander, et al., 1997).

Figure C-3 compares forecasts of precipitation distributions at 0900 UTC on 13 March (derived from the control data) with forecasts using SSM/I and GOES IR data only and with forecasts predicted by the model when lightning data were also assimilated. Those distributions are compared to precipitation distributions given by radar. This figure shows that the MM5 model forecasts without the continuous update from the lightning predicted the squall line too far to the west, whereas the forecast that used lightning data placed the squall line closer to where it actually occurred.

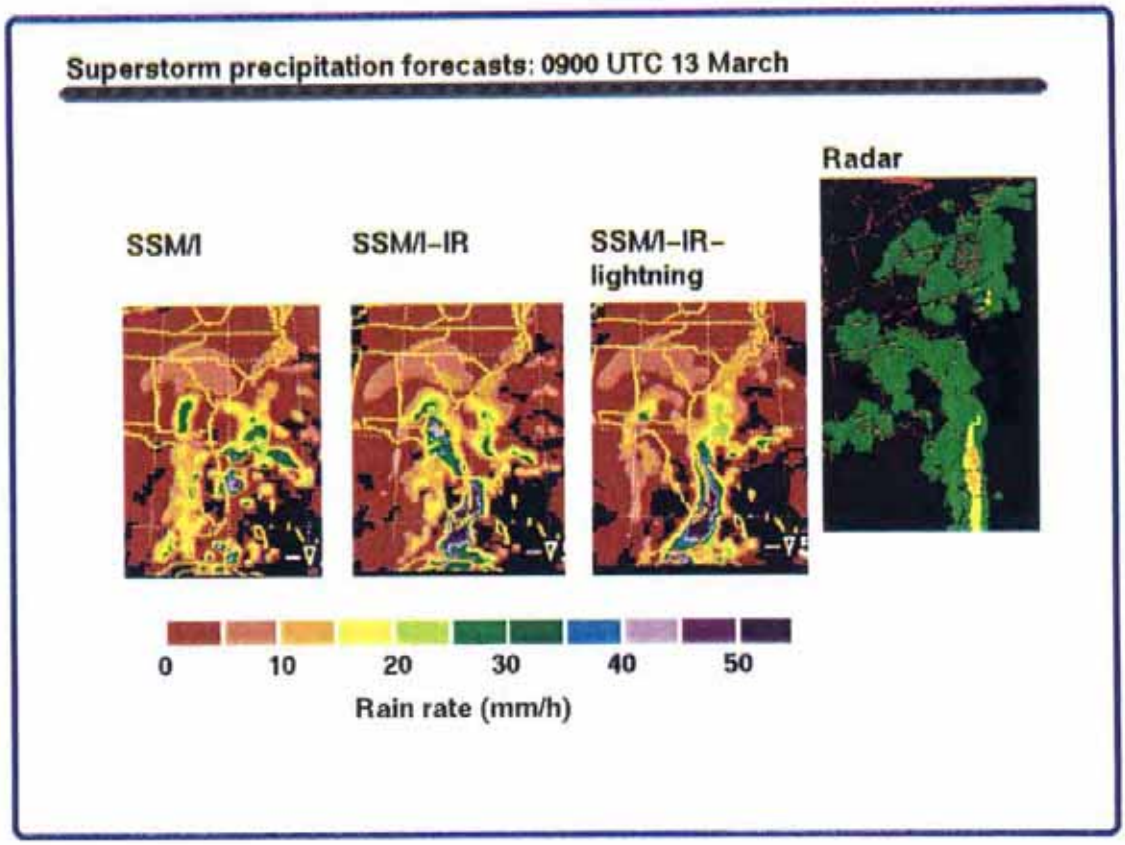

Figure C-3. Comparison of precipitation distribution forecasts on 13 March (derived from the control data) with forecasts using SSM/I and GOES IR data only and with forecasts predicted by the model when lightning data were also assimilated.